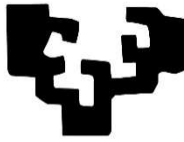eman ta zabal zazu

Universidad
del País Vasco
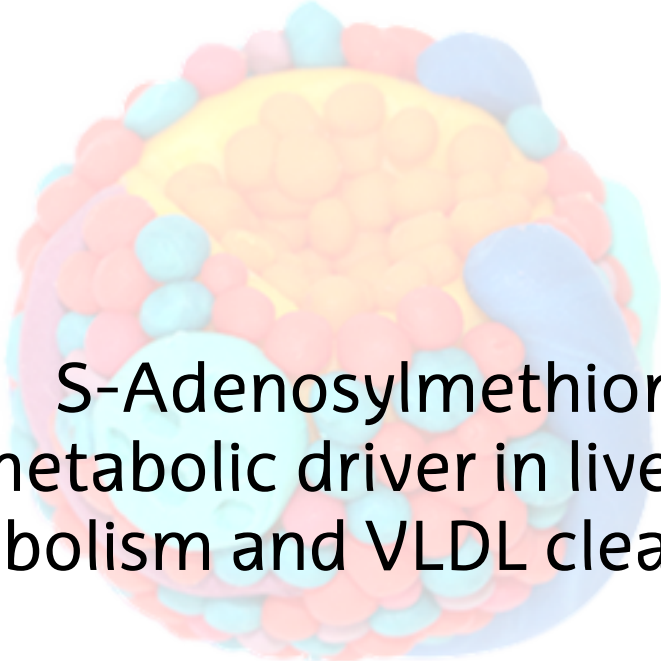
Euskal Herriko
Unibertsitatea

MEDIKUNTZA
ETA ERIZAINTZA
FAKULTATEA

FACULTAD
DE MEDICINA
Y ENFERMERÍA

Departamento de   Fisiologia
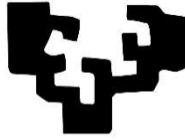Fisiología   Saila

S-Adenosylmethionine: a metabolic driver in liver lipid metabolism and VLDL clearance

Maite Martínez Uña

2017

eman ta zabal zazu

Universidad del País Vasco
Euskal Herriko Unibertsitatea

MEDIKUNTZA ETA ERIZAINTZA FAKULTATEA

FACULTAD DE MEDICINA Y ENFERMERÍA

Departamento de   Fisiologia
Fisiología   Saila

S-Adenosylmethionine: a metabolic driver in liver lipid metabolism and VLDL clearance

Maite Martínez Uña

2017

ABBREVIATIONS

5,10-MTHF	5,10-methyllenetrathydrofolate
5-MTHF	5-methyltetrahydrofolate
AADA	Arylacetamide deacetylase
Acaca	Acetyl-CoA carboxylase 1 gene
ACC	Acetyl-CoA carboxylase protein
AGPAT	1-acylglycerol-3-phosphate acyltransferase
AHCY	S-adenosylhomocysteine hydrolase
ANOVA	Analysis of the variance
Apob	Apolipoprotein B gene
ApoB-100	Apolipoprotein B-100 protein
ApoB-48	Apolipoprotein B-48 protein
ApoCI	Apolipoprotein CI
ApoCII	Apolipoprotein CII
ApoCIII	Apolipoprotein CIII
Apoe	Apolipoprotein E gene
ApoE	Apolipoprotein E protein
ATP	Adenosine triphosphate
BHMT	Betaine methyltransferase
BSA	Bovine serum albumin
CBS	Cystathionine β-synthase
CD36	Platelet Glycoprotein 4
CD	Control diet
CDD	Choline-deficient diet
cDNA	Complementary deoxyribonucleic acid

CE	Cholesteryl ester
Cho	Cholesterol
ChREBP	Carbohydrate-responsive element-binding protein
CIDE-B	Cell death activator CIDE-B
CK	Choline kinase
CKD	Chronic kidney disease
CL	Free cholesterol
CLna	Cardiolipin
CoA	Coenzyme A
CPT1	Cholinephosphotransferase 1
CVD	Cardiovascular disease
DG	Diglyceride
DGAT	Diacylglycerol O-acyltransferase
dKO	Double knock-out
DLS	Dynamic light scattering
DMEM	Dulbecco's modified Eagle's medium
DZA	3-deazaadenosine
EDTA	Ethylenediaminetetraacetic acid
EGTA	Ethylene glycol tetraacetic acid
EKI !/2	Ethanolamine kinase 1/2
ELOVL6	Long chain fatty acid elongase 6
EPT	Ethanolaminephosphotransferase 1
ER	Endoplasmic reticulum
FA	Fatty acids
FASN	Fatty acid synthase
FBS	Fetal bovine serum
FFA	Free fatty acids
FPLC	Fast-Protein Liquid Chromatography

FXR	Farnesoid x receptor
GAMT	Guanidinoacetate methyltransferase
GNMT	Glycine N-methyltransferase
GPAT	Glycerol-3-phosphate acyltransferase
HDL	High-density lipoproteins
Hepes	4-(2-Hydroxyethyl)piperazine-1-ethanesulfonic acid
HFD	High fat diet
HTG	Hypertriglyceridemia
HOMA-IR	Homeostasis model assessment
HuR	Hu-antigen R
IOD	Integrated optical densities
IP	Intraperitoneally
IR	Insulin resistance
KB	Ketone bodies
KH	Krebs-Henseleit
KO	Knock-out
Lac	Lactate
LC/MS	liquid chromatography/mass spectrometry
LD	Lipid Droplet
LDL	Low-Density Lipoproteins
Ldlr	Low-Density Lipoprotein receptor gene
LDL-R	Low-Density Lipoprotein receptor protein
LPC	Lisophosphatidylcholine
LPL	Lipoprotein lipase
Lrp1	Prolow-density lipoprotein receptor-related protein 1 gene
LRP-1	Prolow-density lipoprotein receptor-related protein 1 protein

LXRα	Liver X receptor α
MAT	Methionine adenosyltransferase
Mat1a	Methionine adenosyltransferase 1A gene
MCD	Methionine-choline-deficient diet
MDD	Methionine-Deficient-Diet
MG132	Carbobenzoxy-L-leucyl-L-leucyl-L-leucinal, Z-LLL-CHO
MS	Methionine synthase
MTHFR	5,10- methyllenetrathydrofolate reductase
MTP	Microsomal TG transfer protein
MTs	Methyltranferases
NADPH	Nicotinamide adenine dinucleotide phosphate
NAFLD	Non-alcoholic Fatty Liver Disease
NASH	Non-alcoholic steatohepatitis
o/n	Overnight
OA	Oleic acid
P	Probability of the null hypothesis
P-407	Poloxamer P-407 detergent
pACC	Phosphorylated Acetyl-CoA carboxylase protein
PBS	Phosphate-buffered saline
PC	Phosphatidylcholine
PCYT1	Choline-phosphate cytidylyltransferase A
Pcyt1α	CTP:phosphocholine cytidylyltransferase-α
PCYT2	Ethanolamine-phosphate cytidylyltransferase
PE	Phosphatidylethanolamine
PEMT	Phosphatidylethanolamine methyltransferase
PI	Phosphatidylinositol
PL	Phospholipids
Plin2	Perilipin-2 gene

PLIN2	Perilipin-2 protein
PMSF	Phenylmethylsulfonyl fluoride
PPARs	Peroxisome proliferator-activated receptors
Pparγ	Peroxisome proliferator-activated receptor γ
PS	Phosphatidylserine
PTMA	Prothymosin alpha
PVDF	Polyvinylidene difluoride
Pyr	Pyruvate
qPCR	Quantitative polymerase chain reaction
RT-PCR	Reverse transcription polymerase chain reaction
SAH	S-adenosylhomocysteine
SAMe	S-adenosylmethionine
SCD1	Stearoyl-CoA desaturase 1
SDS	Sodium dodecyl sulfate
SDS-PAGE	Sodium dodecyl sulfate-polyacrylamide gel electrophoresis
SEM	Standard error of the mean
SM	Sphingomyelin
SREBP-1	Sterol regulatory element-binding protein 1
SREBP1c	Sterol regulatory element binding protein 1c
T2DM	Type 2 diabetes mellitus
TEMED	Tetramethylethylenediamine
TG	Triglyceride
TGH	Triglyceride hydrolase
THF	Tetrahydrofolate
TLC	Thin layer chromatography
Tris	Tris(hydroxymethyl)aminomethane

UPLC	Ultraperformance liquid chromatography
VLDL	Very low-density lipoproteins
Vldlr	Very low-density lipoprotein receptor gene
VLDL-R	Very low-density lipoprotein receptor protein
WAT	White adipose tissue
WT	Wild-type

INDEX

1. Resumen/ Summary

1. **RESUMEN/SUMMARY**

1.1. **Resumen**

La enfermedad del hígado graso no alcohólica, EHGNA o NAFLD*,* por sus siglas en inglés, es la causa más frecuente en el mundo de enfermedad crónica hepática. Está enfermedad, generalmente asociada a obesidad, dislipemias y resistencia a insulina, engloba desde la simple esteatosis hepática hasta el desarrollo de esteatohepatitis, cirrosis o incluso hepatocarcinoma. Su desarrollo se ha asociado a un metabolismo errático de S-adenosilmetionina (SAMe) tanto en humanos como en ratones.

La ausencia de la proteína glicina N-metiltransferasa (GNMT) en ratones provoca un considerable aumento, de unas 35 veces superior a valores control, de SAMe en el hígado debido a que GNMT es la encargada principal de su catabolismo hepático. GNMT transfiere el grupo metilo de **SAMe** a la glicina, generando así S-adenosilhomocisteína y sarcosina; su función es actuar como un tampón celular que mantiene la concentración de SAMe constante. Por otro lado, la enzima metionina adenosiltransferasa (MAT) dirige la síntesis hepática de SAMe, y la ausencia del gen *Mat1a,* que codifica las isoformas MAT I y III, y se expresa principalmente en el hígado y páncreas del adulto, da lugar a un descenso en la cantidad de SAMe en ratones. Tanto la falta de la enzima GNMT como la de MAT dan lugar en ratones al desarrollo de distintas etapas de NAFLD. En el caso de la deficiencia en MAT se ha demostrado que bajas cantidades hepáticas de SAMe dan lugar a la reducción del contenido de fosfatidilcolina (PC) con los consecuentes cambios en el metabolismo fosfolipídico. Por otro lado, la deficiencia en MAT1A altera la oxidación de ácidos grasos en la mitocondria. Asimismo, la desactivación génica de *Mat1a* provoca alteraciones en el ensamblaje y secreción de lipoproteínas de muy baja densidad (VLDL), se secretan mayor número de partículas, de menor tamaño y más pobres en triglicérido. Los mecanismos mencionados contribuyen

al desarrollo de hepatoesteatosis en este modelo animal. Así, nos planteamos investigar si los altos niveles de SAMe que encontramos en los ratones que carecen de la enzima GNMT pueden provocar la acumulación de grasa en el hígado y en tal caso, el mecanismo implicado.

SAMe es el principal donador de grupos metilo, participa en la síntesis de PC a partir de fosfatidiletanolamina (PE) mediante la enzima PE metiltransferasa (PEMT), que convierte PE en PC con tres reacciones de metilación consecutivas en las que SAMe dona los grupos metilo. La actividad PEMT se ha reportado como un requisito indispensable para garantizar la correcta secreción de VLDL, secreción que, si está alterada, se ha descrito como un factor clave en el desarrollo de NAFLD en humanos. Por otro lado, las VLDL sirven como fuente de energía secretada por el hígado para los tejidos periféricos, si se produce un desequilibrio entre su tasa de secreción hepática y su tasa de aclaramiento del plasma pueden aparecer dislipemias con su consecuente riesgo de enfermedad cardiovascular.

En este contexto nos planteamos varios objetivos: averiguar el mecanismo implicado en la generación de esteatosis hepática en el ratón deficiente en GNMT; aclarar si cambios en el contenido hepático de SAMe afectan el ensamblaje y la secreción de VLDL tanto cuando sus niveles hepáticos son bajos, caso ratones MAT1A-knock out (KO), como cuando son altos, caso GNMT-KO; y por último saber si los elevados niveles de SAMe pueden tener consecuencias, distintas de las observadas en el hígado, para el resto del organismo.

La hipótesis de trabajo situó a la enzima PEMT como la clave tanto para el desarrollo de NAFLD como para la afectación de la secreción de VLDL ya que SAMe es sustrato de PEMT, y, ante la carencia de GNMT la actividad PEMT podría estar inducida debido al exceso de SAMe en el modelo GNMT-KO. Asimismo, el consecuente incremento de PC podría redirigirse hacia la síntesis de diglicérido (DG) y posteriormente de triglicérido (TG), dando lugar a su acumulación en el hígado, y de la

4

misma manera a su redirección hacia la secreción de VLDL. VLDLs que, si están alteradas, podrían dar lugar a consecuencias a otros niveles sistémicos.

Para el desarrollo del trabajo se utilizaron los modelos animales de ratón: GNMT-KO, MAT1A-KO, PLIN2-GNMT-KO y PLIN2-KO con sus correspondientes controles, de 3 meses de edad en todos los casos y de 8 meses en algunos. Fueron alimentados con dieta control (CD), dieta rica en grasa (HFD) o dieta deficiente en metionina (MDD), según procediera, y de ellos se obtuvieron muestras de sangre y tejidos como hígado, tejido adiposo blanco, corazón y músculo. Se emplearon también muestras humanas de plasma e hígado de 33 pacientes diagnosticados de NAFLD y de 36 sujetos con hígado sano.

Con objeto de analizar diversos procesos metabólicos (síntesis de ácidos grasos, producción de glucosa, de metabolitos ácidos, etc.) se realizaron experimentos *in vitro* en cultivos primarios de hepatocitos aislados mediante una técnica basada en el método de perfusión con colagenasa en dos etapas. También se realizaron experimentos *in vivo* para analizar la tolerancia a glucosa y a insulina o para examinar la producción de VLDLs inhibiendo su aclaramiento con Poloxamer 407. El análisis de los tejidos se realizó tras su homogeneización con Potter-Elvehjem o con Polytron, además, en algunos casos se procedió a la separación subcelular mediante centrifugaciones. En los tejidos, principalmente en el hepático se analizaronactividades enzimáticas, expresión génica, cuantificación de proteínas, y extracción, separación y cuantificación de lípidos

A partir del plasma sanguíneo se realizaron análisis lipoproteicos separando las distintas lipoproteínas (VLDL, LDL y HDL) mediante FPLC y analizando su contenido lipídico (TG, colesterol y PC). Del plasma también se aislaron las VLDL mediante ultracentrifugación, para el posterior análisis de su tamaño y contenido lipídico y apoproteico.

Los análisis estadísticos para buscar las diferencias significativas entre los distintos grupos de estudio fueron: el test de la t de Student's no pareado o el de Mann-

Whitney U para comparar entre dos grupos, y para comparar más de dos grupos de datos el análisis de la varianza (ANOVA) seguido del test de Bonferroni.

En los estudios realizados observamos que a pesar del desarrollo de NAFLD, los ratones GNMT-KO presentan un contexto metabólico favorable, no presentan obesidad ni resistencia a insulina, además sus niveles de ácidos grasos y cuerpos cetónicos en sangre son normales. El análisis de la síntesis *de novo* de ácidos grasos en hígado tampoco presentó cambios con respecto a los animales silvestres, aunque sí se observó un incremento en la tasa de secreción de TG que no es capaz de compensar su acumulación. A la luz de estos resultados no parece que ningún mecanismo habitual participe en el aumento de TG hepático. Por otro lado, el estudio mediante cromatografía en capa fina del contenido hepático en glicerolípidos reveló que el contenido de PE está muy disminuido en los ratones con alto contenido en SAMe, mientras que la cantidad de PC, DG y TG está aumentada. Además, en concordancia, el flujo PEMT, el paso de PE a PC está también aumentado. La administración de MDD a los ratones GNMT-KO, que restablece los niveles de SAMe hasta valores control, restaura todos los valores mencionados, incluso resuelve la esteatosis hepática, lo que pone de manifiesto la clara implicación de SAMe en el proceso de acumulación de TG en estos animales. La inhibición de la enzima PEMT con DZA en hepatocitos KO evita la acumulación de TG en los mismos, por lo tanto, es el incremento del flujo PEMT el que está liderando la hepatoesteatosis. La sobreactivación de PEMT no es un proceso pasajero, sino que se mantiene en el tiempo, ya que se observa también en ratones de 8 meses.

La esteatosis en los animales deficientes en GNMT también se resuelve con la deleción adicionalde perilipina 2 (PLIN2). En los ratones que carecen de estas 2 proteínas se observa un perfil lipídico hepático idéntico al observado en los GNMT-KO, excepto por el TG, que en los ratones doble KO está disminuido. Ese perfil lipídico se corresponde por tanto con el aumento de la actividad PEMT y el consecuente incremento en la tasa de secreción de TG hepático. Además estos animales presentan

menor cantidad de cuerpos cetónicos en sangre mientras que la generación de metabolitos ácidos en hepatocitos está ligeramente aumentada, en concordancia presentan una gluconeogénesis muy activa.

A lo largo de este estudio se observó, como ya se ha mencionado, que los ratones deficientes en GNMT secretan mayor cantidad de TG hepático al torrente circulatorio; además sabíamos que los ratones MAT1A-KO secretaban mayor número de partículas de VLDL (mayor secreción de apolipoproteina B –ApoB-), pero menos TG hepático, lo que hacía que las partículas de VLDL fueran de menor tamaño. En este trabajo observamos que los animales GNMT-KO secretaban menor número de partículas de VLDL (menos apoB) pero con mayor contenido de TG hepático. Estas VLDL presentan, por tanto, mayor tamaño y, además, menos cantidad de PE. En el caso de GNMT-KO, en consonancia con la mayor secreción de VLDL-TG, se observa una mayor movilización hepática de TG junto con un incremento en las actividades DG aciltransferasa (DGAT) y de la proteína transferidora de TG microsomal (MTP). La actividad DGAT además de la TG lipasa y PEMT están disminuidas en el caso de MAT1A-KO y se recuperan junto con los valores de SAMe y las características control de las VLDL al administrárselo a los ratones durante 7 días. La administración de la MDD a los ratones GNMT-KO también restaura las características silvestres de las VLDL. Así, SAMe controla la secreción de VLDL a través de PEMT. Observamos también que SAMe controla la cantidad de ApoB inhibiendo su transcripción mediante la metilación de su promotor y reduciendo la estabilidad de su mRNA que no se une a HuR.

En este trabajo observamos que las VLDL secretadas cuando la concentración hepática de SAMe es muy alta presentan además otras características diferenciales, como es el alto contenido en la apolipoproteína E (ApoE), alto contenido que responde a un incremento de esta proteína en el tejido hepático. Nos planteamos que estas diferencias, además de las ya descritas, podrían afectar al catabolismo de las VLDL una vez en circulación. Así, observamos que el TG en sangre en los ratones GNMT-KO es mucho más bajo que en sus controles y se recupera con la MDD, lo que nos indica que

el metabolismo de las VLDL está acelerado en estos animales. La tasa de aclaramiento de VLDL humanas en ratones que carecen de GNMT no está alterada, por lo que las especiales características fenotípicas de las VLDL parece ser lo que lidera el mayor aclaramiento plasmático de las mismas, aunque la mayor expresión del receptor de VLDL y del receptor de LDL en el hígado podría estar contribuyendo también. El aclaramiento es incluso mayor cuando los animales son sometidos a una HFD, circunstancia bajo la que la hepatoesteatosis aumenta y además se observa acumulación de TG en el corazón, con el consecuente riesgo de enfermedad cardiovascular (CVD). El riesgo de CVD está asociado a NAFLD en humanos, y en humanos hemos observado que existe un grupo de enfermos que presentan bajos niveles de TG en suero al mismo tiempo que bajas cantidades de GNMT en hígado.

Los resultados obtenidos en este trabajo ponen de relevancia la necesidad de mantener una adecuada homeostasis de SAMe para mantener bajo control la acumulación de TG en el hígado, su salida en VLDL y el aclaramiento de estas (Figura RS1).
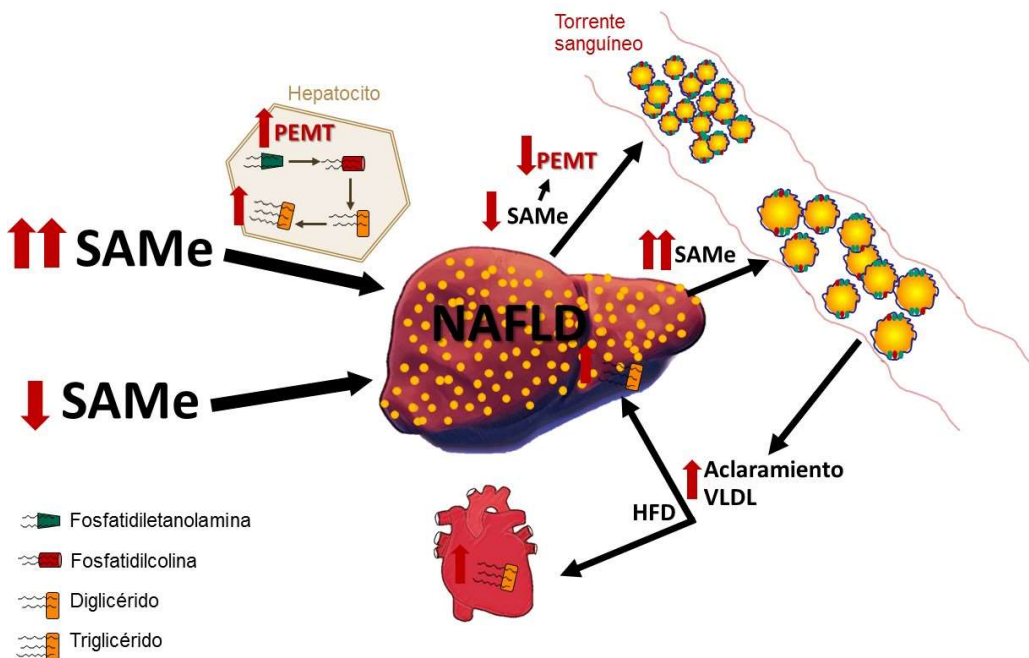
Figura RS1. _Resumen esquemático de los resultados obtenidos_

1.2. **Summary**

Non-alcoholic Fatty Liver Disease, NAFLD, is the most common cause of hepatic chronic disease in the world. NAFLD is usually associated with obesity, dislipidemias and insulin resistance; and it comprises from simple hepatic steatosis to steatohepatitis development, cirrosis or even hepatocarcinoma. Its development has been associated with an impaired metabolism of S-adenosylmethionine (SAMe) in humans and in mice.

Gycine N-methyltransferase (GNMT) protein absence in mice induces a remarkable increase, 35-fold rise over control values, of SAMe due to the fact that GNMT is the principal enzyme in charge of its hepatic catabolism. GNMT transfers SAMe methyl group to glycine producing S-adenosylhomocysteine and sarcosine; its function is to act as a cellular buffer to maintain SAMe concentration steady. On the other hand, methionine adenosyltransferase (MAT) enzyme directs the hepatic synthesis of SAMe. The absence of *Mat1a* gene expression, that codifies for MAT I and III isoforms, and it is expressed mainly in adult liver and pancreas, produces a decrease of SAMe content in mice. Both GNMT and MAT absence prompt the development of different stages of NAFLD development. For MAT deficiency case it has been shown that low hepatic content of SAMe induce a reduction in phosphatidylcholine (PC) content leading the consequent changes in phopspholipd metabolism. What is more, the lack of MAT alters fatty acids oxidation in the mitochondria. Additionally, *Mat1a* gene inactivation induces an impairment in very low density lipoproteins (VLDL) assembly and secretion, more number of particles, larger and poorer in triglyceride (TG) are secreted. All the mentioned mechanisms may contribute to the development of the hepatosteatosis phenotype in this animal model. Fatty liver development also occurs in GNMT-KO mice in which hepatic SAMe levels are markedly increased. Thus, we decided to investigate how high levels of liver SAMe can lead to the accumulation of fat in the liver and the mechanism involved.

SAMe is the principal methyl donor, it participates in PC biosynthesis from phosphatidylethanolamine (PE) through PE methyltranferase (PEMT) enzyme activity. PEMT turns PE into PC after three consecutive methylation reactions in which SAMe donates the methyl group. PEMT activity has been reported to have a key role that guarantees the correct secretion of VLDL. Secretion that if impaired has been described as a key factor in the development of NAFLD in humans. Furthermore, VLDLs are a source of energy secreted by the liver for peripheral tissues; if an imbalance between its hepatic secretion rate and its clearance from plasma takes place dislipidemias may appear with the subsequent risk of cardiovascular disease.

Under this context several objectives were outlined: figure out the mechanism involved in the generation of hepatic steatosis in GNMT deficient mice; clarify if changes in the hepatic content of SAMe disturb the assembly and secretion of VLDL both when SAMe hepatic levels are low, MAT1A-knock out (KO) mice model, and when they are elevated, GNMT-KO mice case; and lastly, discover if SAMe high levels can have consequences others than the ones observed in the liver for the rest of the body.

The working hypothesis pointed out PEMT enzyme as crucial as much for NAFLD development as for VLDL secretion impairment because SAMe is a substrate for PEMT. In the face of GNMT absence, PEMT activity could be induced due to the excess of SAMe in GNMT-KO mice model. In addition, the subsequent increase in PC due to augmented PEMT activity could be rerouted in the direction of diglyceride (DG) and later triglyceride (TG) synthesis; the latter could accumulate in the liver and likewise could be redirected towards VLDL secretion. VLDLs that if impaired could present some consequences at a systemic level.

For the development of the study, the following animal models were used: GNMT-KO, MAT1A-KO, PLIN2-GNMT-KO, PLIN2-KO and their corresponding counterparts of 3-months-of-age in every case and of 8-months-of-age in some cases. They were fed with a control diet (CD), a high fat diet (HFD) or a methionine deficient diet (MDD), depending on the case. Samples of blood and tissues, such as liver, white

adipose tissue, heart and muscle were collected. Serum and liver samples of 33 NAFLD diagnosed patients and of 36 patients with a healthy liver were also used.

With the aim of analysing several metabolic processes (fatty acid synthesis, glucose production, acid metabolites production, etc.) some *in vitro* experiments with primary hepatocytes cultures were performed. *In vivo* experiments were also executed in order to study glucose and insulin tolerance or to examine VLDLs production inhibiting its clearance with poloxamer-407. The analysis of tissues was performed after their homogenization either with Potter-Elvehjem or with Polytron; besides, in some cases a subcellular fractionation through serial centrifugations was also carried out. In the tissues, mainly in the hepatic tissue, enzymatic activities, genetic expression, protein quantification, lipid extraction, separation and quantification were analysed.

An examination of lipoproteins was also made. From serum and by means of FPLC the different lipoproteins (VLDL, LDL and HDL) were separated and their lipid content (TG, cholesterol and PC) analysed. VLDLs were also isolated from serum by ultracentrifigation and later studied for their size and lipid and apoprotein content.

The statistical analyses used to examine the statistical significance of the differences in the results depended on the group of results to be compared. The comparison between two groups was analysed using the unpaired Student's t-test or Mann-Whitney U test. For the examination of more than two groups of data the analysis of the variance (ANOVA) followed by Bonferroni test was applied.

We observed that in spite of the NAFLD development, GNMT-KO mice present a favourable metabolic context; they do not have obesity nor insulin resistance, besides, their fatty acids and ketone bodies levels in serum were normal. The analysis of *de novo* fatty acids synthesis neither presented changes with respect to wild type (WT) animals; although it was observed an increase in the rate of TG secretion from the liver that is not capable of compensating the TG accumulation. In the light of these results no usual mechanism seems to be contributing to the rise of hepatic TG in GNMT-KO model. However, the study by thin layer chromatography of hepatic glycerolipid content

revealed that PE content was noticeably decreased in the mice with high levels of SAMe, while PC, DG and TG content was increased. Moreover, in concordance, PEMT flux, the transformation of PE into PC, is also augmented. The administration of a MDD to GNMT-KO mice, that re-establishes SAMe levels to control values, restores all the mentioned changes, and it even resolves the hepatic steatosis; this discloses the implication of SAMe in the TG accumulation process in the liver of GNMT deficient mice. What is more, PEMT inhibition with DZA in KO hepatocytes avoids the accumulation of TG, therefore, it is the increase in PEMT flux what is leading the hepatosteatosis in these animals. The overactivation of PEMT is not a transitional process but it maintains over months given that it is also observe in mice of 8-months-of-age.

The steatosis in GNMT deficient mice is also resolve with the additional deletion of perilipin 2 (PLIN2). In the mice lacking both proteins the hepatic lipid profile resembles the one observed in GNMT-KO mice except for the TG content, which is diminished in the double KO mice. That lipid profile corresponds, thus, with the increase in PEMT activity and the consequent increase in the rate of secretion of hepatic TG. Besides, the double KO animals present less ketone bodies in serum while the production of acid metabolites in hepatocytes is slightly increased, in concordance they have a very active gluconeogenesis.

During the study it was observed that mice lacking GNMT enzyme secrete an increased quantity of TG into the bloodstream; besides, we already knew that MAT1A-KO mice secreted an increased number of VLDL particles (increased secretion of apolipoprotein B –ApoB-) but less hepatic TG, given rise to smaller VLDL particles. And in this work we found that the number of particles secreted by GNMT-KO animals was less (reduced secretion of ApoB) but with increased content of hepatic TG; hence, these particles have a larger size, and, in addition, a lesser amount of PE. For the case of GNMT-KO, in accordance with the increased secretion of VLDL-TG, an increase mobilization of hepatic TG along with an increase both in DG acyltransferase (DGAT) and in microsomal transfer protein (MTP) activities were observed. DGAT, TG lipase and PEMT activities are diminished for MAT1A-KO case and recovered together with SAMe

values and VLDL control features after SAMe administration to the KO mice for 7 days. The administration of the MDD to the GNMT-KO mice also restores VLDL normal features. All the obtained results led us to conclude that SAMe controls VLDL secretion through PEMT pathway. It was also observed that SAMe control ApoB quantity by inhibiting its transcription by means of its promoter methylation and also by reducing its mRNA stability that do not attach to HuR.

It was also observed in this work that the VLDL secreted when hepatic SAMe concentrations are high present other differential characteristics apart from the ones already mentioned. The VLDLs secreted by GNMT-KO contain an increased amount of apoliprotein E (ApoE) content that responds to an augmentation of this protein in the hepatic tissue. We wondered if all the differential features could be challenging VLDL catabolism once in the bloodstream. Serum TG in GNMT-KO mice was much lower than in the control animals and it recovered after MDD feeding, what shows that VLDL metabolism is accelerated in this animal model. The clearance rate of VLDLs of human origin in mice lacking GNMT was not impaired, therefore, the particular phenotypic features of the VLDLs seem to be behind the increased clearance. The augmented expression of VLDL receptor and LDL receptor in the liver could also be contributing, at least in part, to the increased clearance. VLDL clearance is even greater when GNMT-KO mice are fed with a HFD; under this circumstance the hepatosteatosis is also greater and TG is shown to accumulate in the heart as well, with the consequent risk of cardiovascular disease (CVD). The risk of CVD is associated with NAFLD in humans; and in humans we have observed that there is a group of NAFLD patients that present low levels of TG in serum along with a low amount of GNMT in the liver.

All in all, the results obtained in this work highlight the importance of maintaining an adequate homeostasis of SAMe to control TG accumulation in the liver, its export into VLDL and the clearance of VLDLs (Figure RS2).
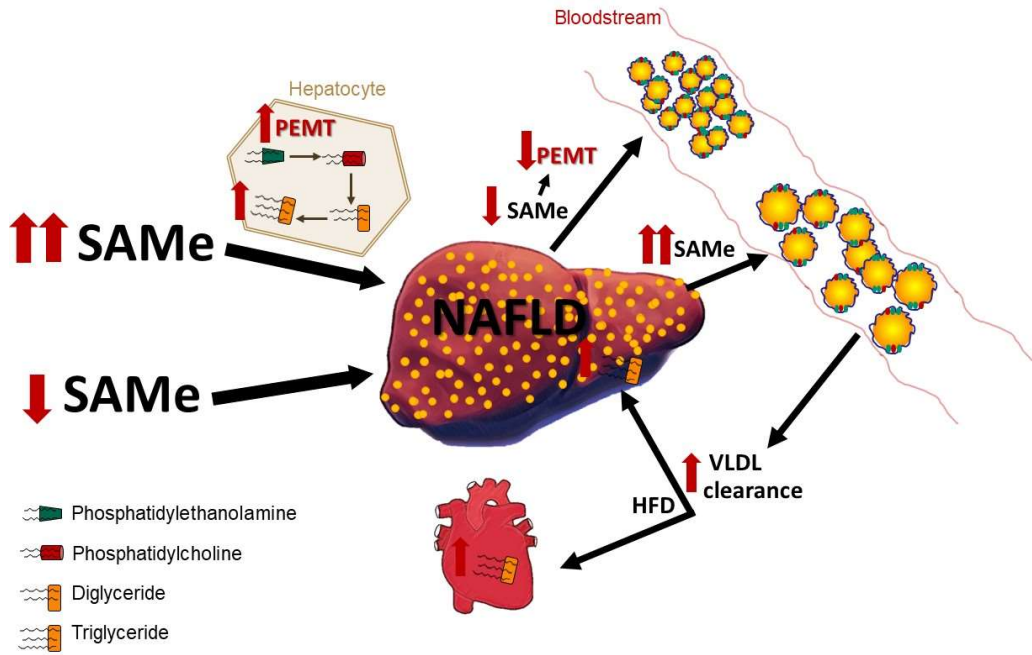
Figure RS2. *Scematic representation of the obtained results.*

2. Introduction

Tell me and I forget, teach me and I may remember, involve me and I learn.

Benjamin Franklin (1706-1790)

2. **INTRODUCTION**

2.1. **S-Adenosylmethionine**

S-Adenosylmethionine (SAMe, also abbreviated as AdoMet and SAM) is a crucial molecule for all living organisms, it is widely known as the principal biological methyl donor, and several cellular processes are dependent on its availability. Therefore, SAMe is considered a key regulator in cellular metabolism, proliferation, differentiation, apoptosis and death[1]. SAMe is synthesized in all mammalian cells, however, liver is the organ in which 85% of transmethylation reactions and 50% of methionine metabolism take place, for that reason liver can be considered as body's SAMe factory[2]. The role of the liver in SAMe homeostasis is essential.

SAMe was first discovered by Giulio Cantoni in 1953[3], back then he demonstrated that the enzymatically catalysed reaction of L-methionine, an essential amino acid, and ATP yielded SAMe. SAMe synthesis and utilization occur mainly in the liver[4]. The reaction of SAMe biosynthesis is catalysed by the enzyme Methionine Adenosyltransferase (MAT, EC 2.5.1.6) and the removal by glycine N-methyltransferase (GNMT, EC 2.1.1.20)[4].

MAT is an essential enzyme to sustain life, consequently, it has been extremely well conserved through evolution, and all mammalian cells and tissues that have been studied express it[2]. There are three isoforms of MAT enzyme that synthesize SAMe: MATI, MATII and MATIII, MATI and MATIII are products of *Mat1a* gene while MATII is codified by *Mat2a*. *Mat1a* gene is exclusively expressed in the liver and pancreas of adults, whereas *Mat2a* is expressed in all tissues but to a lesser degree since its expression decreases after birth, conversely to *Mat1a*, whose expression increases after birth[4].

SAMe catabolism is the link to four key metabolic pathways: polyamine synthesis, transmethylation, transsulfuration and 5'-deoxyadenosyl 5'-radical mediated biochemical transformations[2] (Figure I1).

- **Polyamine synthesis:** to enter this pathway SAMe is first decarboxylated and then the propylamino moiety is donated to putrescine to form spermidine and to spermidine to form spermine, both reactions yield methylthioadenosine (MTA) as a by-product[1]. MTA is rapidly metabolized trough the methionine salvation pathway and regenerates SAMe. Polyamines are ubiquitous in all living cells and play a crucial role in many biological processes[2].

- **Transmethylation:** the methyl group of SAMe can be donated to a large variety of acceptor molecules in reactions that are catalysed by methyltransferases (MTs)[1]. The acceptor molecules range from nucleic acids to proteins, carbohydrates, lipids or small molecules, accordingly, over 200 proteins in the human genome have been identified as known or putative SAMe-dependent MTs[2].

- **Transsulfuration:** this pathway is particularly active in the liver. It requires SAMe first to transfer its methyl group to form S-adenosylhomocysteine (SAH), which is hydrolyzed by SAH hydrolase (AHCY) to produce Homocysteine (Hcy). Hcy is then converted to cysteine plus α-ketobutyrate, due to the concerted action of cystathionine β-synthase (CBS) and cystathionase; cysteine is the rate-limiting precursor of glutathione (GSH), the major endogenous antioxidant[2]. The steps from Hcy onwards are really what constitutes transsulfuration pathway.

- **Radical reactions:** upon one-electron reduction, SAMe is a source of 5'-deoxyadenosyl radicals, which by removing a hydrogen atom from substrates such as small molecules, proteins, RNA or DNA initiate many metabolic reactions and biosynthetic pathways[5].
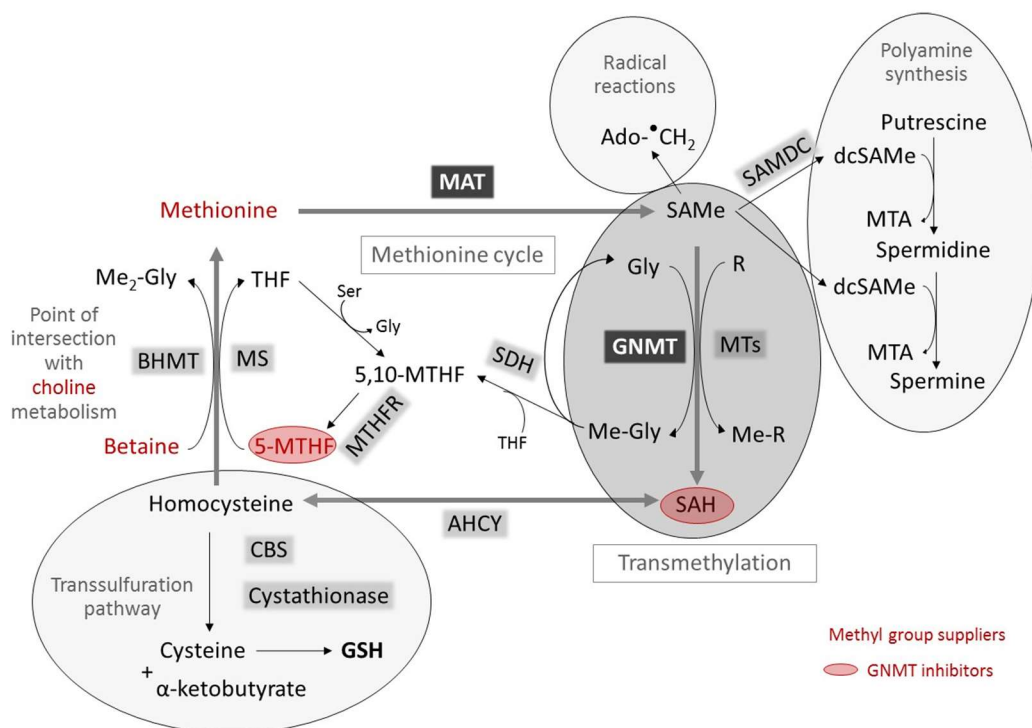
Figure I1. *SAMe metabolism in liver.* MAT, Methionine Adenosyltransferase; SAMe, S-Adenosylmethionine; Ado-$^{\bullet}CH_2$, 5'-deoxyadenosyl radical; SAMDC, S-Adenosylmethionine decarboxylase; dcSAM, decarboxylated SAMe; MTA, Methylthioadenosine; R, Methyl accepting substrate; MTs, Methyltransferases; Me-R, Methylated product; Gly, Glycine; GNMT, Glycine N-Methyltransferase; Me-Gly, Sarcosine; SAH, S-Adenosylhomocysteine; AHCY, SAH hydrolase; CBS, Cystathionine β-synthase; GSH, Glutathione; THF, Tetrahydrofolate; SDH, Sarcosine dehydrogenase; 5,10-MTHF, 5,10-methyllenetrathydrofolate; 5-MTHF, 5-methyltetrahydrofolate; MS, Methionine synthase; Ser, Serine; BHMT, Betaine methyltransferase; Me$_2$-Gly, dimethylglycine.

As it has been mentioned above, SAMe is widely known for its transmethylation capacity. In this reaction, by giving its methyl group SAMe is transformed in SAH, which is then hydrolysed to form Hcy. Hcy can follow two paths, either the already cited transsulfuration pathway or it can be re-methylated to form methionine, completing the methionine cycle. Re-methylation can be catalysed by two different enzymes: methionine synthase (MS), which requires vitamin B$_{12}$ and 5-methyltetrahydrofolate (5-MTHF) to perform correctly; and betaine methyltransferase (BHMT) that needs betaine to function[1] (Figure I1).

There are many MTs, yet the available evidence indicates that the quantitatively most important pathways for SAMe-dependent transmethylation in mammals are guanidinoacetate methyltransferase (GAMT) that synthesizes creatine, Phosphatidylethanolamine methyltransferase (PEMT) to form Phosphatidylcholine (PC), and GNMT that produces sarcosine (Figure I1). And among those, GNMT is the main enzyme that regulates SAMe levels; when GNMT is absent or reduced, SAMe and methionine accumulate in plasma whereas GAMT or PEMT reduction does not trigger the accumulation, probably due to GNMT activity[6].

GNMT is the most abundant MT in the liver where it accounts for 1-3% of cytosolic protein and it is activated by SAMe[7]. GNMT transfers SAMe methyl group to glycine producing SAH and sarcosine (N-Methylglycine). Sarcosine has no known essential metabolic function, however it is demethylated by sarcosine dehydrogenase (SDH) to restore glycine, and its methyl group is transferred to tetrahydrofolate (THF) forming 5,10-methyllenetrathydrofolate (5,10-MTHF), which enters into the folate cycle to recover methionine through its conversion to 5-MTHF thanks to 5,10-MTHF reductase (MTHFR). 5-MTHF is an inhibitor of GNMT (Figure I1). Through this set of reactions SAMe methyl group is saved from being used in undesired methylation reactions. Therefore, GNMT function is to act as a cellular buffer that maintains SAMe concentration constant[2].

PEMT activity is also important in the liver not only because it contributes to SAMe levels regulation but also because it accounts for approximately 30% of PC biosynthesis[8]. Two pathways contribute to PC synthesis in the liver: CDP-choline pathway (or Kennedy pathway) and PEMT pathway (Figure I2). In PEMT pathway PE is converted into PC through three consecutive methylations, in which SAMe donates the methyl group, of PE[8]. By means of PEMT pathway SAMe plays a role in lipid metabolism through the methylation of phospholipids, and may be responsible for membrane fluidity and for the establishment of a proper PC/PE ratio[9]. Choline to synthesized PC can be acquired from the diet or obtained from the PC synthesized via PEMT[10]. Choline

can then be oxidized to betaine[10] that manner contributing to methionine recovery through methionine cycle (Figure I2).
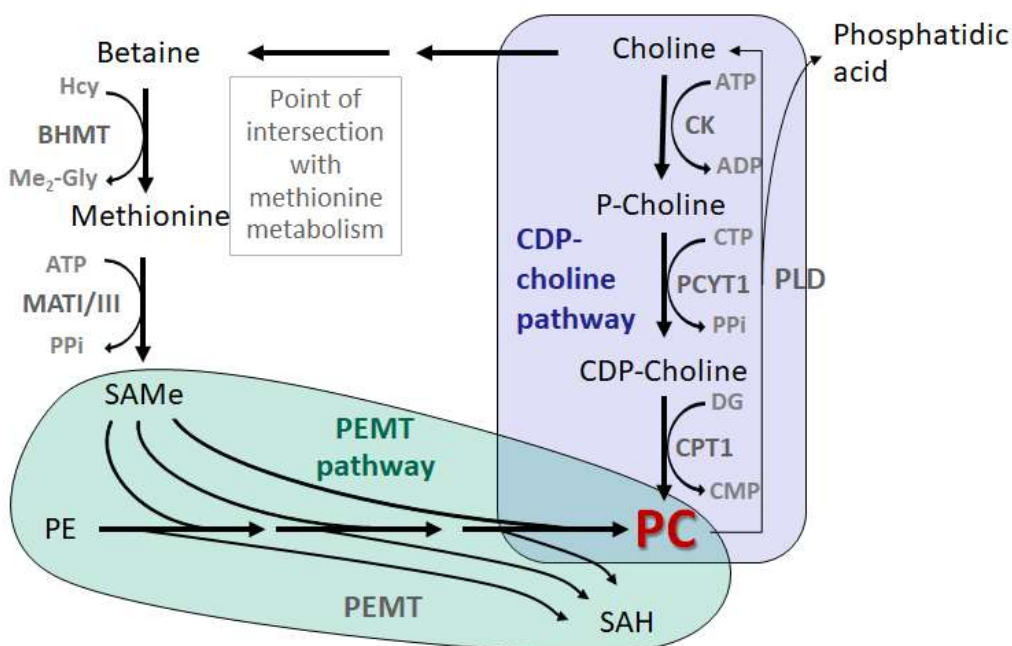
Figure I2. *Phosphatidylcholine biosynthetic pathways.* CK; Choline kinase; PCYT1, Choline-phosphate cytidylyltransferase A; CPT1, Cholinephosphotransferase 1; PLD, Phospholipase D; PC, phosphatidylcholine; Hcy, homocysteine; BHMT, Betaine methyltransferase; Me_2-Gly, dimethylglycine; MAT1A, Methionine Adenosyltransferase 1A; SAMe, S-Adenosylmethionine; PE, phosphatidylethanolamine; PEMT, phosphatidylethanolamine methyltransferase; SAH, S-Adenosylhomocysteine.

Many different pathways can contribute to methionine cycle, therefore its regulation needs to be tightly controlled. In addition to methionine, SAMe, SAH and Hcy are the main compounds of methionine cycle. SAMe is an activator of MTs while SAH acts as an inhibitor of most MTs[11], thus SAMe to SAH ratio can be viewed as an index of transmethylation potential in the cell[12]. Because of SAMe relevance as a regulator of multiple hepatic functions, its hepatic content must be maintained steady independently of methionine daily intake, or of choline and betaine ingestion, the other two compounds that can supply the methyl group for methionine synthesis, or of the endogenous synthesis of 5-MTHF (Figure I1). Hence, if methionine hepatic content is high, it is rapidly transformed to Hcy first thanks to the concerted action of MATIII and

GNMT, which are activated by methionine and SAMe, respectively, and then to AHCY, whose substrate is SAH. Furthermore, SAMe activates transsulfuration pathway through CBS and inhibits methionine recovery by inhibiting MTHFR, and consequently 5-MTHF synthesis, a compound that acts as an inhibitor of GNMT. Through these concerted actions SAMe levels are controlled, when SAMe levels are high Hcy is channelled through the trassulfuration pathway and when they are low Hcy is used to form methionine and regenerate SAMe[11]. The main enzyme that contributes to the maintenance of SAMe/SAH ratio is GNMT, which is controlled not only by SAMe levels but also by 5-MTHF. This way, GNMT removes excess of SAMe and avoids aberrant methylations[13].

The importance of SAMe to ensure the correct functioning of liver has been widely recognised. Given its participation in multiple cellular processes SAMe is undoubtedly a relevant molecule for life. However, a further comprehension of the diverse mechanisms in which it is involved is needed.

2.1.1. **Relevance of SAMe in liver function**

The fact that methionine metabolism is altered in patients with liver disease has been recognised since 1948, when Kinsell *et al.[14]* demonstrated that after a methionine load patients with liver injury exhibit a noticeable impairment in methionine clearance, thereby establishing a central role of liver in methionine metabolism[4]. Moreover, patients with cirrhosis and patients hospitalized for alcoholic hepatitis (some of them just with fibrosis) have diminished MAT1A expression and decreased SAMe biosynthesis, which can lead to reduced transmethylation and GSH synthesis[1]. Further evidence suggests that hepatic MAT activity is also impaired in Non-Alcoholic Steatohepatitis (NASH) patients, since after intravenous injection of trace amounts of L-[1-^{13}C]methionine and L-[C$_2$H$_3$]methionine a lower rate of methionine transmethylation was observed in NASH patients compared to control subjects[15]. Likewise, steatohepatitis, increased hepatocyte apoptosis, fibrosis, and HCC can be consequences

of *Gnmt* mutations in patients that present abnormally elevated plasma methionine and SAMe levels[4, 16]. Besides, a GNMT polymorphism (1289C>T) has been associated with HCC[17]. These observations point out that the liver needs the right amount of SAMe to provide an adequate supply of methyl groups, and that excess or lack of SAMe can induce liver injury[4].

SAMe treatment has proven to ameliorate liver injury in multiple animal models, including galactosamine-, acetaminophen-, alcohol-, thioacetamide-, endotoxemia-, CCl4-, bile duct ligation-, NASH-, and ischaemia-reperfusion-induced injury, protecting not only against acute injury but also reducing fibrosis in multiple experimental models[2]. In humans there is less evidence, even so, SAMe treatment has been shown to increase survival in patients with less advanced alcoholic liver cirrhosis[4]; there is also some evidence that recommends SAMe treatment for cholestasis in pregnancy and for chronic hepatitis C; and a clinical trial is examining the efficacy of SAMe in NASH patients[2]. The mechanisms involved in the hepatoprotective role of SAMe include, among others, its ability to rise GSH levels, inactivate CYP2E1, suppress TNF-α expression or protect against apoptosis[2].

Nevertheless, despite promising pre-clinical data confirming that SAMe depletion contributes to aggravate liver injury and supporting the hepatoprotective role of SAMe therapy, hitherto no confident enough clinical trials have been performed that establish a clinical utility for SAMe[18].

In the development of new therapies or in the search of new targets a better understanding of the mechanisms involved in the initiation and progression of liver injury caused by SAMe or methionine metabolism impairment would be very helpful. For that purpose knockout mice for the main enzymes involved in SAMe metabolism, MAT and GNMT, were generated[19, 20]. Both animal models present an impaired SAMe metabolism and both develop spontaneously different stages of Non-Alcoholic Fatty Liver Disease (NAFLD)[13, 19], a disease with an increasing incidence nowadays. Since these mice were created they have been subjected to many studies, being the present work one of them.

2.2. **Non-Alcoholic Fatty Liver Disease**

Accordingly to World Gastroenterology Organization (WGO), NAFLD is a disorder defined by excessive fat accumulation in the liver (> 5% of hepatocytes histologically) in the form of triglycerides (TG) (steatosis)[21] and in the absence of excessive alcohol consumption or other known liver pathologies[22]. A subgroup of NAFLD patients, in addition to excessive hepatic fat, evolve to necroinflammation with varying stages of fibrosis, a condition entitled as NASH and histologically indistinguishable from alcoholic steatohepatitis (ASH)[21, 23].

Historically, simple steatosis has been considered a benign condition, reversible, asymptomatic and with few clinical complications; its presence does not correlate with increase morbidity or mortality[21]. However, liver steatosis is the starting point for the progression to NASH, and this evolution increases the risks of cirrhosis, liver failure and hepatocarcinoma (HCC).

In addition to the spectrum of liver damage that NAFLD concept comprises, from simple steatosis to inflammation and fibrosis, cirrhosis, liver failure and HCC; there is now growing evidence that supports NAFLD as a multisystem disease that affects extra-hepatic organs and regulatory pathways[24]. For instance, the risk of type 2 diabetes mellitus (T2DM), cardiovascular disease (CVD), cardiac diseases and chronic kidney disease (CKD) increases with NAFLD[24].

2.2.1. **Epidemiology**

Nowadays NAFLD is a common cause of chronic liver disease worldwide, and is becoming a major public health problem mainly in western countries. The latest meta-analysis assessment on its prevalence estimates that 25% of the adult population in the world has NAFLD[25]. And that the overall prevalence of NASH, the first stage malignant progression of NAFLD, is between 1.5% and 6.45%[25]. The fluctuation in numbers is due to diagnosis reasons; NASH, in contrast to hepatic steatosis, cannot be assessed by

imaging techniques, and a liver biopsy is still needed for its right diagnosis[26]. NAFLD is also a problem for children and adolescents health, its prevalence among them has been estimated to be 7.6% in general population studies and 34.2% on obesity clinics based studies[27]. Significantly, the main burden of NAFLD is its association with comorbidities and with a higher overall mortality and liver-related mortality[28]. However, the incidence of cardiovascular and malignancy mortality among NAFLD patients seems to be higher than liver-related mortality[25, 29], finding that supports NAFLD as a multisystem disease.
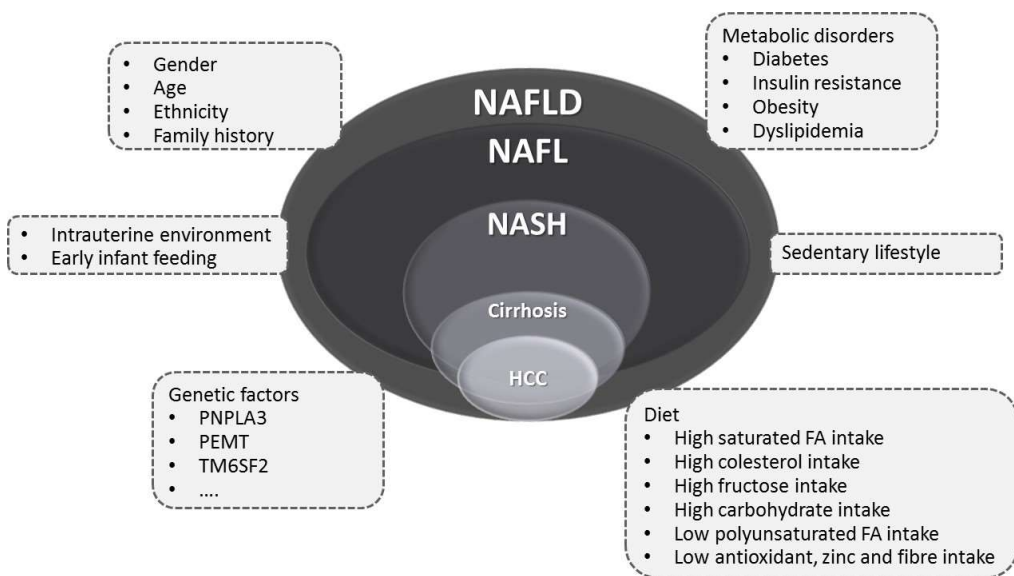
Figure I3. Factor*s associated with NAFLD development and progression.* Schematic representation of factors that influence NAFLD. NAFLD, non-alcoholic fatty liver; NAFL, non-alcoholic fatty liver; NASH, non-alcoholic steatohepatitis; HCC, hepatocarcinoma; FA, fatty acid; PNPLA3, patatin-like phospholipase domain-containing 3; PEMT, phosphatidylethanolamine methyltransferase; TM6SF2, transmembrane 6 superfamily member 2. Modified from Brunt *et al.*, 2015[26].

NAFLD usually appears with other metabolic disorders, such as T2DM and/or insulin resistance (IR), obesity, dyslipidemia, hypertriglyceridemia (HTG) and hypertension[25]. 40-80% of T2DM and 30-90% of obese patients have been reported to present fatty liver[26]. In consequence, NAFLD is increasingly recognized to be the hepatic manifestation of the metabolic syndrome[25]; which is a collection of complex conditions

that include central obesity, hypertension, hyperglycaemia, HTG and low HDL (high-density-lipoproteins), all risk factors for development of CVD, stroke and diabetes[30].
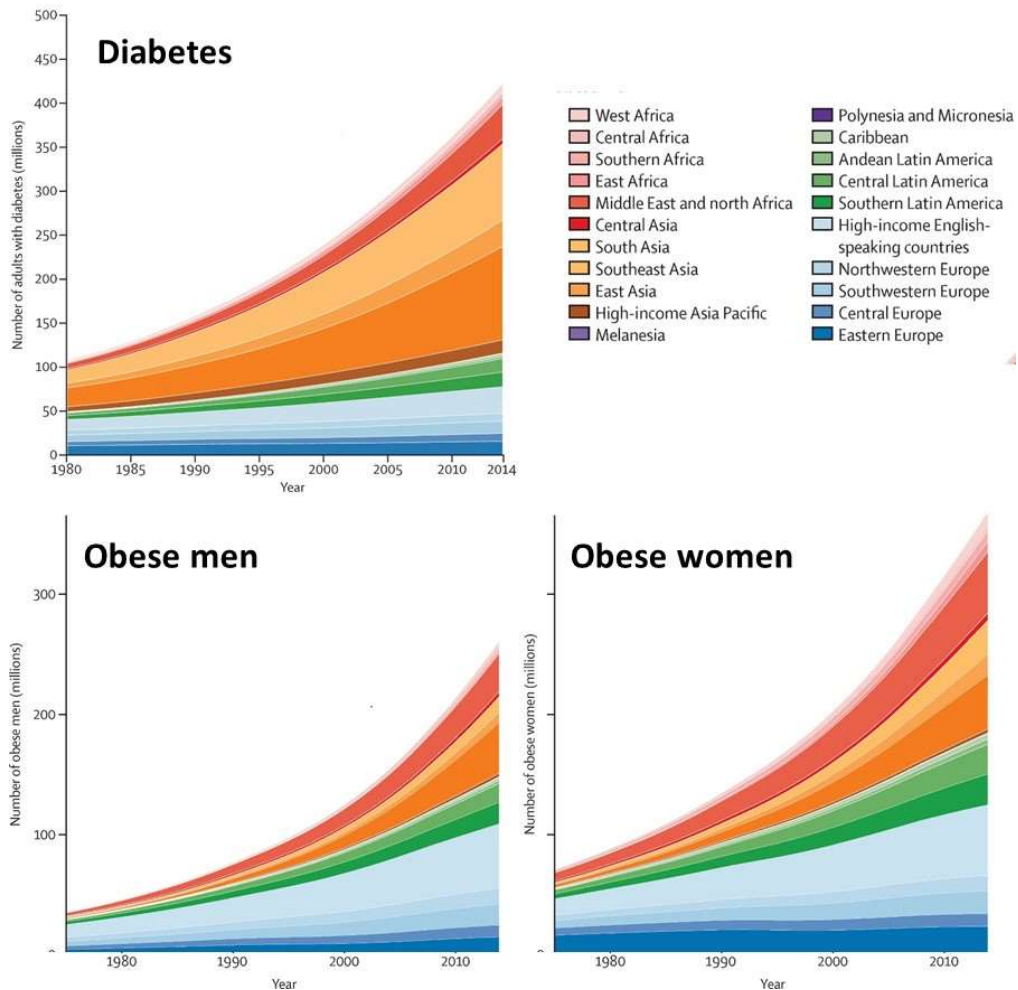
Figure I4. *Trends in the number of adults with diabetes and in the number of obese.* Stacked plots showing the number of people with diabetes in the world over the period 1980-2014 by region; and the number of obese people over the period 1974-2014 decomposed by sex and region[31, 32].

The factors that influence NAFLD development and progression are a current scope of study, to date many have been identified, as it can be observed in Figure I3. Many of the factors are environmental; however, there are also genetic factors that can contribute to NAFLD development. For instance, PEMT and some polymorphisms of PNPLA3 and TM6SF2 genes have been associated with progressive NAFLD[26]. Among all

the risk factors, obesity and T2DM may be the most studied. NAFLD prevalence has been on the increase the last decades along with obesity spread and diabetes (Figure I4), an increment that may be accounted for changes in dietary habits and the increase in sedentary lifestyle[31-33]. Obesity has been stablished as an independent risk factor for NAFLD development, a 3.5 fold increase in risk has been described[25, 34]. Although more than 50% and 82% of NAFLD and NASH patients, respectively, are obese, there are many non-obese people with NAFLD[25]. With respect to diabetes, it is also an independent risk factor for NAFLD progression to NASH, cirrhosis and mortality[25]. Although all the associations are strong, the mechanisms involved in the development and progression of NAFLD are still unclear and a current field of research.

2.2.2. **Pathophysiology**

NAFLD has been considered a "two-hit" process of pathogenesis for almost 20 years[35]. The "first hit" would be the accumulation of TG in hepatocytes, process that may increase the vulnerability of the liver to several possible "second hits" that in turn could lead to the hepatic damage characteristic of NASH: inflammation, fibrosis and cellular death[30]. However, it is now known that the "two hits" do not occur necessarily always in the same order or even sequentially[30]. Therefore the "two-hit" hypothesis is obsolete; it cannot explain the multiple molecular and metabolic changes that happen in NAFLD[36, 37]. And NAFLD pathogenesis may be better explained by a "multiple hit" hypothesis that considers multiple factors acting together to induce NAFLD. The hits can include nutritional factors, oxidative stress, endoplasmic reticulum (ER) stress, IR, hormones secreted by adipose tissue, gut-derived factors and genetic and epigenetic factors[30, 36, 37].

In any case, hepatic steatosis is a pre-requisite for NAFLD diagnosis[26]. Intrahepatic content of TG, under physiological conditions, responds to low steady-state concentrations due to a precise balance between: (1) acquisition by uptake of FFA from the plasma and by *de novo lipogenesis* (DNL) and (2) disposal of TG by FA oxidation and

by its export through VLDL[38] (Figure I5). Any imbalance between lipid acquisition and removal may lead to the NAFLD hallmark: TG accumulation in the cytoplasm of hepatocytes[37, 38].

Under a pathophysiological condition such as it might be obesity, an impairment of lipids acquisition may lead to hepatic steatosis, hence obesity-induced NAFLD. In obesity patients, the expansion of adipose tissue with its associated dysfunction may promote IR, which in turn may lead to a compromised ability of adipocytes for fat storage resulting in the release of FFA into the circulation. FFA become then available for its uptake by other organs such as the liver, where some transporters such as Fatty Acid Transport Protein 5 (FATP5) and Platelet Glycoprotein 4 (CD36), which are also upregulated in obesity, take up those circulating FFA[26] (Figure I5). FFA account for approximately 60% of hepatic TG in human subjects[39], consequently, adipose tissue derived FFA constitute a great source for NAFLD development. The remaining 40% TG that accumulates in fatty liver derives from dietary sugars and fats, and a 26% of it is attributable to DNL[39].

An imbalance in DNL plays a significant role in NAFLD pathogenesis. FA are synthesized in the hepatocytes from acetyl-CoA through a series of polymerization reactions catalysed by several enzymes. Acetyl-CoA carboxylase (ACC) catalyses the production of malonyl-CoA from acetyl-CoA, an irreversible step followed by Fatty Acid Synthase (FASN) activity, which leads to the formation of palmitic acid. Palmitic acid can then suffer elongation and desaturation reactions catalysed by long chain fatty acid elongase 6 (ELOVL6) and stearoyl-CoA desaturase 1 (SCD1) enzymes, respectively. The formation of TGs requires further enzymatic reactions catalysed by: (1) Glycerol-3-phosphate acyltransferase (GPAT), leads the esterification of the FA with glycerol-3-phosphate to form lysophosphatidic acid, a concerted action of (2) 1-acylglycerol-3-phosphate acyltransferase (AGPAT) and (3) lipin 1 that leads to the synthesis of diacylglycerols (DG) which are further acylated to form TG through (4) diacylglycerol O-acyltransferase (DGAT) activity. The mentioned enzymes, hence, lipogenesis regulation is mainly controlled at the transcriptional level by the expression and activation of

nuclear transcription factors such as, peroxisome proliferator-activated receptors (PPARs), liver X receptor α (LXRα), farnesoid x receptor (FXR), sterol regulatory element binding protein 1c (SREBP1c) and carbohydrate responsive element binding protein (ChREBP)[38, 40] (Figure I5). Insulin and glucose upregulate SREBP1c and ChREBP, respectively, thus, in cases of obesity, IR and diabetes, DNL might be impaired contributing to NAFLD development[26].

The balance of hepatic TGs is also controlled by FA disposal through mitochondrial β-oxidation, a crucial process for ATP and ketone bodies (KB) production. Acetyl-CoA generated from FA in the mitochondrial matrix through β-oxidation cycle enters the tricarboxylic acid (TCA) cycle, where it is further oxidized and NADH and $FADH_2$ are generated for ATP synthesis by the electron transport chain. If acetyl-CoA production exceeds the capacity of TCA cycle, then two molecules of acetyl-CoA condense to form acetoacetate, which can be converted to β-hydroxybutyrate or spontaneously turn into acetone, molecules known as KB that provide a source of energy for extrahepatic tissues[38, 40] (Figure I5). Contribution of impaired β-oxidation to NAFLD development is controversial given that in patients with NAFLD both situations, increased and decreased β-oxidation, have been found[38]. However, NAFLD has been associated with hepatic mitochondrial structural and functional abnormalities that could affect hepatic energy production but not FA oxidation, what could represent an adaptive uncoupling of FA oxidation and ATP production[40].
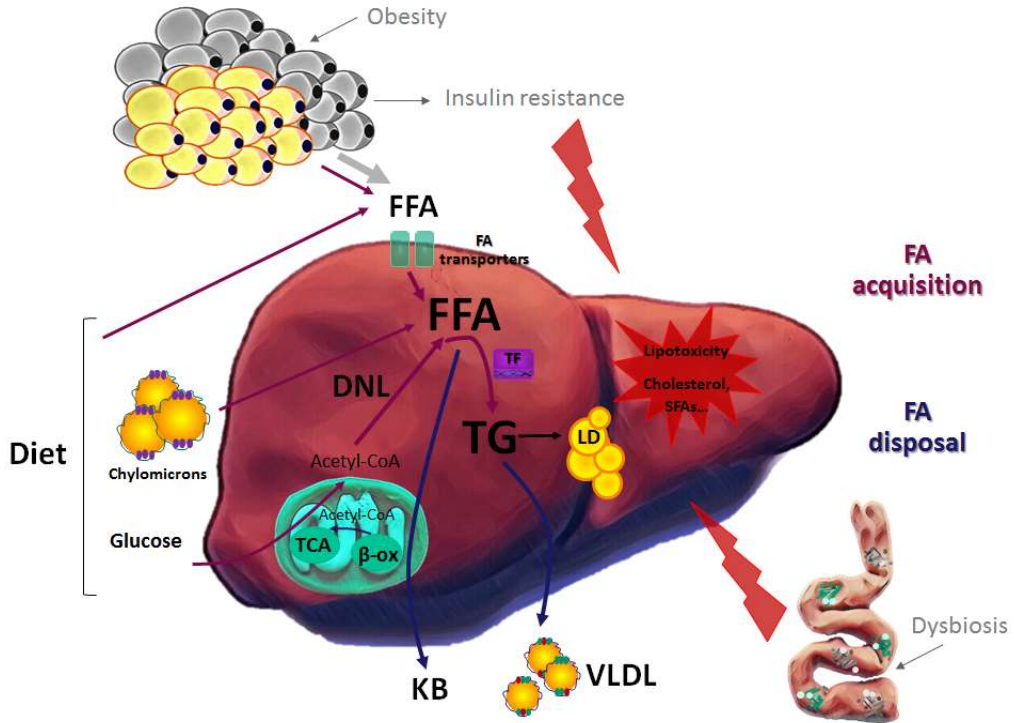
Figure I5. *Potentially dysregulated mechanisms for NAFLD development.* Schematic representation of fatty acids (FA) metabolism in the liver and other factors that can lead NAFLD development. FFA, free fatty acids; DNL, *de novo lipogenesis*; TF, Transcription factors; TG, Triglycerides; LD, lipid droplets; SFAs, long-chain saturated fatty acids; TCA, tricarboxylic acid cycle; β-ox, β-oxidation; KB, ketone bodies; VLDL, very low-density lipoproteins.

FA that are not oxidized are esterified to TGs, which are either stored within the hepatocytes in lipid droplets (LD) (further described in section 2.2.2.1) or incorporated into VLDL to be secreted into the blood, thus mobilising fat from liver[40, 41] (Figure I5). The mechanisms by which hepatocytes decide whether to store or to secrete TGs are not entirely clear, nevertheless, the origin of FA may be an important factor[40]. What is more, VLDL secretion rate appears to depend not only on the availability of hepatic TGs, but also on the overall capacity for VLDL assembly (process further described in section 2.3.1.)[38]. A diminished secretion of VLDL is usually associated with hepatosteatosis when it is caused by genetic factors or externally induced. However, surprisingly, studies with

NAFLD patients have demonstrated that hepatic steatosis results in oversecretion of VLDL-TG, although not sufficient to prevent or reverse NAFLD[40].

Hepatic steatosis is the hallmark for NAFLD diagnosis, however, for its progression to NASH, to the presence of hepatocyte injury, other mechanisms besides the above mentioned might take place in parallel or progressively[30, 37]. For instance, liver lipotoxicity, the accumulation of certain lipids including free cholesterol and long-chain saturated fatty acids (SFAs)[30], may trigger the development of mitochondrial dysfunction, oxidative stress, ER stress, or even the inflammatory response leading to the whole spectrum of NAFLD pathologies[30, 36, 37] (Figure I5).

What is more, given that the liver is at the intersection of the whole body energy metabolism, the cross-talk between the liver and other systemic organs, such as the adipose tissue or the gut should be tightly regulated in order to maintain energy homeostasis. Otherwise, mechanisms leading to NAFLD development or progression may be triggered. For example, obesity triggers adipose tissue inflammation, hence inducing the secretion of cytokines and chemokines that may affect IR and consequently liver lipid metabolism[30]. In relation with the gut, interactions between the intestine, mainly through its microbiota, and the liver are emerging as important determinants for NAFLD pathogenesis. Intestinal microbiota of NAFLD patients differs from that of healthy individuals. And the intestinal dysbiosis can alter dietary choline metabolism and bile acids pools, weaken the intestinal barrier or enable the translocation of bacteria or bacterial products, such as endotoxin, alcohol or short-chain FA into portal circulation; alterations that can affect hepatic lipid homeostasis and NAFLD progression[26, 30] (Figure I5).

Taking everything into account NAFLD can now be considered as a complex multifactorial disease. Its development requires the concurrence of various factors and the consequent activation of several cellular responses and molecular pathways that point out the liver as the "principal actor" and some other organs as affecting and affected "bit players"[24].

2.2.2.1. **Lipid Droplets, Perilipin2 and Non-Alcoholic Fatty Liver Disease**

A key feature of NAFLD is TG accumulation in the form of LD in hepatocytes[42] and the increased association of perilipin and non-perilipin proteins to LD[43]. Of the perilipins, Perilipin2 (PLIN2, formerly known as adipophilin -ADFP- or adipose differentiation-related protein –ADRP-) is the most upregulated in the livers of rodents and humans with NAFLD[43].

LD are cellular organelles lipid-filled and balloonlike that are present in basically all eukaryotic cells when they take in more than their fair share of lipids[44]. Lipids in LD organised in a core of neutral lipids (primarily TGs and cholesterol esters) delimited by a membrane monolayer of phospholipids[42] . They have long been considered to be inert but they are now thought to be dynamic structures at the hub of lipid and energy metabolism[42] by means of the LD-specific associated proteins[43]. Among those LD-coating proteins we found PLIN2, a protein that belongs to PAT-domain or perilipins proteins family, and that is the best characterised in fatty liver diseases[45]. Perilipins are the proteins in charge for maintaining the TG content in LD of hepatocytes and are vital in the overall lipid turnover of LD and therefore in the pathology of NAFLD[46].

PLIN2 has been localised not only on the surface but also inside the core of LD[44] and in hepatocytes PLIN2 not only plays and important role in lipid storage and in the biogenesis of LD but it also participates in the control of VLDL secretion[46]. PLIN2 promotes TG accumulation, inhibits fatty acid oxidation, and impairs glucose tolerance[43]. The presence of PLIN2 on LDs is greatly influenced by the lipid content in the cell, if FA synthesis is reduced this protein is degraded via proteasome[46].

PLIN2 ablation in mice results in a 60% reduction in hepatic TG and, what is more, it protects against liver steatosis when animals are fed with a high fat diet (HFD), a diet capable of inducing NAFLD[47]. And if PLIN2-KO mice are bred with obesity-prone leptin deficient mice, they have reduced steatosis despite some compensation with other

perilipins, increased VLDL secretion and improved insulin sensitivity[48]. In contrast, overexpression of PLIN2 is associated with LD pools expansion and with increased cellular TG mass even when the cells are cultured in delipidated serum, suggesting that increased expression of PLIN2 by itself is capable of inducing lipid accumulation in cells[45]. Besides, it has been shown that during liver injury, PLIN2 expression is significantly increased and found prominently on the LD surface of hepatocytes[46]. Accordingly, PLIN2 is upregulated in human NAFLD and appears to be a reliable marker of hepatic LDs[43]. Thus, expression of PLIN2 in the surface of LD in the hepatocytes is a pathophysiological change in human fatty liver disease[45]. All these findings emphasise the relevance of PLIN2 in fatty liver development.

2.2.2.2. **Extrahepatic complications of Non-alcoholic Fatty Liver Disease**

As it has been stated before, NAFLD is a major cause of liver disease worldwide, and its association with higher overall mortality is mainly attributable to CVD and malignancy[25, 28, 29]. These notions lead to the idea that NAFLD could be an important risk factor or even a driver of extrahepatic diseases[23].

NAFLD is a pro-inflammatory condition characterized by the coexistence of pro-inflammatory mediators, oxidative stress, IR and lipotoxicity in which a pathogenic crosstalk between the liver and the adipose tissue may take place. Liver /adipose tissue axis mediators include hormonal/cytokine signals from both sides; a network that if dysregulated promotes the development of atherosclerosis, T2DM and malignancy[23]. Consequently, that pathogenic crosstalk has been pointed out as the likely key factor behind the induction of systemic abnormalities during NAFLD development[23].

So far, NAFLD is a well stablished independent risk factor for CVD and T2DM[23, 24]. NAFLD and CVD present some common risk factors, such as those related with the metabolic syndrome, dyslipidemias or visceral adiposity, for instance[49]; and cumulative

studies show that NAFLD diagnosed patients also present a diverse number of subclinical markers of CVD[23]. The case of T2DM and NAFLD relationship is complex, although ostensibly, there is a lineal relationship between NAFLD and T2DM, fatty liver patients are at risk of developing T2DM, and the other way round T2DM patients are at risk of developing NAFLD[24].

CKD and colorectal cancer have also received attention as extrahepatic consequences of NAFLD. Several clinical studies stablish NAFLD as a risk factor for their development[23, 24]. And emerging evidence suggests that NAFLD is also linked to obstructive sleep apnea syndrome, osteoporosis, psoriasis and several endocrinopathies (e.g. polycystic ovarian syndrome, hypothyroidism or hypercortisolemia)[23, 24].

Because the clinical burden of NAFLD is not restricted to liver-related morbidity, but it is in fact related to its independent association with the abovementioned diseases, prevention and treatment approaches should not only reduce the risk of progressive liver disease but also have an impact on extrahepatic and overall prognosis[23].

2.2.3. **Treatment**

Nowadays NAFLD management is accomplished through the modulation of lifestyle, lowering energy intake and doing regular exercise[26]. Dietary interventions that achieve weight loss have been proven to improve steatosis, inflammation and hepatocyte injury[26, 50]. Exercise alone, with minimal or no weight loss, can also reduce hepatic fat content[50]. However, there is no approved drug for the treatment of NASH and the multiple pathways described and being described to be involved in NAFLD pathogenesis suppose an obstacle for its development[50].

All things considered, NAFLD is a complex disease, its development and progression can be attributed to subtle individual variations, including host genetic

factors and environmental factors that interact to produce the disease phenotype and determine its progression[26]. Therefore, NAFLD may appear as a constellation of various phenotypes that will require patient-tailored treatment, depending on the underlying cause[26].

2.2.4. **Animal models of NAFLD**

In order to study the pathogenesis of NAFLD, and also for examining the therapeutic effects of diverse agents, different animal models have been and are nowadays being designed and investigated. Animal models for NAFLD development analysis include both genetically modified animals in which NAFLD appears spontaneously and diet- or agent-induced NAFLD establishment. Different genetic or dietary approaches produce different severities along NAFLD spectrum and likely, each approach works by distinctive mechanisms.

In the case of this study our interest lies mainly in the modifications of methionine and SAMe metabolism that can induce the development of NAFLD and the side effect of a high fat diet (HFD) on those cases.

2.2.4.1. **Methyl groups-deficient diet-induced NAFLD**

The deficiency in methyl groups is usually induced by a methionine-choline-deficient diet (MCD). MCD diet has been extensively used for the induction of NAFLD/NASH, it rapidly induces TG accumulation in the liver of mice during the first week of diet, after which it maintains[51]. Choline deficient diet (CDD) and methionine deficient diet (MDD), each one alone, are also capable of inducing the onset of hepatic steatosis. Nevertheless TG accumulation is more noticeable in CDD case, while in MDD case it is less marked[51]. SAMe metabolism is altered in the three mentioned diets[51, 52], although only MCD and MDD diets are capable of inducing a decrease in hepatic SAMe

levels[51]. This further supports the relevance of this molecule and of methyl-groups metabolism in liver correct functioning.

The existing experimental studies indicate that methyl donors shortage (choline and methionine) is causally related to lipid accumulation in the liver, and that the involvement of PC is probable[53]. When there is a lack of choline/methionine in rat hepatocytes, the biosynthesis of PC via PEMT and CDP-choline pathways is diminished what causes a decreased secretion of VLDL. This disturbance is corrected when either choline or methionine are added to the medium as sources of methyl groups[54]. Therefore, there seems to be a close relationship between methyl donors, PC biosynthesis and VLDL secretion, relationship that if impaired may lead to NAFLD development.

2.2.4.2. S-Adenosylmethionine chronic deficiency- or excess-induced NAFLD

2.2.4.2.1. Methionine Adenosyltransferase 1A knockout mice

The relevance of Methionine Adenosyltransferase 1A (MAT1A) knockout (KO) mouse model to human liver disease lies in the fact that *Mat1a* expression is highly reduced in the majority of patients with liver cirrhosis[55].

MAT1A-KO mice were generated with the aim of elucidating the role of *Mat1a* gene in hepatic growth and dedifferentiation in 2001 by Lu S.C. and Mato J.M. groups[19]. They were developed by recombination and directed mutagenesis of *Mat1a* on the genetic base of C56BL/6 mouse strain.

The lack of MAT1A, enzyme responsible for SAMe synthesis, causes hypermethioninemia and a reduction of 74% in SAMe content in liver. Hepatic glutathione levels also fall, and two other metabolites of methionine metabolism, SAH

and MTA, are normal in KO mice livers. Besides, DNA methylation levels in liver are not affected because of MAT1A absence[19].

The MAT1A-KO mouse model has provided some insight into the consequences of chronic SAMe deficiency and altered signalling pathways that may lead to hepatic degeneration[2].

It has been stated that MAT1A-KO mice are more prone to liver injury[19]. These mice are more predisposed to develop fatty liver induced by CDD at 3 months-of-age. And at 8 months they develop spontaneously NASH that can progress to hepatocarcinoma when they get older, by 18 months[56]. MAT1A absence produces no changes in liver histology when 3 months old mice are fed a normal diet. However, if fed a CDD diet for 6 days KO mice develop severe macrovesicular steatosis in the liver while WT animals present little histologic change or only mild steatosis (Figure I6)[19]. At 8 months of age WT counterparts' livers remained normal histologically, but the livers of the KO animals fed a normal diet showed macrovesicular steatosis that involved 25-50% of hepatocytes and mononuclear cell infiltration, mainly in the periportal areas (Figure I7)[19].
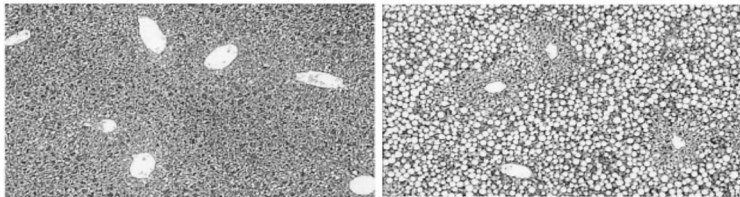
FigureI6. *Effect of CDD diet on liver histology in MAT1A-KO mice*[19]*.* Representative Trichrome-stained sections of liver samples of 3-month-old (left) WT and (right) MAT1A-KO mice fed a CDD diet for 6 days (×100).
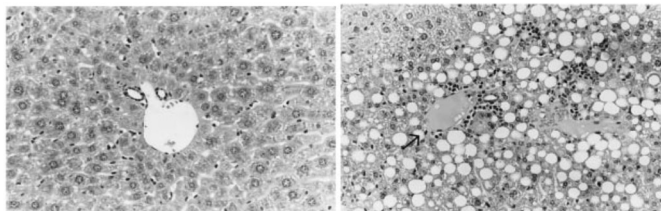
Figure I7. *Liver histology from 8-month-old MAT1A-KO mice fed a normal diet*[19]*.* (Left) WT. (Right) MAT1A-KO mouse. Hematoxylin and eosin × 148, n=3.

To date, MAT1A-KO mouse model has proven to be adequate for the study of NASH human condition. A comparative study of gene expression profiling has identified a gene-pathway associated with NASH in both NASH patients and MAT1A-KO mice that can distinguish between healthy individuals and WT animals, respectively[57].

The involvement of *Mat1a* gene or SAMe deficiency in the development of different liver injuries is a theme of study. So far, several dysfunctional mechanisms that may interfere in disease development have been elucidated. MAT1A-KO mice present increased oxidative stress and genomic instability, dysregulated ERK and LKB1/AMPK signaling, cancer stem cell expansion, decreased prohibitin 1 expression and abnormal lipid homeostasis[2].

The abnormal lipid homeostasis in MAT1A-KO mice is a topic of interest for our research group. Our group have found that MAT1A-deficient mice show impaired assembly and secretion of VLDL, what could contribute to steatosis development in these animals. Specifically, a decrease in TG stores mobilization, in TG secretion and in PC synthesis via PEMT were found in MAT1A-KO mice[58]. A decreased PC liver content can lead to the activation of SREBP-1, consequently increasing lipogenesis[59]. It has also recently been shown that a altered FA oxidation in the mitochondria might be also contributing to fatty liver in MAT1A-KO mice[60]. Besides, ApoB availability is increased leading to changes in VLDL features, which are smaller and TG-poorer than those secreted by WT animals[58]. Accordingly with what has been described, the secretion of this type of particles could induce alterations in their plasmatic metabolization. In any case, further investigation is needed to understand the mechanism by which SAMe alters lipid homeostasis.

2.2.4.2.2. Glycine N-Methyltransferase knockout mice

Gycine N-Methyltransferase (GNMT) KO mouse model is relevant for the study of liver diseases. It has been demonstrated that GNMT expression is reduced or absent in HCC[61] and in the livers of patients at risk of developing HCC, such as hepatitis C virus-

and alcohol-induced cirrhosis patients[55]. Moreover, GNMT has been proposed to be a tumour-susceptibility gene for liver cancer[17]. Finally, the finding of several children with mutations in GNMT and presenting mild to moderate liver disease accompanied with elevated serum aminotransferases[16, 62] has provided further evidence suggesting that GNMT defects can lead to liver disease.

GNMT-KO mouse was created with the objective of elucidating the role of *Gnmt* gene in liver disease. The homozygous GNMT-KO was generated by homologous recombination on the genetic base of C56BL/6 mouse strain in 2006 by Luka and Mato research groups[20].

The absence of GNMT, enzyme accountable for SAMe catabolism, increases methionine as well as SAMe levels both in plasma and in liver; SAMe experiences a 35-fold rise. Consequently, since hepatic SAH levels fall, hepatic SAMe/SAH ratio increases about 100-fold with respect to WT animals[20]. GNMT deficiency in humans presents with very high levels of methionine and SAMe in plasma, and normal levels of homocysteine[16]. Therefore, GNMT-KO mice resemble the human condition in terms of SAMe metabolism. The findings that both methionine and SAMe are elevated when GNMT correct functioning fails indicate that the hepatic reduction in total transmethylation flux cannot be compensated by other MTs that are abundant in the liver, such as GAMT or PEMT, situation that leads to the accumulation of hepatic SAMe and increases the transport of this molecule to the blood. Accordingly, disruption of PEMT or GAMT in mice has little or no effect on hepatic SAMe content[63]. These results demonstrate that hepatic SAMe content is regulated by the combined action of the enzymes MAT and GNMT.

With respect to liver injury, GNMT absence in mice induces the development of different stages of NAFLD, by 3-months-of-age they present steatosis and fibrosis, signs that worsen by 8-months when hepatocarcinoma (HCC) is also found in the liver of these mice (Figure I8)[13].
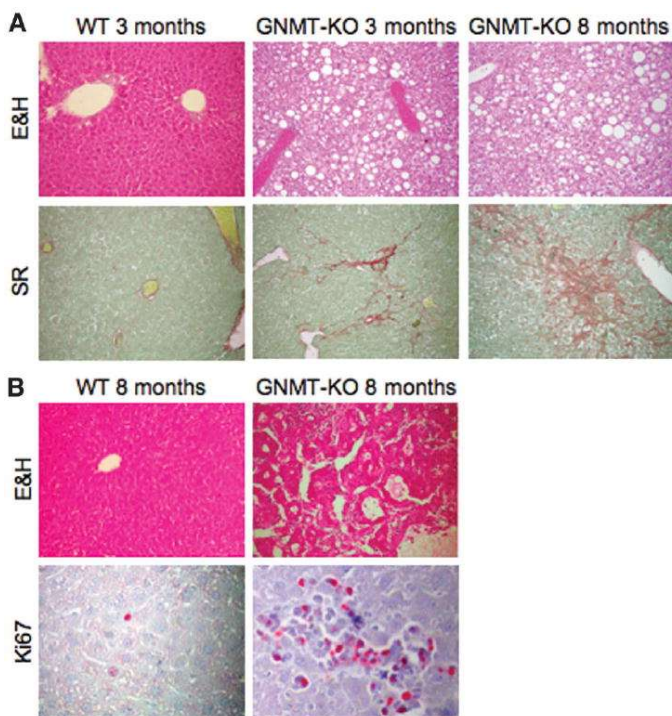
Figure I8. *GNMT absence induces steatosis, fibrosis and hepatocarcinoma[13].* (A) 3-months-old WT and GNMT-KO and 8-months-old KO liver mice (E&H) eosin and hematoxylin staining (first row) and (SR) Syrius red staining (second row) for collagen deposits. (B) 3-months-old WT and GNMT-KO liver mice E&H staining (first row) and Ki67 (red spots) staining (second row). Original magnification X40.

GNMT-KO mice not only present an impaired lipid metabolism as a consequence of altered expression of several lipid metabolism-related genes, high SAMe levels also induce DNA and histone hypermethylation, what induces the silencing of several tumour suppressor genes leading in the end to abnormal growth and malignant transformation[2]. The treatment of GNMT-KO mice with nicotinamide, a substrate for nicotinamide N-methyltransferase (NNMT, an enzyme expressed in the liver) that uses SAMe, leads to the reduction of SAMe hepatic levels normalising lipid metabolism and DNA methylation demonstrating that SAMe excess is responsible for the mentioned phenotype in GNMT deficient mice[2, 64].

In any case, GNMT-KO mice need to be further investigated to unravel the many mechanisms in which the excess of SAMe may be exerting an effect; for instance, to discover the machinery behind lipid accumulation in the liver.

2.2.4.3. **High Fat Diet-induced NAFLD**

NAFLD is more prevalent in patients with obesity and diabetes[22], and epidemiological studies propose diets rich in fat as a risk factor for both, obesity and insulin resistance[65]. Provided that fat is the most energy dense macronutrient in human nutrition, it is not surprising that consumed in excess increases the probability of obesity. Accordingly, high fat diets (HFD), in which the majority of caloric intake (45-75%) is from fat, and nowadays HFD supplemented with fructose, trans-fats or cholesterol, have been pointed out as useful tools to induce obesity, insulin resistance and the different stages of NAFLD in animal models[66].

An increased dietary supply of fat to the liver may promote steatosis by increasing hepatic lipid uptake or *de novo* lipogenesis[67]. In accordance, expression of SREBP-1c, SREBP-2 and Stearoyl-CoA desaturase genes have shown to be increased in HFD-subjected liver[63, 68] and so has been CD36 protein[69]. HFDs are sufficient to induce obesity, insulin resistance, dyslipidemia, hepatic steatosis, oxidative stress, mild fibrosis and increased expression of proinflammatory cytokines in the white adipose tissue of mice and rats[63, 70, 71]. However, the extension of the pathophysiological outcome of HFDs is variable. The results obtained with these diets may depend on animal/rodent species and strain (genetic background), the fat content in the diet, the composition of the dietary fat, and the duration of the treatment[63, 70].

HFD models, in general, do not present liver injuries as severe as those found in MCD models and the feeding times required to achieve more severe damage are significantly longer in the HFD case as compared to MCD[66, 72]. Hence, the mechanims involved in liver injury are different. Nevertheless, the MCD causes weight lose[51], which is not commonly observed in NAFLD patients. Besides, HFD is a widely used strategy to induce steatosis and NAFLD in animal models since it has been said that these diets more closely resemble the pathological and molecular alterations found in humans with NAFLD[72]. What is more, HFDs are being combined with genetic animal models of NAFLD,

so the combination may better help to understand the intricate processes that lead to NAFLD onset and progression.

2.3. **Very Low-Density Lipoproteins**

Liver plays a central role in the whole body energy homeostasis by means of different mechanisms, one of which is the secretion of lipoproteins, a process that under physiological conditions permits an adequate interchange of lipids between the liver and the rest of the body.

Lipoproteins are soluble complexes of proteins and lipids that transport lipids in the circulation of all vertebrates. They classify into chylomicrons, very low-density (VLDL), intermediate-density (IDL), low-density (LDL) and high-density (HDL) lipoproteins, accordingly to their relative content of proteins and lipids that determines the density of the lipoprotein class. Their diameters inversely correlate with their density, being chylomicrons the larger lipoproteins and HDL the smallest (see Figure I9). Lipoproteins consist of a central fluid spherical droplet of neutral lipids (TG and cholesteryl esters) surrounded by a surface lipid monolayer containing phospholipids, unesterified cholesterol and the corresponding proteins. The proteins (apolipoproteins –apo-) are critical regulators of lipid transport and play a role in lipoprotein assembly, lipid transport and lipid metabolism by mediating interactions with receptors, enzymes and lipid transport proteins[73].

VLDLs are synthesized in the liver for the export of endogenous lipids to peripheral tissues through circulation. VLDLs are secreted enriched in TG along with some cholesteryl esters and with one apolipoprotein B, ApoB-100 in humans and in the case of mice ApoB-100 or ApoB-48. The main constituent of its lipid monolayer is PC, but they also contain PE and other minority phospholipids. The hydrophilic layer is also composed of other apoproteins such as apolipoprotein E (ApoE), or the different isoforms of apolipoprotein C, CI, CII and CIII (ApoCI, ApoCII and ApoCIII).
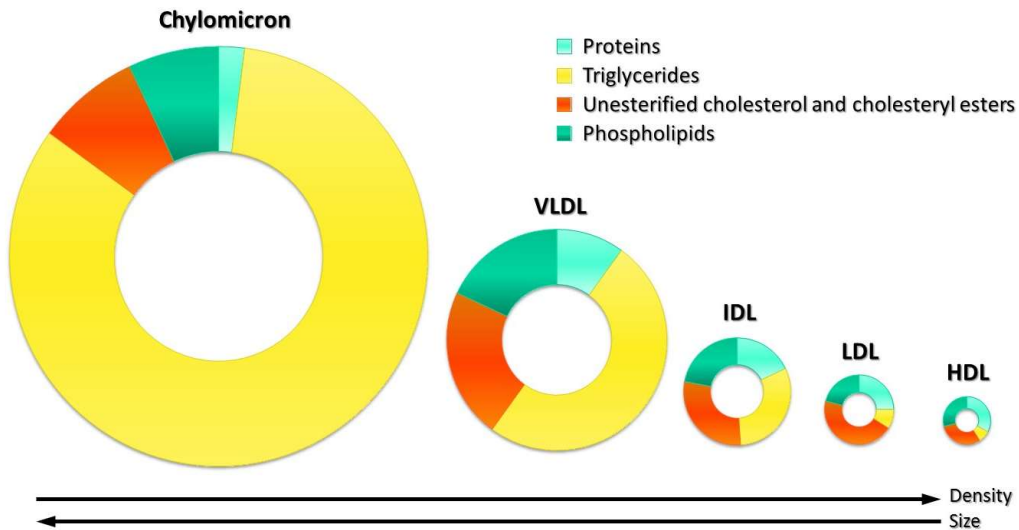
Figure I9. *Schematic representation of lipoprotein size, density and composition.*

Under physiological conditions, VLDL-TG secretion rate is well matched to the supply of hepatic TGs for the metabolic demands of oxidative tissues, with the excess TGs directed toward adipose tissue for storage. The production of VLDLs needs to be synchronized with their secretion, otherwise, abnormalities in their production may occur that may impair lipids recruitment for VLDL assembly and lead to adverse consequences such as hepatic steatosis[74, 75]. Findings regarding VLDL secretion in NAFLD patients are controversial, some studies show that VLDL-TG secretion is increased[76], whereas other report that it is decreased[75]. And it has also been shown that alterations in the hepatic uptake of lipoproteins can lead to hepatoesteatosis as well[77].

Plasma levels of VLDL are defined by the steady-state resulting from the rate of hepatic secretion and the rate of removal from plasma, an imbalance between those processes will lead to dyslipidemia. For instance, it has been shown that changes in the size of VLDL particles secreted by the liver result in significant disturbances of plasma lipoprotein metabolism[78]. Dyslipidemia is associated with increased risk of cardiovascular disease[79], one of the extrahepatic complications of NAFLD[23].

The abovementioned clinical scenarios caused by abnormal assembly and secretion and/or catabolism of VLDLs highlight the importance of these lipoproteins both in liver lipid metabolism and in the whole body lipid homeostasis.

2.3.1. **VLDL assembly and secretion**

The biogenesis of VLDLs and their secretion into bloodstream by the liver is a complex but highly organised process that plays a central role in overall lipid homeostasis. VLDL biosynthesis initiates in the ER and is regulated by a variety of factors that must guarantee the release of adequate amounts of TGs from the liver. The elements that can affect VLDL production include lipids and some proteins and enzymatic activities[80].

The initiation of VLDL assembly depends mainly on the supply of hepatic triglycerides and on the activity of microsomal triglyceride transfer protein (MTP), if these are deficient, ApoB, the other critical factor, will be degraded and little assembly of secretion-competent VLDL will take place.

The biogenesis of VLDL is accomplished in a multistep process for which the precise molecular mechanisms and subcellular localization for the addition of lipids are still an active area of research[81]. VLDL assembly starts with ApoB translation from its mRNA by ribosomes while crossing the ER membrane and entering its lumen[82]. In a first step, during the translocation process ApoB is partially lipidated thanks to MTP activity, giving rise to a lipid-poor primordial VLDL particle[83]. Lipid transfer to ApoB by MTP requires a physical interaction between both proteins[84]; the association prevents ApoB degradation, facilitates its translocation to the ER lumen and along with the participation of several chaperone proteins promotes ApoB proper folding[82, 85, 86]. In a second step of VLDL formation, the primordial, nascent VLDL particles are further lipidated; whether this process takes place in the ER or in the Golgi apparatus or how does it occur, fusion with LDs, involving a pool of MTP…, is incompletely defined[82, 83]. Hitherto, it is known that before the mature particle is secreted into the plasma, VLDLs

transit the Golgi apparatus, they depart the ER in COPII-coated specialized vesicles termed VLDL transport vesicles (VTV); VTVs are meant to fuse with *cis*-Golgi and deliver their VLDL cargo to the Golgi lumen[83]. Once in Golgi apparatus VLDL are additionally processed and ApoB gets further glycosylated[83], this last process could be considered as a third step in the process of assembly and secretion of VLDL (see Figure I11).

Therefore, VLDL assembly and secretion is an intricate process that can be challenged, hence regulated, at many different stages, such as ApoB protein or MTP activity regulation, lipids supply or other apoproteins participation.

ApoB is a glycoprotein essential for VLDL production, in fact, hepatic VLDL secretion rates are largely controlled by rates of ApoB degradation[82]. There are two isoforms of this apolipoprotein: ApoB-100 and ApoB-48, a truncated form of ApoB that matches the N-terminal 48% end of ApoB-100 and is produced by an mRNA editing mechanism[87]. *Apob* gene expression, in general, is viewed as constitutive and ApoB regulation by metabolic factors is mainly post-translational[81]. However, there is evidence of translational regulation by insulin and the possibility that MTP inhibition slows down *Apob* translation[81]. Hitherto, the molecular mechanisms by which *Apob* mRNA translation is regulated remain incompletely understood. Another target for ApoB regulation and consequently for VLDL secretion concerns *Apob* mRNA stability; mRNA stability can be modulated through the binding of some proteins, such as the ubiquitously expressed Hu-antigen R (HuR) protein, to AU-rich elements (ARE). *Apob* mRNA contains ARE sequences and has been shown to bind to HuR protein[88]. As alluded to above, the intracellular degradation of ApoB further regulates VLDL assembly and secretion, if the availability of lipids, including TGs, phospholipids, cholesterol and cholesteryl esters, at the site of ApoB synthesis in the ER is not adequate, ApoB initial lipidation fails and the apolipoprotein is directed to proteasome-mediated ER-associated degradation (ERAD) pathway[81, 82]. If lipidation step is successful but VLDL maturation is interrupted in a later step, another regulatory control degrades ApoB by a post-ER presecretory proteolytic process (PERPP). This process depends on autophagy

and it is increased by insulin, fish oil fatty acids, such as Omega-3, and by ER stress[82] (see Figure I10).
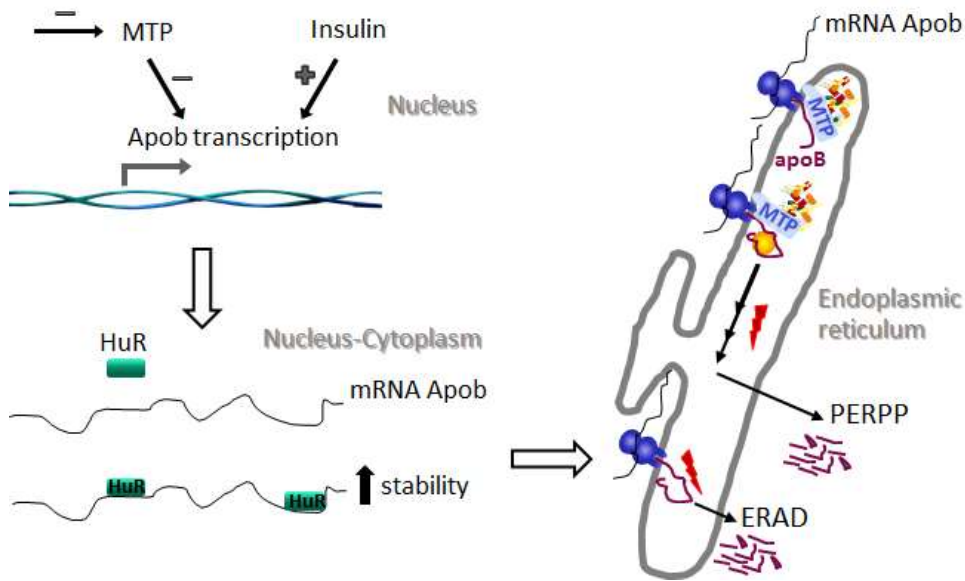
Figure I10. *ApoB regulation.* Apoprotein ApoB regulation from transcription to traduction. MTP, microsomal triglyceride transfer protein; HuR, PERPP, post-ER presecretory proteolytic process; ERAD, proteasome-mediated ER-associated degradation.

MTP lipid transfer activity is another major determinant for VLDL secretion[86]. MTP is shown to have 3 functional domains: an ApoB-binding domain, a lipid transfer domain and a membrane association domain[86] and it localizes in ER and in Golgi apparatus[89]. For MTP to be able to acquire and transfer lipids to the site of VLDL assembly within the ER lipids must be available in its vicinity[80]. Then, MTP can transfer both neutral and polar lipids to the developing VLDL particle, however, its phospholipid transfer domain can alone generate VLDL particles[90]. If MTP is chemically inhibited VLDL assembly fails. Furthermore, MTP activity requirement is more pronounced for ApoB-100 than for ApoB-48, consequently MTP inhibition effectively diminishes ApoB-100 and TG secretion while it has little effect on lipid-poor ApoB-48 secretion[80, 91]. TG biosynthesis is not affected by MTP action of recruitment of TG from ER/Golgi membranes[80], what is more, MTP activity is required for TG accumulation in the microsomal lumen[91].

Altogether, different studies indicate that alterations in MTP activity have a direct effect on VLDL production[80].

As repeatedly mentioned, lipid availability together with ApoB and MTP is the other main factor that regulates VLDL assembly and secretion. Lipid components of VLDL are mainly synthesized by ER-associated enzymes, impairment in lipids disposal or a malfunction of the enzymes could lead to an inadequate secretion of VLDL particles.

TGs incorporated into VLDL particles are preferentially synthesized within liver from plasma FA, which either come from adipose tissue or the diet, or from FA *de novo* synthesized by hepatocytes. Besides, most of VLDL-TG secreted (60–70%) is derived from the hydrolysis of TG stored in cytosolic LD followed by re-esterification[78, 92, 93]; hence, the mobilization of lipids from LDs towards the ER represents a potentially regulated step in VLDL assembly and secretion[93-95]. For VLDL assembly, TGs stored in cytosolic LDs are hydrolysed essentially by two different lipases: TG hydrolase (TGH) and arylacetamide deacetylase (AADA), then the DGs generated are re-esterified on the luminal side of ER with either the released FAs or with others thanks to the action of a diglyceride acyl-transferase (DGAT)[78] (Figure I11). Thus an impaired activity of any of those enzymes may disturb VLDL secretion; rationally, inhibition of TGH in primary rat hepatocytes decreases VLDL secretion[94] likewise does AADA deficiency in Huh7.5 cells[96]; in addition, overexpression of either DGAT enzymes, DGAT1 or DGAT2, in McA-RH7777 cells resulted in increased secretion of VLDL[80]. On another hand, factors that promote LDs assembly and its cellular concentration, such as insulin or PLIN2, have been reported to reduce VLDL production[95]. PLIN2 as well as CIDE-B are proteins found in association with LDs whose presence also influences VLDL assembly (Figure I11). The mentioned proteins have been shown to have opposite effects, while PLIN2 overexpression reduces VLDL secretion[95] and its knock-out increases it[48], CIDE-B knock-out animals present reduced VLDL secretion[97]. What is more, CIDE-B has been found interacting with ApoB, which suggests that LDs are functionally in close contact with the ER, where initial VLDL assembly takes place[80].
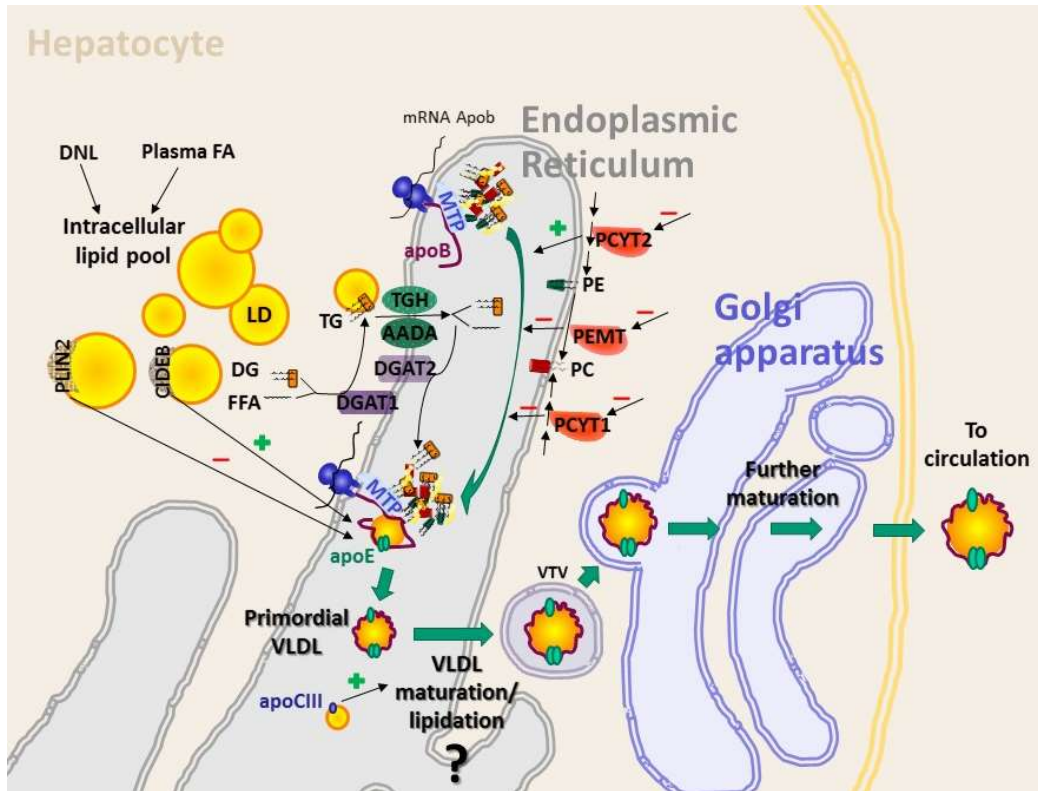
Figure I11. *VLDL assembly and secretion process, main influencing elements.* The intricate process of VLDL assembly involves many different actors, the principal ones are represented here. DNL, de novo lipogenesis; FA, fatty acid; PLIN2, perilipin2 ; CIDEB, cell death activator CIDE-B; LD, lipid droplets; TG, triglyceride; DG, diglyceride; FFA, free fatty acid; MTP, microsomal triglyceride transfer protein; TGH, triglyceride hydrolase; AADA, arylacetamide deacetylase; DGAT, diacylglycerol O-acyltransferase; PCYT1, Choline-phosphate cytidylyltransferase; PCYT2, Ethanolamine-phosphate cytidylyltransferase; PE, phosphatidylethanolamine; PC, phosphatidylcholine; PEMT, phosphatidylethanolamine methyltransferase; VTV, VLDL transport vesicles; (+) stimulated process; (-) reduced process.

Nevertheless, with respect to lipids, not only TG mobilization of liver lipid storage pool and *de novo* synthesis of FA contribute to hepatic VLDL synthesis but also phospholipids pool and its biosynthesis[80]. Among phospholipids, PC is the major component of VLDL and as stated before in *section 2.1*, in the liver, PC can be synthesized by CDP-Choline and PEMT pathways. The inhibition of any of these two pathways by means of knocking-out either PEMT or CTP:phosphocholine cytidylyltransferase-α (Pcyt1α) enzymes led to a reduction in VLDL secretion; thus, both

enzymes' activities are required for an adequate assembly and secretion of VLDL and an impairment of PC biosynthesis decreases VLDL secretion from the liver[98-100] (Figure I11). Therefore, adequate amounts of PC synthesis in the liver are required for the satisfactory secretion of VLDL. In addition to PC, other phospholipids such as PE, phosphatidylserine, phosphatidylinositol or sphingomyelin (SM) are components of VLDL[101], hence, their presence may contribute to VLDL assembly. For instance, SM depletion in rat hepatocytes by sphingomyelinase reduces VLDL secretion by 40-50%[102]; conversely, reduced synthesis of CDP-ethanolamine, precursor of PE, in CTP:phosphoethanolamine cytidylyltransferase (Pcyt2) heterozygous mice (Pcyt2^{+/-}) resulted in elevated plasma VLDL[80].

Finally, in addition to all the cited lipids and enzymatic activities needed for the proper synthesis of VLDL, and besides apolipoprotein ApoB, other apolipoproteins contained in VLDLs have been shown to participate in its assembly, independently of other roles, such as lipoprotein clearance. For example, ApoE is synthesized in the liver, and its presence on nascent VLDL particles promotes VLDL secretion[100] (Figure I11). When it is expressed in human or rat hepatocytes, VLDL secretion is stimulated; and on the contrary, when it is absent in apoE-KO mice, VLDL production is markedly reduced[103]. It has been suggested that ApoE facilitates ApoB maturation[103] and an early lipidation step in VLDL assembly process in the ER[73]. Apolipoprotein CIII (ApoCIII) and apolipoprotein AV (ApoAV) have also been shown to participate in VLDL production. ApoCIII has a role in nascent VLDL maturation process, it stimulates the incorporation of newly synthesized TG into microsomal compartments facilitating the expansion of VLDL particles[82] (Figure I11); and ApoAV can attenuate the production of VLDL, although the mechanism involved is unclear[73]. The mechanisms by which the mentioned apolipoproteins participate in VLDL production are independent of their role in VLDL clearance.

All the above stated agents can determine not only the secretion rate of VLDL but also the physical features of the particles, such as size and composition. Features that lately can affect VLDL metabolism[104, 105].

2.3.2. **VLDL catabolism**

VLDLs deliver TGs through the bloodstream to peripheral tissues; essentially, to the muscle, which utilises them for energy production, and to adipose tissue, where TGs are stored for future energy consumption. VLDL plasma levels depend on the rate of hepatic secretion and the rate of clearance from the plasma, an imbalance between the two processes may lead to dyslipidemia and its further consequences, such as CVD[82, 103].

VLDL clearance starts intravascularly by lipoprotein lipase (LPL) action, an enzyme that localizes in the outside of capillary endothelial cells plasma membrane and dictates VLDL catabolism. VLDLs bind and activate LPL by virtue of their apolipoprotein content. In adipose tissue insulin is also required for LPL activation. Once bound, LPL hydrolyses TG allowing FFA to be assimilated by tissues. VLDLs hydrolysis process by LPL leads to the formation of smaller denser particles known as IDL or VLDL remnants. These particles can be directly captured by lipoprotein receptors in the liver or, if remain in circulation, be further catabolised to LDL with loss of every apoproteins, except for the single ApoB and enrichment in cholesteryl esters[82, 106].

VLDL clearance, as well as VLDL assembly and secretion, is determined by several factors such as VLDL lipid and apoprotein composition or lipoproteins receptors[106].

VLDL lipid composition and size may affect how VLDLs interact with cell surface proteins, therefore affecting its catabolism[106, 107]. For instance, it has been suggested that a reduced content of PC on the surface of nascent VLDL particles promotes their clearance in mice[107]. Moreover, a higher susceptibility to hydrolysis by LPL has been observed when VLDL size and TG content are increased[108]. The lipid composition could alter the number and type of apolipoproteins that bind to VLDL particles surface, hence altering the interactions with other VLDL catabolism-related proteins[106].

Apolipoproteins stabilize lipoprotein particles and also act as receptor ligands and activate enzymatic activities to facilitate lipoproteins metabolism within the plasma compartment[82]. Differential apolipoprotein content in VLDL highly influences VLDL

catabolism[73, 106, 109, 110]. For example, ApoCII promotes VLDL-TG hydrolysis, it is an activator of LPL; while ApoCIII interferes with its activity promoting HTG by this LPL-dependent pathway and also by an LPL-independent pathway that may involve the inhibition of lipoprotein receptors[106, 110]. ApoE plays as well an important role in VLDL clearance[106, 110], it is a high affinity ligand for several lipoprotein receptors such as LDL receptor (LDL-R), prolow-density lipoprotein receptor-related protein 1 (LRP-1) and VLDL receptor (VLDL-R)[103, 111]. Those LDL-R family proteins upon interaction with ApoE internalize plasma lipoproteins via clathrin coated pit-mediated endocytosis[111]. LDL-R is mainly expressed in the liver, and it mediates the clearance not only of ApoE-containing but also of ApoB-containing lipoproteins, hence LDLs[73, 112]. On the other hand, VLDL-R is considered to function as a peripheral lipoprotein receptor for VLDL, and it is expressed abundantly in FA-active tissues, such as heart, skeletal muscle and fat where it mediates VLDL uptake through LPL-dependent lipolysis or receptor-mediated endocytosis[112-115] (Figure I12).

Pathophysiological changes in any of the mentioned factors may lead to dyslipidemia or other metabolic complications. For instance, VLDL-R augmented hepatic expression due to ER stress induces steatosis in mice[77]. It has been shown that subjects with HTG secrete VLDL with more ApoCIII than ApoE leading to ApoCIII-mediated reduce VLDL clearance what induces the accumulation of atherogenic lipoproteins[116]. HTG often coexists with other metabolic disorders such as obesity, metabolic syndrome or type 2 diabetes[117], and it is strongly associated with NAFLD[82], conditions that increase CVD risk[82, 117].
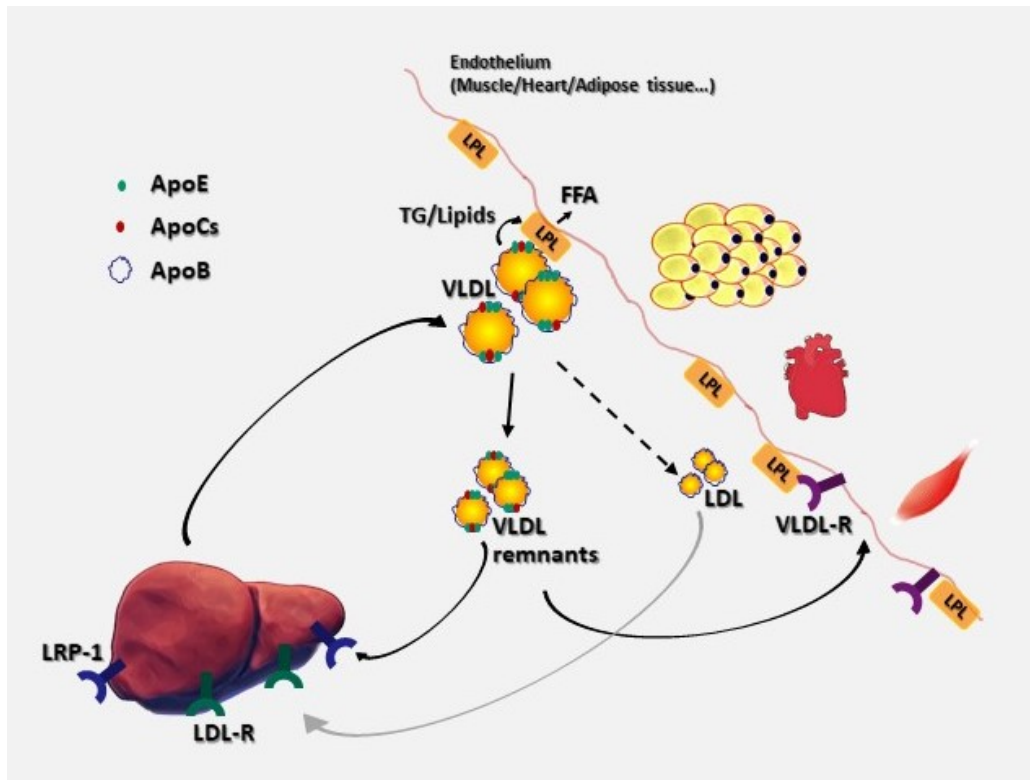
Figure I12. *Schematic representation of VLDL clearance process.* VLDL clearance involves the participation of different actors present either in tissues or in VLDLs themselves. ApoE, apolipoprotein E; ApoCs, apolipoproteins C; ApoB, apolipoprotein B; TG, triglyceride; FFA; free fatty acids; VLDL, very low-density lipoproteins; LDL, low-density lipoproteins; VLDL-R, VLDL receptor; LRP-1, prolow-density lipoprotein receptor-related protein 1; LDL-R, LDL receptor.

3. Objectives

The important thing is not to stop questioning. Curiosity has its own reason for existing.

Albert Einstein (1879-1955)

3. **OBJECTIVES**

Non-alcoholic Fatty Liver Disease (NAFLD) is the most common cause of chronic liver disease worldwide[25], but mainly in western contries, it is generally linked to obesity, dyslipidemia and insulin resistance[118]. Its development has been associated with dysregulated metabolism of S-adenosylmethionine (SAMe) both in humans[16, 55, 57, 62] and in mice[19, 20].

The deletion of Glycine N-methyltransferase (GNMT) protein in mice leads to a huge increase in hepatic SAMe[20]. This happens because GNMT, enzyme in charge of SAMe catabolism, is the main methyltransferase that regulates SAMe content in the liver[2]. On the other hand, Methionine Adenosyltransferase (MAT) enzyme leads hepatic SAMe synthesis[2]. The absence of MAT1A gene, which codifies the subunits MATI and MATIII, produces a decrease in liver SAMe[19]. Low hepatic content in SAMe has been shown to reduce phosphatidylcholine (PC) content leading to SREBP-1 activation and lipogenesis in *C. elegans* model; besides, the reduced PC quantity in HepG2 cells or in the liver of choline-phosphate cytidylyltransferase A knock out (KO) mice also leads to the activation of SREBP-1[59]. In addition, knocking out MAT1A in mice disrupts Very Low Density Lipoproteins (VLDL) assembly. Liver-secreted VLDL particles are small and triglyceride (TG)-poor in this animal model[58]. MAT1A absence has also recently been shown to altered FA oxidation in the mitochondria[60]. The mentioned processes may prompt the development of hepatosteatosis in this animal model[58-60]. Fatty liver development also occurs in GNMT-KO mice[13] in which, as mentioned above, hepatic SAMe levels are markedly increased. This led us to wonder how high levels of liver SAMe can lead to the accumulation of fat in the liver.

SAMe is the principal donor molecule of methyl groups[2], it is involved in the synthesis of PC from phosphatidylethanolamine (PE) via PE methyltransferase (PEMT) enzyme by three consecutive methylation reactions[119]. A requirement for PEMT activity in the liver has been reported to ensure normal VLDL secretion[99, 120], secretion that if

impaired has been described as a key factor in human NAFLD development[75]. VLDLs serve as an energy source to peripheral tissues, if an imbalance between its hepatic secretion rate and its plasma rate clearance occurs, dyslipidemia may appear leading to the consequent risk of cardiovascular disease[79, 121]. Thus, in this project we also wondered if there is an involvement of SAMe metabolism in all these processes.

Considering the abovementioned context, the main objectives of this work were (Figure O1):

- Unravel the mechanisms by which GNMT deficient mice develop hepatic steatosis.

- Analyse if SAMe controls VLDL assembly and secretion both in MAT1A-KO and in GNMT-KO mice.

- Decipher the extrahepatic consequences of chronic high SAMe levels in NAFLD.
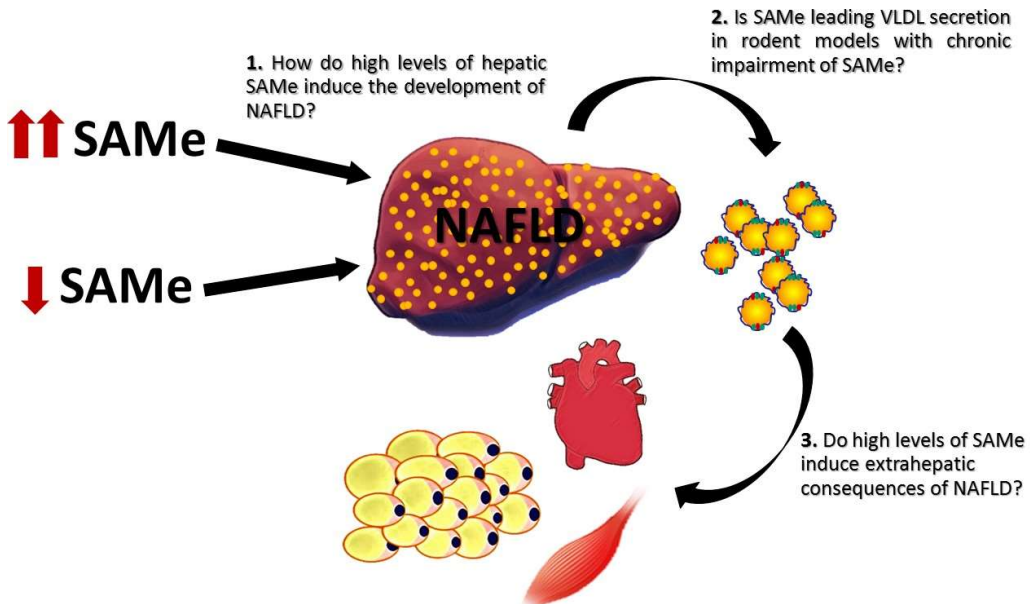
Figure O1. *Schematic representation of the questions asked during the progress of this work.*

4. Experimental procedures

4. EXPERIMENTAL PROCEDURES

4.1. Animal experiments

4.1.1. Animal models and diets

Male MAT1A Knockout (KO), GNMT-KO, PLIN2-KO and GNMT/PLIN2-KO mice, along with their wild-type (WT) counterparts, were the animal models use for the experiments. They were all produced in the animal facilities of CIC bioGUNE, and housed at 24°C with a 12-hour light-dark cycle with food and water available *ad libitum*.

The animal experimentation was performed according to both, the Spanish guide for the care and use of laboratory animals and the international animal care and use committee standards. All the animal procedures were approved by the University of the Basque Country UPV/EHU and CIC bioGUNE Animal Care and Use Committees.

4.1.1.1. MAT1A Knockout mice

The husbandry of male Mat1a KO and WT littermates has been described before[19].

3-month-old MAT1A-KO male mice and their WT littermates fed a rodent chow diet (Teklad Global 18% Protein Rodent Diet 2018S; Harlan Laboratories INC., USA) were administered daily, during 7 days, 100 mg/kg of S-Adenosylmethionine (SAMe) or vehicle alone by oral gavage[122].

4.1.1.2. GNMT Knockout mice

GNMT-KO male mice and their WT counterparts husbandry have already been described[20].

3-month-old an 8-month-old GNMT-KO male mice and their WT littermates were maintained on a rodent chow diet (Teklad Global 18% Protein Rodent Diet 2018S; Harlan Laboratories INC., USA) until further experimentation. 3-month-old mice were also fed either a methionine deficient diet (MDD) (S8946-E020 EF AIN 76A 0,15% L-methionine, SSNIFF, Soest, Germany) for 21 days or a high fat diet (HFD) (Mouse Diet, High Fat, Fat Calories (60%), Soft Pellets, F3282; Bio-Serv, USA) during 6 weeks, prior to being euthanised.

4.1.1.3. **PLIN2 Knockout and GNMT/PLIN2 Knockout⁻ mice**

The PLIN2-KO and GNMT/PLIN2-KO mice were generated by Richard H. Finnell (Department of Nutritional Sciences, Dell Paediatric Institute, The University of Texas at Austin, Austin, Texas) at the animal facilities of CIC bioGUNE, following the procedure detailed in the next section.

Both PLIN2-KO and GNMT/PLIN2-KO male mice, along with their WT littermates, age 3-month-old, were fed a rodent chow diet (Teklad Global 18% Protein Rodent Diet 2018S; Harlan Laboratories INC., USA) before being euthanised for further experimentation.

4.1.2. **Serum extraction and tissue harvesting**

After 2 or 8 hours of food deprivation, depending on the type of experiment, animals were anesthetised (sodium pentobarbital, 60 mg/kg body weight, given intraperitoneally (IP)) and euthanised. Blood and liver were extracted in every case, while other tissues such as heart and white adipose tissue were extracted just in some cases.

Blood was extracted from the inferior vena cava when sacrifice of mice followed and drawn in heparin capillary tubes by tail vein when not. After room temperature blood coagulation, and in order to obtain serum, blood was centrifuged for 30 minutes at 2000 x g 4ºC (Heraeus centrifuge, Biofuge Primo R). The supernatant was centrifuged again during 10 minutes at 10000 x g 4ºC for the elimination of any possible cellular fraction. Serum was ready for further analysis.

Liver, heart and white adipose tissue were removed, washed with saline at 4ºC, cut into small pieces, snap frozen in liquid nitrogen, and stored at -80ºC until later analysis. A small part of the tissues was also fixed in 4% formaldehyde for paraffin inclusion, cut (4µm width) and haematoxylin/eosin stained (performed by Neiker-Tecnalia or at CIC bioGUNE).

4.1.3. *In vitro* experiments – Primary culture hepatocytes

The hepatocyte isolation was performed in 2 hour fasted animals. The isolation technique was based on the two-step collagenase perfusion method described by Seglen[123]. Mouse strain hepatocytes were isolated by perfusion with collagenase type IV. In brief, mice were anesthetised with pentobarbital (60 mg/kg body weight), the abdomen was opened and a catheter was inserted into the inferior vena cava. Liver was perfused with Krebs-Henseleit medium (KH) (NaCl 118mM, $NaHCO_3$ 25mM, KCl 4.7 mM, $MgSO_4$ 1.2 mM, KH_2PO_4 1.2 mM, glucose 20mM, Hepes 6.5 mM) (37°C, oxygenated), portal vein was cut, and superior vena cava was ligated to close the circuit. Once washed liver was perfused for 5 minutes with KH plus 0.05% (w/v) of EGTA. Subsequently, liver was perfused during 12 minutes with supplemented KH ($CaCl_2$ 2.5 mM, collagenase 300µg/ml and tripsin inhibitor 60 µg/ml added) (37°C, oxygenated). After the perfusion, liver was placed in a petri dish containing KH supplemented with $CaCl_2$ and there it was carefully disaggregated by manual agitation. The digested liver was then filtered through a sterile nylon gauze (200µm pore size). Hepatocytes were collected and washed three times (50 x g, 3 minutes, 4ºC) in supplemented KH with 0.5 µg/ml of amphotericin in order to remove dead cells. After the last washing, supernatant was removed and hepatocytes were suspended in serum-free Dulbecco's modified Eagle's medium (DMEM; Sigma-Aldrich). An aliquot of 200 µl of the cells in suspension was dilute 1:4 and mixed with trypan blue 1:1. Cells were counted on a *Fuchs Rosenthal* haemocytometer to determine cell number and viable cells percentage. Viability was always superior to 90%.

Hepatocytes suspension was diluted to the appropriate concentration, calculated in order to plate 2×10^6 cells/dish (p60 dishes). Dishes were previously coated with a fibronectin and collagen mixture [DMEM, fibronectin 0.00094% (w/v), $NaHCO_3$ 0.94% (w/v), Bovine Serum Albumin (BSA) 0.0094% (w/v) and collagen 20.3 μg/ml]. Hepatocytes were then incubated with attachment DMEM [supplemented with 2g/l $NaHCO_3$, 15% Fetal Bovine Serum (FBS; Biochrome), 1% (v/v) of an antibiotic mix and 0.1% (v/v) of gentamicin (50mg/ml)] at 37 ºC and 5% CO_2 for at least 2 hours to permit the adhesion of the cells to the dish.

4.1.3.1. **Radiolabelled substrates incorporation**

After the attachment period, hepatocytes were incubated with culture DMEM [supplemented with 2g/l $NaHCO_3$, 1% (v/v) of an antibiotic mix and 0.1% (v/v) of gentamicin (50mg/ml)] with either [^{3}H]acetate (20 μM, 20 μCi/ml) for *de novo lipogenesis* experiments or [^{3}H]oleate (20 μM, 2 μCi/ml) for *fatty acid esterification* experiments. Both radioisotopes were from Perkin Elmer (Boston, MA). Radioactivity incorporation was measured after 30, 60 and 120 minutes of incubation with the radiolabelled substrates. For [^{3}H]ethanolamine (American radiolabelled chemicals, Inc. St. Louis, MO) incorporation, *PEMT flux* studies, hepatocytes were incubated with 5 μCi/ml for 4 hours. In all of three cases, after incubation periods, cells and mediums were collected separately, cells were washed twice with ice-cold phosphate-buffered saline (PBS) (NaCl 150 mM, sodium phosphate buffer 10 mM pH 7.4). Lipids were extracted[124] from both cells and culture medium and separated by thin layer chromatography (TLC)[125]. Lipid species were visualised by exposure to iodine vapour, the bands corresponding to the lipids object of study were scraped; TG and DG for *de novo lipogenesis* and for *fatty acid esterification*, and PE and PC for *PEMT flux*. The associated [^{3}H] radioactivity was determined by scintillation counting and expressed relative to the cell protein.
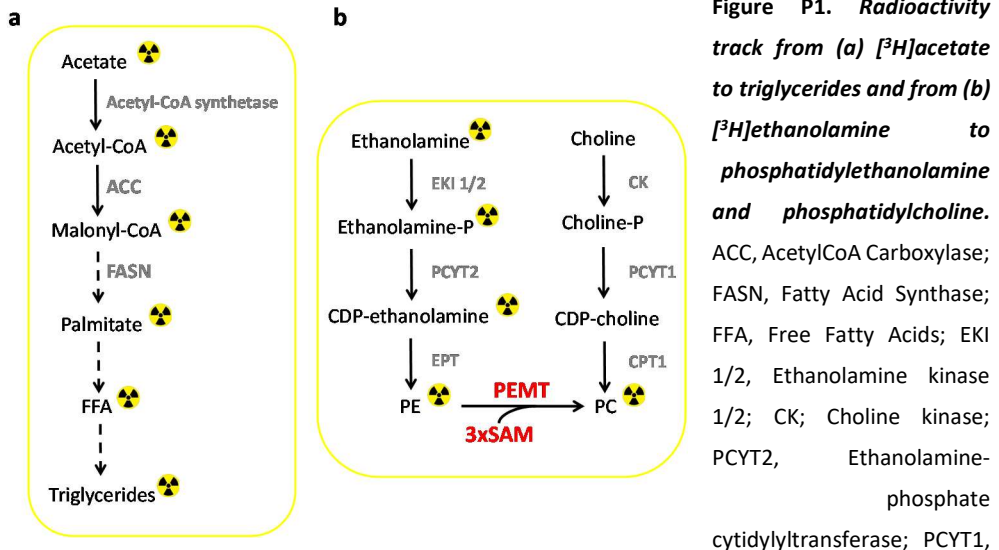
Figure P1. *Radioactivity track from (a) [³H]acetate to triglycerides and from (b) [³H]ethanolamine to phosphatidylethanolamine and phosphatidylcholine.* ACC, AcetylCoA Carboxylase; FASN, Fatty Acid Synthase; FFA, Free Fatty Acids; EKI 1/2, Ethanolamine kinase 1/2; CK; Choline kinase; PCYT2, Ethanolamine-phosphate cytidylyltransferase; PCYT1, Choline-phosphate cytidylyltransferase A; EPT, Ethanolamine phosphotransferase 1; CPT1, Choline phosphotransferase 1; PE, phosphatidylethanolamine; PEMT, phosphatidylethanolamine methyltransferase; SAM, S-Adenosylmethionine; PC, phosphatidylcholine.

4.1.3.2. **Soluble acid metabolites**

In the case of [³H]oleate incorporation mentioned in the previous paragraph, a part of the harvested medium (400µl) was used for acid soluble metabolites assessment[126, 127]. Mediums were centrifuged for 5 minutes at 2,500 x g to remove dead cells. Then, 60 µl 20% fatty acid free bovine serum albumin (FA-free BSA) was added to 400 µl medium for lipid binding. 32 µl of 70% perchloric acid were added later as precipitant agent in order to allow BSA to precipitate and delipidate the medium. A 21,000 x g for 5 minutes centrifugation followed and radioactivity was measured in an aliquot of the supernatant. The radiolabel incorporated into acid soluble metabolites was determined by scintillation counting and expressed relative to the cell protein.
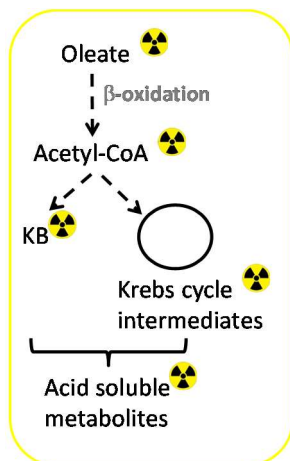
Figure P2. *Radioactivity track of [³H] from [³H]oleate to acid soluble metabolites.* KB, Ketone bodies.

4.1.3.3. **Phosphatidylethanolamine methyltransferase activity inhibition**

To inhibit PEMT activity, after attachment, cells were washed and incubated with culture DMEM with or without 10µM 3-deazaadenosine (DZA) for 4 hours[128]. Cells and medium were harvested and TG was measured in both using a commercially available kit (Menarini Diagnostics).

4.1.3.4. **Glucose production**

To assess glucose production, mice were fasted overnight before primary hepatocytes isolation. After attachment period, isolated hepatocytes were starved for 1 hour in Krebs-Henseleit buffer without D-Glucose. Cells were then incubated for 2 hours in KH buffer supplemented with or without gluconeogenic substrates: lactate and pyruvate added together at 30 mM/3 mM or glycerol at 25 mM as described by Sun *et al.*[129]. Cells and medium were harvested separately and glucose levels were measured in harvested medium using a commercially available kit from Menarini diagnostics.

Gluconeogenic substrates
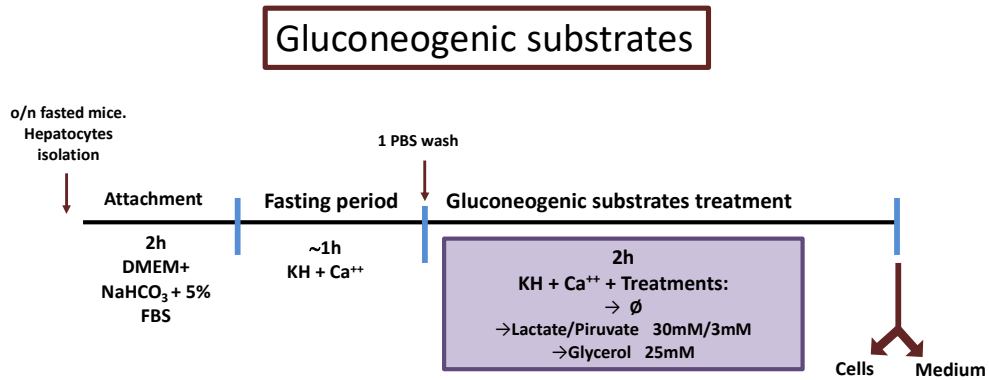
Figure P3. *Timeline for glucose production experiment.* FBS, fetal bovine serum; KH, Krebs-Henseleit; PBS, phosphate buffer saline; Ø, nothing.

4.1.3.5. **Turnover and secretion of triglycerides**

For glycerolipids turnover experiments, primary hepatocytes attachment period was 6 hours, after that time hepatocytes were washed and incubated overnight in culture DMEM as described[94]. Following overnight incubation, cells were incubated for 4 hours with 0.4 mM [^{3}H]oleic acid (5 µCi/dish) and [^{14}C]glycerol (0.5 µCi/dish) this period is denominated pulse. [^{3}H]oleic acid and [^{14}C]glycerol were from Amersham Radiochemicals (UK) and PerkinElmer Inc (Waltham, MA) respectively. After a 1 hour wash in culture DMEM, cells were incubated in culture DMEM without the radiolabelled substrates for 4 more hours, this period is named chase. After both pulse and chase periods, cells and medium were separately harvested. Lipids were exhaustively extracted from hepatocytes and incubation medium[124] and separated by TLC[125]. Lipid species were visualised by exposure to iodine vapour, the bands corresponding to triglycerides were scraped, and the associated [^{3}H] and [^{14}C] radioactivity was determined by scintillation counting. The percentage of the total [^{3}H]-TG and [^{14}C]-TG secreted to the medium in each period was calculated.
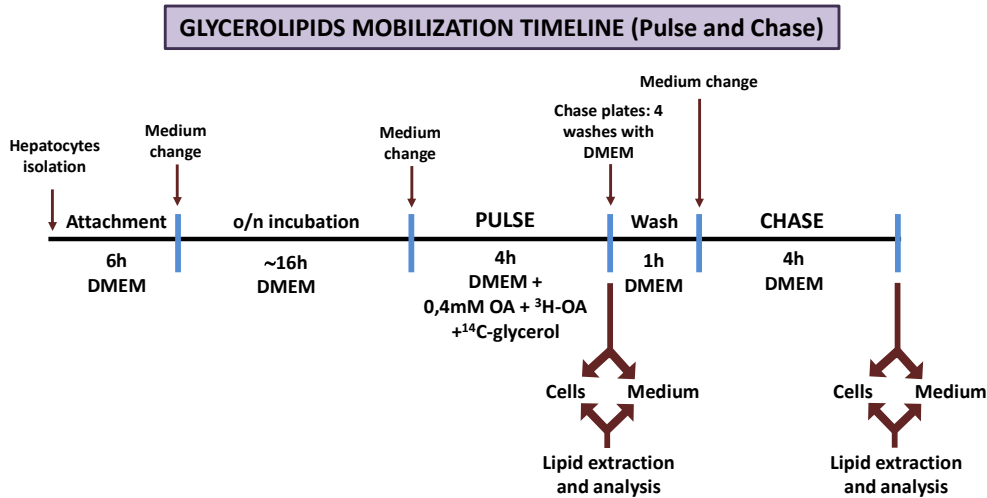
Figure P4. *Timeline for glycerolipids mobilization experiment.* o/n, over night; OA, oleic acid.

4.1.3.6. **Proteasome and autophagy inhibition**

For proteasome and autophagy inhibition assessment, after attachment, primary mice hepatocytes were incubated in culture DMEM for 12 hours with or without MG132 (10μM), to inhibit proteasome activity, or for 24 hours in culture DMEM without or with a mixture of the lysosomal function inhibitors leupeptin (100 μM) and ammonium chloride (20 μM), to inhibit autophagy through lysosomes. After the incubation cells and medium were separated, cells lysed, and kept for further analysis.

4.1.4. *In vivo* **experiments**

4.1.4.1. **Glucose and insulin tolerance tests**

For glucose tolerance test mice were fasted for 3 hours, and then administered a glucose solution (2 g/kg body weight) by oral gavage. Blood glucose levels were measured before and 15, 30, 60, and 120 minutes postgavage using blood strips (Arkray Factory, Inc., Shiga, Japan).

For insulin sensitivity studies mice were injected intraperitoneally 1 U insulin/kg body weight and glucose levels were monitored as described for glucose tolerance test.

4.1.4.2. **VLDL production and hepatic triglyceride secretion rate**

In vivo VLDL production in mice was measured after a 2 hours fasting period aiming to avoid circulating chylomicrons in the blood stream. For this purpose a group of mice were injected with Poloxamer P-407 (Invitrogen Life Technologies) in saline at a dose of 1 g/kg intraperitoneally, as described by Millar *et al.*[130]. P-407 is an inhibitor of lipoprotein lipase enzyme (LPL), an enzyme that hydrolyses TG from VLDL[130]. This way, VLDL metabolism is blocked and newly secreted VLDL particles can be analysed. Each secreted VLDL particle contains one apolipoprotein B, which in mice can be either apoB100 or apoB48.

Blood samples were drawn prior to injection and 6 hours after the injection for serum TG measurement (see section 4.2.8.1.). TG secretion rate was calculated by subtracting the TG values obtained prior to injection from those obtained 6 hours after the injection.

At the same time, another group of mice were not injected with P-407, their blood samples were used for circulating VLDL particles characterization.

VLDL particles were isolated and characterised for its size (see section 4.1.4.2.2), apolipoprotein content (see section 4.1.4.2.3) and lipid content (see section 4.2.6.).

4.1.4.2.1. **VLDL isolation**

VLDLs were isolated from 100µl-600µl of serum. The amount of serum was filled to 1.5ml with NaCl 0.9%. For VLDL flotation serum density was adjusted to 1.02 g/mL with a floating buffer (NaCl 0.2 M, EDTA 0.01 M, sodium azide 7.7 mM, chloramphenicol 1.55 mM and KBr q. s. to adjust 1.02 g/ml density, pH 7.4), reaching a final volume of 3 ml (i.e. 1.5ml of floating buffer were added). Serum was then ultracentrifuged during 2.5 hours at 100,000 rpm at 16 ºC in a TLA 110 rotor (Optima TL; Palo Alto) as described

by Aspichueta *et al.*[131]. The VLDL fraction, the one we collected for further analysis, was the upper 1.5 ml part of each sample.

4.1.4.2.2. **VLDL particle size analysis**

The diameter of VLDL lipoproteins was measured with an optical detector, Zetasizer 4 (Malvern Instruments), at Unidad de Biofísica CSIC-UPV/EHU. The Zetasizer equipment size measurement is based on a process called dynamic light scattering (DLS). DLS measures Brownian motion of VLDL particles and relates it to its size.

Brownian motion is the random movement of particles suspended in a liquid due to their collision with the quick molecules in the liquid that surround them. The particles in a liquid move about randomly and their speed of movement is used to determine the size of the particle.

For this size measurement, a laser (633 nm) is driven towards particles illuminating them and the intensity fluctuations in the scattered light are analysed.

It is known that small particles move more quickly in a liquid than larger particles, which move slowly. Using this knowledge and the relationship between diffusion speed and size, the size can be determined. The relationship between particle size and diffusing speed due to Brownian motion is defined by Stokes-Einstein equation (**$D = kT/6\pi\eta r_s$** where **k**: Boltzmann constant; **T**: absolute temperature; **η**: viscosity; **r_s**: effective radius of the spherical particle).

Serum isolated VLDL fraction was used for the diameter analysis, the measurements were performed in quintuplicate for each sample.

4.1.4.2.3. **Electrophoretic separation and quantification of VLDL apolipoproteins**

The apolipoproteins apolipoprotein B-100, apolipoprotein B-48 and apolipoprotein E were resolved by SDS-PAGE in a 3% to 15% gradient gel as described

by Laemmli[132]. For gel preparation a commercially available dissolution 30% acrilamide:bisacrilamide (37.5:1) (v/v) was used and the gradient was produced through communicating vessels principle. Polymerization was initiated by addition of 0.05% (w/v) ammonium persulfate and 0.1% (v/v) TEMED.

VLDL proteins were denatured with a denaturing buffer (Bromophenol blue 0.04% (w/v); glycerol 50% (v/v); 2-mercaptoethanol 25% (v/v); SDS 10% (v/v) and Tris-HCl 300 mM; pH 6.8) at 100 °C for 5 minutes.

A calibration curve of five points of phosphorylase b (from 0.05 to 0.8 µg) was loaded in each gel plus a molecular weight size markers PageRuler™ Plus Prestained Protein Ladder (10-250kDa) (Fermentas).

The electrophoresis run lasted 1 hour at 175 V and a maximum of 150 mA in electrophoresis buffer (glycine 192 mM; SDS 0.1% (w/v); Tris-HCl 25 mM; pH 8.3). After the run the gel was washed three times for 5 minutes with distillated water and stained with Gel Code® Blue Stain Reagent (Thermo Scientific) for 1 hour in continuous agitation in a rocking platform. And then was washed again with distillated water for 1 hour in agitation.

Apolipoproteins bands were quantified by optical densitometry using a GS-800 densitometer and Quantity One software (BioRad). Gel images were digitalised (Figure P5) and the integrated optical density (IOD) of apolipoproteins and phosphorylase *b* bands quantified. Each IOD value was corrected by subtracting the IOD value of a same-size band taken from background.

Calibration curves were constructed by plotting the IOD of the phosphorylase b standard versus the amount of protein loaded. Apolipoprotein quantity was determined by IOD interpolation in the calibration curve. Apolipoprotein concentration is given as nmol/dL serum considering each apolipoprotein molecular weight: ApoB-100 520 kDa, ApoB-48 250 kDa and ApoE 36 kDa.
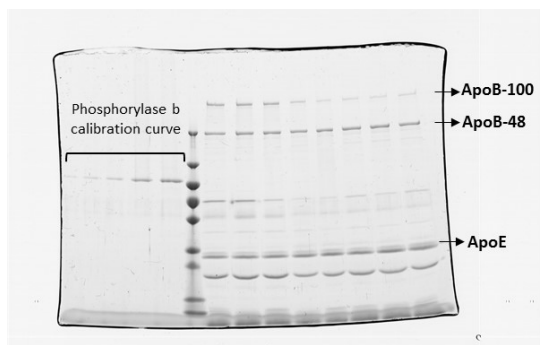
Figure P5. *Representative image of a resolved SDS-PAGE gel of VLDL apolipoproteins.*

4.1.4.3. **VLDL clearance**

VLDL clearance was assessed by labelling human VLDL with radioactivity, injecting them via tail vein to the mice and measuring the remaining radioactivity in mice blood at different points of time after injection.

Labelled human VLDL particles were obtained by a method previously described[133, 134]. VLDL were isolated from healthy human plasma by ultracentrifugation at d≤1.006 g/ml for 2.5 h at 100,000 rpm (Optima max XP centrifuge, Beckman coulter, TLA-110 rotor) at 16 °C. Isolated VLDL were added to a glass tube evenly coated with 400 µCi of [3H]TG (PerkinElmer Life Sciences). For every 2.2 ml of VLDL-radioisotope mixture, 1 ml of the 1.21 bottom fraction (obtained from sequential ultracentrifugation of the human plasma at d≤1.21 g/ml) as a source of cholesteryl ester transfer protein was added. The mix of VLDL, [3H]TG and cholesteryl ester transfer protein enriched fraction was incubated overnight with steady shaking at 37 °C. The now radiolabelled VLDL were re-isolated by ultracentrifugation as mentioned before. After, the VLDL preparation was extensively dialyzed using Econo-pac 10 DG columns (Biorad) and filtered through 0.45-µm syringe filters prior to use for turnover experiments. Mice were injected with such a mixture of the labelled VLDL that each mouse received 5 x 10^6 dpm of [3H]TG-VLDL (0.1 mg of TG per mouse) via the tail vein. Blood was collected 0.5, 5, 10, and 30 min after injection. At 30 min, mice were perfused with cold PBS and livers, hearts, white adipose tissue and muscle were harvested, flash frozen in liquid nitrogen,

and stored at -80 °C until further use. Radioactivity was determined in 30 µl of plasma and 100 µl of tissue homogenate, on a 1214 wallac rackbeta scintillation counter (PerkinElmer).

4.2. **General techniques**

4.2.1. **Tissue homogenization**

Tissues were mechanically homogenated either with a motor-driven Potter-Elvehjem (Potter S, B.Braun Biotech International) or with a Polytron PT 1200 C (Kinematica). Potter was used, 20 strokes at 750 rpm, when further fractionation of the tissue was needed. And Polytron, 30 seconds at power 6, in the rest of the cases. Homogenization buffer depended on the following technique to be applied, otherwise specified it was PBS (NaCl 150 mM, sodium phosphate buffer 10 mM pH 7.4).

4.2.2. **Subcellular fractionation of hepatic tissue**

The starting amount of liver was 300 mg; 5 volumes of homogenization buffer (sacarose 250 mM, sodium azide 0.02% w/v, EDTA 5 mM and Tris-HCl 50 mM pH 7.4) were added to the tissue and it was then homogenized with a Potter-Elvejhem. Every step was performed at 4 °C. The obtained homogenate was centrifuged at 500 x g (Sorvall RT-7 centrifuge, RTH-750 rotor) for 10 minutes to let the nucleus and other cellular rests to deposit. The remaining supernatant was then immediately centrifuged at 22,000 x g (Sorvall RC-6 Plus centrifuge, SM24 rotor) for 10 minutes in order to eliminate mainly mitocondria and lysosomes. The pellet was kept and the supernatant centrifuged at 159,000 x g (Optima max XP centrifuge, Beckman coulter, TLA-110 rotor) for 40 minutes, to separate cytosol and microsomes (cellular membranes). The pellet, the microsomes, was washed with 3 ml of washing buffer (NaCl 0,5 M and Tris-HCl 20 mM pH 7.4) so lipid droplets and membrane-associated-proteins could be eliminated

and the cytosol stored. Microsomes were resuspended in homogenization buffer. The microsomes isolation method is based on the one described by Wang *et al.*[135].

4.2.3. Enzymatic activities measurement

4.2.3.1. Diacylglycerol acyltransferase activity

DGAT activity was evaluated quantifying the radioactivity incorporated into TG after the esterification of DG with a fatty acid labelled with radioactivity, as it has been described before[136]. DG and Oleoyl-CoA were used as cold substrates, carriers of the reaction, and [14C]-Oleoyl-CoA as the radioactive substrate.

4.2.3.2. Triglyceride lipase activity

The activity of TG lipase was analysed by the quantification of the radioactivity contained in the oleic acid released when radioactively labeled triolein is hydrolysed. [14C]-triolein, the radioactive substrate, is first incorporated in micelles along with cold triolein, PC and taurocholate. The method has been previously described[137].

4.2.3.3. Phosphatidylethanolamine methyltransferase activity

PEMT activity assay is also a radiometric assay and was performed as detailed previously[138]. 1,2 dioleoyl sn-glicero 3-phosphoethanolamine-N-methil (PMME) and cold SAMe as carriers along with [3H]SAMe were used. In order to calculate the activity the following formula was used:

$$\text{PEMT activity} = \frac{\left[\dfrac{cpm*5}{0.5*2.2*10^{16}}\right]\dfrac{SAM}{{}^3\text{H-SAM}}}{(\text{min})(\text{protein mg})} \ (\text{mmol CH}_3 \text{ incorporated/min/protein mg})$$

4.2.3.4. **Microsomal transfer protein Triglyceride transfer activity**

The measurement of MTP TG transfer activity was performed in isolated microsomes, following the manufacturer' instructions (Chylos, Woodbury, NY). The assay is based on the detection of the fluorescence emitted by a fluorophore joint to TG when the TG is transferred (by MTP) from donor vesicles, where the fluorophore is quenched, to acceptor vesicles (Figure P6).

100 mg of liver tissue were used for this enzymatic assay. Tissue was homogenized in a Potter-elvhejem with 1 ml of MTP assay buffer (EGTA 1mM, MgCl$_2$ 1 mM, Tris-HCl 1 mM pH 7.6). Samples were centrifuged at 7,437 x g for 30 minutes at 4 °C, the supernatant was collected, and this was the fraction used for the assay. Black 96-well plates were used. Triplicate measurements of 100 µg of protein sample plus the rest of compounds in the proportions indicated by the manufacturer were done. The reaction took place at room temperature with steady shaking during 30 minutes.
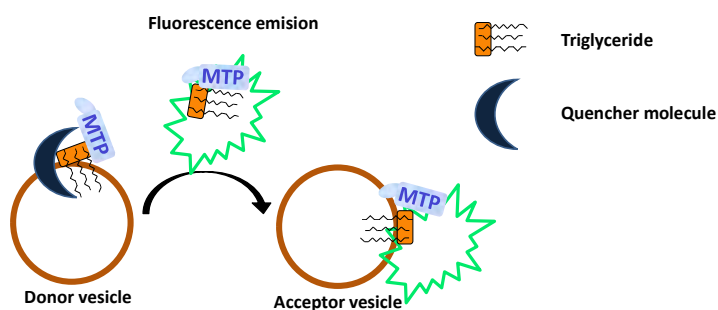
Figura P6. *Schematic representation of MTP triglyceride transfer activity. Figure taken from the PhD thesis of Ainara Cano.*

MTP TG transfer activity is expressed in percentage of TG transfer per mg of protein per hour, considering the 100% of the emitted fluorescence the one emitted by vesicles disrupted with 2-propanol.

4.2.4. **Gene expression analysis**

4.2.4.1. **Total RNA isolation and quantification**

Total RNA was isolated using Trizol (Invitrogen, UK), liver pieces were homogenated in trizol at 4°C. Trizol manufacturers' instructions were followed to isolate RNA, which was finally dissolved in DEPC water. RNA concentration was determined in a NanoDrop ND-1000 Spectrophotometer measuring the sample absorbance at 260 nm. Contamination with proteins was measured at 280 nm and the 260/280 ratio was always higher than 1.85. In order to check RNA integrity an electrophoresis in 1% agarose gel with SYBR® Safe (Life Technologies) for bands visualization was performed.

4.2.4.2. **cDNA synthesis**

Previously to cDNA synthesis, 2.5 µg of isolated RNA were treated with DNAse to avoid DNA contamination of the samples. "Dnase I, Amplification Grade" kit from Invitrogen was used following the manufacturer directions for this purpose.

RNA retrotranscription was performed using the commercially available kit "SuperScript III First-Strand Synthesis System for RT-PCR" from invitrogen. Starting with 1.8 µg of DNA-free RNA, the manufacturer instructions were followed to obtain the cDNA. A final treatment with RNAse H was performed to avoid RNA contamination of the sample. cDNA samples were diluted 1/10 before real time-qPCR assessment.

Table P1. *Sequence of primers used for real-time qPCR.* f: forward primer sequence, r: reverse primer sequence. Oligonucleotides were synthesized by Invitrogen Life Technologies.

Gene Name	Protein name	NCBI Reference Sequence	Oligonucleotides sequences (5'-3')
Acaca	Acetyl-CoA carboxylase 1	NM_133360.2	f: TGGTGCAGAGGTACCGAAGTG
			r: GTCGTAGTGGCCGTTCTGAAAG
Apob	Apolipoprotein B	NM_009693.2	f: GTGATCCCCACAGCAATAAGCA
			r: AGATTCCCAGGACCATGGAAAA
Apoe	Apolipoprotein E	NM_009696.3	f: TGGAGGCTAAGGACTTGTTTCG
			r: CTCGGCTAGGCATCCTGTCA
Cidec	Cell death activator CIDE-3	NM_178373.3	f: ATGGTGCCAGAGTGGTTAGC
			r: AGAGTCCCAGGTGAGAGACC
Cs	Citrate synthase, mitochondrial	NM_026444.3	f: TTGTTTTGTTTCAGGGGCCTT
			r: AGGGGAGAAGGGGTCACTTT
Fasn	Fatty acid synthase	NM_007988.3	f: *GATCCTGGAACGAGAACACGA*
			r: *GACATTTCCTGAAGTTTCCGC*
Fitm1	Fat storage-inducing transmembrane protein 1	NM_026808.1	f: CGCTGTGTTTGCCAAGTACC
			r: TACCAGGCAAACGTGCCTAC
G0s2	G0/G1 switch protein 2	NM_008059.3	f: GCCACCGAATCCAGAACTGA
			r: TTGATTGCTCGCACAGCCTA
G6pdx	Glucose-6-phosphate 1-dehydrogenase X	NM_008062.2	f: *GGGAAGAGTTGTACCAGGGTG*
			r: *TTCAGGTAGAAGGCCATCCCG*
Gapdh	Glyceraldehyde-3-phosphate dehydrogenase	NM_008084.2	f: *TTGATCGCAACAATCTCCAC*
			r: *CGTCCCGTAGACAAAATGGT*
Ldlr	Low-density lipoprotein receptor	NM_001252658.1	f: AGGCTGTGGGCTCCATAGG
			r: TGCGGTCCAGGGTCATCT
Lrp1	Prolow-density lipoprotein receptor-related protein 1	NM_008512.2	f: CTGAAGGCTCCGAGTACCAG
			r: GTAGGAGATTGTGCCCGTGT
Me1	NADP-dependent malic enzyme	NM_001198933.1	f: GGATGCGTAGGAGTGCTTCA
			r: TGAGCACGCTGTAGAAGAGC
Plin2	Perilipin-2	NM_007408.3	f: *CAGAAAATTCAGCGTGCTCAGG*
			r: *TGCTCAACACAGTGGGACTCAT*
Pparg	Peroxisome proliferator-activated receptor gamma	NM_011146.3	f: *GAATGCGAGTGGTCTTCCAT*
			r: *TGCACTGCCTATGAGCACTT*
Pygl	Glycogen phosphorylase, liver form	NM_133198.2	f: AGACCGTTCTGTGCTCCCTC
			r: CCACATTCTCTACGCCCACG
Scd1	Acyl-CoA desaturase 1	NM_009127.4	f: *TGGCTGGGCAGGAACTAGTG*
			r: *TGTTCCCCAAGGGCTTCATC*
Srebf1	Sterol regulatory element-binding protein 1	NM_011480.3	f: *CCTGCCTTCAGGCTTCTCAGG*
			r: *GAGGCCAAGCTTTGGACCTGG*
Vldlr	Very low-density lipoprotein receptor	NM_001161420.1	f: TGACGCAGACTGTTCAGACC
			r: GCCGTGGATACAGCTACCAT

4.2.4.3. **Real time quantitative PCR assay**

For real time qPCR cDNA quantification, SYBR® Green (Applied Biosystems) was the fluorescence dye used. Every sample was assayed in triplicate and 40 cycles with a melting temperature of 60°C for 1 minute and 95 ºC for 15 seconds were performed. The equipment for the qPCR was AbiPrism 7000 "Sequence Detection System" from Applied Biosystems.

Ct (cycle threshold) values were determined for each sample and extrapolated to a standard curve. The standard curve was constructed with serial dilutions of a mixture of cDNA. The expression levels are showed as arbitrary units which represent the relative quantity of the corresponding cDNA in the samples. Expression levels were normalised to the average level of *Gapdh* in each sample.

Primers were designed for *mus musculus* and synthesized by Invitrogen Life Technologies. Melting curve was checked to test the specificity of the PCR products. PCR was performed with primers described in Table P1.

4.2.4.3. **APOB promoter bisulfite pyrosequencing**

CpG island of the *APOB* promoter was predicted using the CpG Island searcher software (www.uscnorris.com/cpgislands2/cpg.aspx) within the 1000pb upstream of the start site. The pyrosequencing assay was designed using PSQ Assay Design software (Qiagen). Genomic DNA was bisulfite converted using the EpiTect Bisulfite Conversion Kit (Qiagen), according to manufacturer's instructions. In a following PCR amplification locus specific primers were used with one primer biotinylated at the 5´ end (PCR and sequencing primer sequences are shown in Table S4). For amplification reactions the PyroMark PCR Kit (Qiagen) was used according to standard protocol. After initial denaturation, PCR consisted of 45 cycles of each 94 °C for 30 s, annealing temperature for 30 s, and 72 °C for 30 s followed by a final synthesis at 72 °C for 10 min. Amplification was verified by agarose gel electrophoresis. Using the VacuumPrep Tool (Qiagen) single strands were prepared followed by a denaturation step at 85 °C for two minutes and

final sequencing primer hybridization. Pyrosequencing was performed using the PyroMark Q24 system and the DNA methylation analysis software Pyro Q-CpG (Qiagen), which was also used to evaluate the ratio T:C (mC:C) at the CpG sites analysed. All assays were optimised and validated using commercially completely methylated Mouse DNA (Millipore) as the positive control and DNA amplified with illustra GenomiPhi V2 kit (GE Healthcare) as the negative control. Water blanks and genomic DNAs were included with each assay. This procedure was performed in collaboration with Idoia Martín-Guerrero and Africa García-Orad.

Table P2. *Pyrosequencing primers.*

Pyrosequencing primers	Sequence (5'-3')	PCR product
APOB_CpG_island_Forward	Biotin-TGGTGGTTTTTTGGAGAAAGTT	203pb
APOB_CpG_island_Reverse	ACCCCAACCTATTTACTTTTCCATACAA	
Sequencing reaction	AATAATAATCTCACTACTAATTCA	

4.2.5. **Protein analysis**

4.2.5.1. **Protein quantification**

Protein concentrations were measured using a commercially available kit based on bicinchoninic acid method (Thermo Fisher Scientific Inc, Rockford, IL). Manufacturer' instructions were followed. A micro-assay was performed in 96 well-plates, triplicates of each sample were determined. Samples protein concentration was calculated by interpolation of absorbance values in a bovine serum albumin standard curve prepared for each plate.

4.2.5.2. **Protein expression analysis**

Serum, liver homogenate and cell samples were used for protein expression analysis. Both, liver homogenate and cell samples were lysed, the lysis buffer contained 150mM NaCl, 1% NP-40, 2mM EDTA, 10% glycerol, 10mM NaF, 50mM HEPES pH 7.4, 2mM Na_3VO_4, 10mM $Na_4P_2O_7$, and 2mM PMSF and 0.1mM Leupeptin as protein inhibitors. Liver homogenate and cell lysates samples were quantified for protein content as detailed before in section 4.2.5.1.

4.2.5.2.1. **SDS-PAGE Electrophoresis**

Proteins were resolved by electrophoresis after denaturation in denaturing buffer (Bromophenol blue 0.04% (w/v); glycerol 50% (v/v); 2-mercaptoethanol 25% (v/v); SDS 10% (v/v) and Tris-HCl 300 mM; pH 6.8) at 100 ºC for 5 minutes. The electrophoresis was performed in denaturing and reducing conditions as described by Laemmli[132].

The polyacrylamide percentage of the gel depended on the protein aimed to be resolved: for apolipoprotein B and acetyl-CoA carboxylase a gradient gel from 3 to 15% was used, for apolipoprotein E 10% polyacrylamide and for CD36 8% polyacrylamide gel was employed. Gels were prepared as stated in section 4.1.4.2.3. A weight size marker, PageRuler^{TM} Plus Prestained Protein Ladder (10-250kDa) (Fermentas), was loaded in every gel.

The electrophoresis was run in vertical at 175 V and a maximum of 150 mA in electrophoresis buffer (glycine 192 mM; SDS 0.1% (w/v); Tris-HCl 25 mM; pH 8.3).

4.2.5.2.2. **Proteins electrotransference**

After the electrophoresis, the resolved proteins were transferred to a PVDF membrane in a wet electrotransference chamber. The membranes were activated by one minute immersion in methanol previous to the set-up of the transfer, which was as

detailed in figure P7. During the set-up preparation all the material was maintained submerged in transfer buffer (electrophoresis buffer one half diluted and 20% of methanol).

The transfer was performed at a constant voltage of 100V for 1 or 2 hours. The wet electrotransference chamber was maintained in ice and with continuous agitation to keep the temperature.

The efficiency of the transfer was check by Gel Code® Blue Stain Reagent (Thermo Scientific) staining of the gels for 1 hour.

Figure P7. *Representation of the set-up for wet transfer of proteins.* Proteins migrate to the positive pole, the anode.
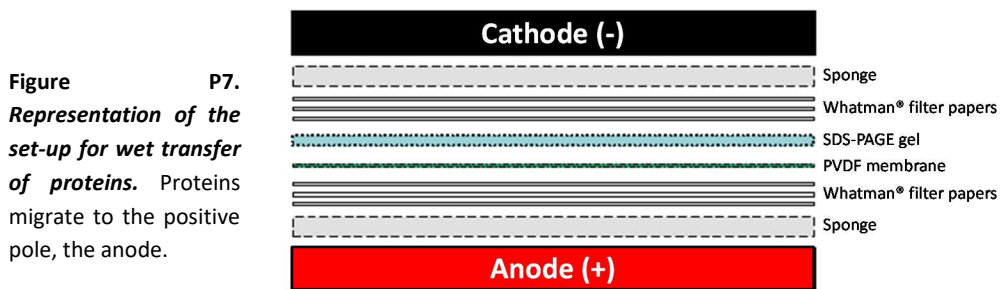
4.2.5.2.3. **Protein immunodetection**

After the transfer, membranes were blocked under different conditions depending on the protein to be detected, as detailed in Table P3. The base buffer used in every incubation was TBST (Tris Buffer Saline-Tween20) (NaCl 150 mM, Tween20 0.05% (v/v), Tris-HCl 10 mM pH 7.6). Following the membrane blocking the primary antibody incubation started under the conditions specified in Table P3.

After primary antibody incubation three 15-minutes washes with TBST were performed. The secondary antibodies conjugated with horseradish peroxidase were incubated as detailed in Table P4, the type of antibody used depended on the source of the primary antibody. Following the secondary antibody incubation another three 15-minutes washes were completed, and the membrane was maintained in TBST until the developing was done.

Every incubation was performed with continuous agitation in a rocking platform.

Table P3. *Primary antibodies for protein expression analysis information and incubation conditions.* TBST, Tris Buffer Saline-Tween20; BSA, Bovine Serum Albumin; h, hour; rt, room temperature; o/n, overnight.

Target protein	Manufacturer	Host species	Blocking	Incubation
Acetyl CoA Carboxylase	Cell signaling	Rabbit	TBST-5% BSA, 1h, rt	TBST-5% BSA 1:1000 o/n, 4ºC
Apolipoprotein B	abcam	Rabbit	TBST-3% milk, 1h, rt	TBST-1% BSA 1:1000 o/n, 4ºC
Apolipoprotein B	Chemicon	Goat	TBST-5% milk, 1h, rt	TBST-5% BSA 1:5000 o/n, 4ºC
Apolipoprotein E	abcam	Rabbit	TBST-5% milk, 1h, rt	TBST-1% BSA 1:1000 o/n, 4ºC
Calregulin	Santa Cruz Biotech.	Goat	TBST-5% BSA, 1h, rt	TBST-1% BSA 1:1000 o/n, 4ºC
CD36	Novus Biologicals	Rabbit	TBST-3% BSA, 1h, rt	TBST-1% BSA 1:1000 o/n, 4ºC
Phospho-Acetyl-CoA Carboxylase (Ser79)	Cell signaling	Rabbit	TBST-5% BSA, 1h, rt	TBST-5% BSA 1:1000 o/n, 4ºC
Transferrin	Santa Cruz Biotech.	Goat	TBST-3% milk, 1h, rt	TBST-1% BSA 1:1000 o/n, 4ºC

Table P4. *Secondary antibodies for protein expression analysis information and incubation conditions.* IgG, immunoglobulin G; TBST, Tris Buffer Saline-Tween20; BSA, Bovine Serum Albumin; h, hour; rt, room temperature.

Target IgG	Manufacturer	Incubation method	Dilution
Rabbit IgG	Sigma	TBST-1% BSA, 1h, rt	1:2000
Goat IgG	Thermo Scientific	TBST-1% milk, 1h, rt	1:10000

4.2.5.2.4. **Developing and quantification**

For the developing membranes were covered with ECL luminol reactive (Amersham™ ECL™ Western Blotting Detection Reagents, GE Healthcare) and incubated in total darkness for 1 minute to let the oxidation reaction take place. Finally,

the membrane was protected with a transparent plastic sheet before exposing the photographic film (Hyperfilm ECL, GE Healthcare) to the oxidised luminol light for the time required for each protein. The film was then developed and fixed with photography liquids (AGFA).

Quantification was made by optical densitometry using GS-800 densitometer and Quantity One software (BioRad). Images of the films were taken and digitalised in order to quantify integrated optical density (IOD) of the bands of the aim proteins.

4.2.5.2.5. **Stripping**

For the analysis of other protein levels in the same membranes stripping was performed. For this, membranes were washed with TBST and then incubated with Restore™ Western Blot Stripping Buffer (Thermo scientific) for 30 minutes. Membranes were washed again with TBST before a new round of incubation with primary antibody was started.

4.2.5.3. **Determination of Apob mRNA binding to HuR**

In collaboration with M.L. Martinez-Chantar´s Laboratory (CIC bioGUNE), binding of Apob mRNA to HuR was evaluated by immunoprecipitation followed by quantitative real-time PCR as described before (Martinez-Lopez et al., 2012). Liver homogenates were centrifuged at 16000 x *g* for 30 min and supernatants used for immunoprecipitation of RNA-protein complexes by incubation (1 h, 4 °C) with a 50% (v/v) suspension of Protein A-Sepharose beads (Sigma-Aldrich, St. Louis, MO) precoated (overnight) with 30 µg of either IgG1 (BD Pharmingen, San Diego, CA) or anti-HuR (Santa Cruz Biotechnology Inc., Santa Cruz, CA) antibodies. Beads were washed using NT2 buffer (50 mM Tris-HCl, pH 7.4, 150 mM NaCl, 1 mM MgCl2, and 0.05% Nonidet P-40). For the isolation of RNA in the immunoprecipitates, beads were incubated with 100 µl NT2 buffer containing 20 U RNase-free DNase I for 15 min at 37 °C, washed with NT2 buffer, and further incubated in 100 ml NT2 buffer containing 0.1% SDS and 0.5 mg/ml

proteinase K (15 min, 55 °C). RNA was extracted and precipitated in the presence of GlycoBlue (Ambion). Apob mRNA bound to HuR was measured by real time PCR and normalised to GAPDH. Prothymosin alpha (PTMA) mRNA binding to HuR was used as positive control.

4.2.6. **Lipid analysis**

Lipid analyses were performed for liver and heart homogenates (see section 4.2.1.), isolated liver microsomes (see section 4.2.2.), isolated VLDL (see section 4.1.4.2.1.), radiolabelled incorporation experiments (see sections 4.1.3.1. and 4.1.3.5.) and for some enzymatic activities measurements (see sections 4.2.3.1., 4.2.3.2 and 4.2.3.3.).

4.2.6.1. **Lipid extraction**

Lipids were extracted following the Bligh and Dyer method[124]. Glass material previously cleaned with chromic acid for avoiding biological contamination was used. 8 ml of a chloroform:methanol (1:2, v/v) mixture was added to 500-1000 µl of the aqueous sample (either containing a determined amount of protein or a determined volume for the same set of samples). The organic-aqueous mixture was vigorously shaken during 2 minutes in a vortex. After the organic and aqueous phases separation was evident, 2.5 ml of chloroform and 4 ml of extra water were added to the previous mix. Shaking as before was performed again. Then, samples were centrifuged at 1,000 x g for 15 minutes at 4 °C to allow the correct separation of aqueous, protein and organic phases. The organic phase (the inferior one), which contained the lipids we were interested in, was next transferred to another glass tube using a glass Pasteur pipette. The remaining lipids were extracted again from aqueous and protein phases by the addition of 4 ml chloroform:methanol (1:2, v/v) and 2 ml water, the vigorous shaking, and the following centrifugation at 1,000 x g for 10 minutes at 4 °C for phases separation. The organic phase was collected again and added to the previous one. To

obtain a cleaner organic phase, the one obtained was washed with a 1.5 mM $CaCl_2$ solution accounting for a third part of the organic phase volume. The mix was shaken in a vortex for 15 seconds, centrifuged at 1,000 x g for 10 minutes at 4 °C, and the organic phase recovered to another clean glass tube. After that, the organic solvent was evaporated with a concentrator-evaporator (Savant A290, Thermo) at 40 °C during approximately 1 hour. The obtained lipid extract was dissolved in the appropriate volume of toluene or isopropyl alcohol (the solvent depended on the next analysis of the sample) and stored in nitrogen atmosphere at -20 °C until later analysis.

4.2.6.2. **Lipid separation by thin layer chromatography**

Lipids were separated by Thin Layer Chromatography (TLC) following the procedure described by Ruiz and Ochoa[125]. Pre-coated Silica Gel G-25 glass plates (Macherey-Nagel) of 20x20 cm were used for the lipid separation. Plates were impregnated by capillarity in a chromatographic glass chamber with a 1 mM EDTA-Na$_2$ pH 5.5 solution, dried overnight at room temperature, and carefully stored until use.

Previous to the chromatographic development, aiming the removal of impurities, plates were washed overnight in a mixture of chloroform:methanol:water (60:40:10, v/v/v) following the same direction as the impregnation; then plates were dried at room temperature and after dehydrated at 100 °C for 30 minutes in a heater. After that, plates followed different paths, depending on the objective:

- · Major lipid species separation only, when the resolution of phospholipids species was not needed.

- · Major lipid and phospholipid species separation, when differentiation of phospholipids was needed.

- · Lipids visualization with iodine vapour, when lipid spots were being scraped from the silica plate for radioactivity counting.

· Lipids visualization following plate charring after 10% cupric sulphate (w/v) in 8% phosphoric acid (v/v) for 10 seconds staining, when lipid spots were being quantified.

4.2.6.2.1. **Separation of major lipid species**

This method allows the separation of phospholipids (PL), fatty acids (FA), diglyceride (DG), free cholesterol (CL), triglyceride (TG) and cholesteryl ester (CE). For this purpose, three consecutive chromatographic developments, with different mixes, as detailed in table P5, were applied. Before initiating the developments, the corresponding amount of sample and standards were applied in the plate at 1.5 cm distance from the bottom edge in every case.

Table P5. *Solvent mixtures* (mobile phases) used for the development and separation of neutral lipids in TLC plates; and the distance to be reached by each solvent.

Mobile phase composition	Ratio (v:v)	Distance from the bottom edge (cm)
Chloroform:methanol:water	60:40:10	1.8
n-hepatne:diethyl ether:acetic acid	70:30:2	11.5
n-heptane	100	13

After each development plates were thoroughly dried, with warm air and at room temperature, a crucial step for the pursued separation of lipids.

4.2.6.2.2. **Separation of major lipid and phospholipid species**

This chromatography pursued the separation of lisophosphatidylcholine (LPC), sphingomyelin (SM), phosphatidylcholine (PC), phosphatidylserine (PS), phosphatidylinositol (PI), phosphatidylethanolamine (PE), cardiolipin (CLna), fatty acids

(FA), diglyceride (DG), free cholesterol (CL), triglyceride (TG) and cholesteryl ester (CE). After applying the sample, the plates followed 6 consecutive chromatographic developments, with different mobile phase composition each, as detailed in table P6. Plates were carefully dried between developments.

Table P6. *Solvent mixtures* (mobile phases) used for the development and separation of neutral lipids and phospholipids in TLC plates; and the distance to be reached by each solvent.

Mobile phase composition	Ratio (v:v)	Distance from the bottom edge (cm)
Chloroform:methanol:water	60:40:10	1.8
Chloroform:methanol:water	65:40:5	2.3
Ethyl acetate:2-propanol:ethanol:chloroform: methanol:0.25% KCl	35:5:20:22:15:9	5.5
Toluene:diethyl ether:ethanol	60:40:3	8.5
n-heptane:diethyl ether	94:8	12
n-heptane	100	13

4.2.6.2.3. **Visualization of lipids**

After the chromatographic developments, two main ways for visualizing lipids were used.

When lipid spots were going to be scraped from the plates, iodine vapour system was used. This method is based upon the observation that iodine has a high affinity for both unsaturated and aromatic compounds. The plate was introduced in a covered chamber containing crystals of iodine and it remained there until yellow to light brown colour spots appeared over the entire plate, where the separated lipids were. Then, the TLC plate was carefully removed and the spots were identified and circled with a dull pencil. Those drawn spots were later scraped for radioactivity quantification in that portion of silica dust containing a determined specific lipid.

If the lipid spots were going to be directly quantified from the TLC plate, lipids were charred after dipping the plate in a solution of 10% cupric sulphate (w/v) in 8% phosphoric acid (v/v) for 10 seconds, wiping dry the glass back, thoroughly drying the plate under a stream of hot air until the lipid spots became evident and immediately heated at 200 °C for 3 minutes. Before losing any colour and after scrupulously wiping the back part of the plate, an image of the plate was acquired with a GS-800 densitometer (BioRad).

Figure P8. *Image example of a thin layer chromatography development for major lipid and phospholipids species separation.* CE, Cholesteryl ester; TG, Triglyceride; DG, Diglyceride; CL, Free Cholesterol; FA, Fatty Acids; CLi, Cardiolipin; PE, Phosphatidylethanolamine; PI, Phosphatidylinositol; PS, Phosphatidylserine; PC, Phosphatidylcholine; SM, Sphingomyelin; LPC, Lysophosphatidylcholine.
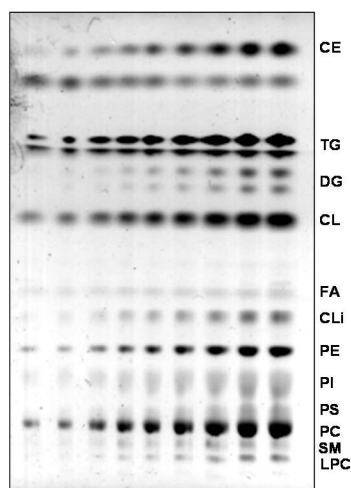
4.2.6.3. **Lipid quantification**

Lipid spots were quantified in the acquired images as integrated optical densities (IOD) with the software Quantity One (BioRad). For quantification, standards of the lipid species to be quantified were included in each plate so a calibration curve could be constructed later. The quantity ranges (nmol) of the standard lipids included were as followed: LPC (0.12-2.67), SM (0.04-0.9), PC (0.32-7.88), PS (0.13-3.24), PI (0.1-2.47), PE (0.16-4.09), CLna (0.02-0.48), CL (0.18-4.51), DG (0.15-3.73), TG (0.54-13.49), and CE (0.09-2.15). The calibration curves were constructed by plotting the IOD of the lipid standard versus the amount of lipid loaded. Calibration curves were used for the lipid amount determination.

4.2.7. **Serum lipoproteins separation by Fast Protein Liquid Chromatography**

Serum lipoproteins, VLDL, LDL y HDL, were separated according to their size. An ÄKTA-FPLC (Fast-Protein Liquid Chromatography) system (GE Healthcare) equipped with a Superose™ 6 10/300 GL column (GE Healthcare Europe GmbH, Germany) was used for this purpose. 50 mM phosphate-buffered 150 mM NaCl, pH 7.4 as mobile phase was used at a constant flow rate of 0.3 ml/min. After system equilibration 200 μl of serum previously filtered through a nitrocellulose 0.45 μm pore-filter (Millipore, Ireland) were injected and 40 fractions of 450 μl each were collected through a Frac-950 collector system. Standard enzymatic, colorimetric methods were used to measure TG (Menarini Diagnostics, Spain) and PC (Spinreact) in each fraction as detailed in 4.2.8.1. and in 4.2.8.2., respectively.

4.2.8. **Other biochemical analysis**

Other biological compounds such as TG, PC, free fatty acids (FFA) and ketone bodies (KB) were determined in serum using commercially available kits. All the procedures are based on a series of coupled reactions in which the appearance of a coloured compound is directly related to the amount of the biological compound to be measured. 96-well plates were used for all of the determinations.

4.2.8.1. **Triglyceride determination by kit**

TG quantification was performed both in 2-propanol suspended lipid-extracts and in non-lipid extracts, such as serum or FPLC fractions.

A kit from Menarini diagnostics was used for TG measurement; the instructions of the manufacturer were followed. A TG standard curve was included in each plate, the standard was provided as well by the manufacturer. The absorbance was measured at

500 nm after 5 minutes incubation at 37 °C. TG samples concentration was calculated by interpolation of the absorbance values in the standard curve.

4.2.8.2. **Phosphatidylcholine determination by kit**

PC was quantified in FPLC fractions. Spinreact was the supplier of PC determination kit. The standard curve in each plate was made with the standard supplied by the manufacturer. After 30 minutes of reaction at 37 °C the absorbance was measured at 505 nm. PC samples concentration was obtained by interpolation of the absorbance values in the standard curve.

4.2.8.3. **Fatty Acids and Ketone Bodies determination by kit**

A kit from Wako Chemicals was used in these cases. The instructions of the manufacturer were followed both to perform the experimental measurement and to make the calculations with the obtained absorbance values.

4.2.8.4. **S-Adenosylmethionine determination in the liver**

SAMe determination was performed at the metabolomic unit of CIC bioGUNE.

Liver specimens were homogenized in 0.4 M perchloric acid on ice for 5 minutes and centrifuged at 1,000 x g for 15 minutes at 4 °C. The aqueous layer was quantitatively removed, neutralised with 3 M KOH, and centrifuged at 3,000 x g for 10 minutes at 4 °C.

SAMe levels were determined by liquid chromatography/mass spectrometry (LC/MS) using a Waters Acquity ultraperformance liquid chromatography (UPLC) system equipped with a column oven, and a Waters Acquity UPLC BEH C18 column (2.1 × 100 mm, 1.7 μm). A 3-μL aliquot of sample was injected into the UPLC column, which was maintained at 50 °C and eluted at 600 μL/min. The mobile phase consisted of water with 0.05% formic acid (solvent A) and acetonitrile with 0.05% formic acid (solvent B). Separation was carried out starting with 1% solvent B for 1 minute, followed by a linear

gradient from 1% to 95% solvent B for 10 minutes and staying at 95% B for 6 minutes. The UPLC system was coupled to a Waters Micromass LCT Premier Mass Spectrometer equipped with a Lockspray ionization source operating in electrospray positive ion mode (W mode, resolution 10,000 full width at half maximum). Full-scan time-of-flight MS spectra were acquired between *m/z* (mass-to charge ratio) 80 and 1,000 using the dynamic range enhancement mode, with a total scan time of 0.4 seconds. Leucine enkephalin was used as a reference compound for accurate mass measurements. The reference was infused into the Lockspray reference channel, and the masses of the analyte channel were automatically mass-corrected by the software. A set of samples, prepared from all standard compounds, was acquired over the concentration range of 10 pg/ μL to 50 ng/μL in order to test the linearity of the system. After analysing all concentration levels, calibration curves were generated and chromatogram traces of the protonated species of the standards were extracted with a mass window of 0.05 Da. Liver SAMe levels were automatically calculated from the calibration curves.

4.3. **Human samples**

This study included 33 non-diabetic patients with cholelithiasis and a clinical diagnosis of NAFLD (Table R2, Results Part 3), who underwent a liver biopsy during programmed laparoscopic cholecystectomy. Inclusion criteria for patients with NAFLD were based on the absence of alcohol intake and the presence of biopsy-proven steatosis without necro-inflammation and/or fibrosis along with negative serum tests for hepatitis B virus (HBV), hepatitis C virus (HCV) and human immunodeficiency virus (HIV). NAFLD patients were classified into two groups depending on serum TG levels (Table R3, Results Part 3); NAFLD-1 group comprised 11 individuals with serum TG levels higher than the media of the whole NAFLD patients and NAFLD-2 included 22 subjects with serum TG levels lower than the media in NAFLD group. 36 patients with asymptomatic cholelithiasis in whom a liver biopsy was performed during programmed laparoscopic cholecystectomy also took part in the study (Table R2, Results Part 3). All had histologically normal liver (NL), normal fasting glucose, cholesterol and TGs, normal

serum aminotransferase levels and no evidence of HBV, HCV and HIV infections. In addition, none of these individuals consumed >20 g alcohol per day. Neither NAFLD patients nor subjects with NL used potentially hepatotoxic drugs.

The study was performed in agreement with the Declaration of Helsinki and with local and national laws. The Human Ethics Committee of the University Hospital Santa Cristina and the University of Basque Country approved the study procedures and written informed consent was obtained from all patients before inclusion in the study.

4.3.1. **Clinical and laboratory assessment in human samples**

After a 12 h overnight fast, clinical and anthropometric data as well as venous blood samples were obtained from each patient at the time of liver biopsy. Plasma insulin was determined by a chemiluminescent microparticle immunoassay (ARCHITECT insulin; Abbot Park, Illinois, USA). Insulin resistance was calculated by the homeostasis model assessment (HOMA-IR)[139].

For lipoprotein analysis, serum samples from NAFLD-1 or NAFLD-2 patients were pooled and TG content in serum lipoprotein subfractions was quantified. Lipoproteins were separated by FPLC as previously detailed (see section 4.2.7.).

4.3.2. **Liver tissue studies in human samples**

Hematoxylin-eosin and Masson´s trichrome-stained paraffin-embedded liver biopsy sections were evaluated by an experienced hepatopathologist blinded to the clinical data. Steatosis was assessed as defined by Kleiner et al[140]. The percentage of hepatocytes containing lipid droplets in each liver biopsy was grade as follows: grade 0, < 5% of steatotic hepatocytes; grade 1, 5-33% of steatotic hepatocytes; grade 2, >33-66% of steatotic hepatocytes; and grade 3, >66% of steatotic hepatocytes.

Lipid analysis of human liver tissue samples was performed as already explained after homogenization (see section 4.2.1.), lipid extraction (see section 4.2.6.1.), separation (see section 4.2.6.2.2.) and quantification (see section 4.2.6.3.).

4.3.3. Immunohistochemistry of human samples

GNMT protein expression was analysed in 17 NAFLD patients (6 from NAFLD-1 group and 11 from NAFLD-2 group) and in 5 subjects with normal liver. Immunostaining was performed on formalin-fixed paraffin- embedded liver biopsy sections. Slides were boiled in a microwave oven for 20 minutes in 10 mM buffer citrate, pH 6.0; and then left in the buffer for 30 minutes at room temperature. Preparations followed an overnight incubation with the primary rabbit antibody against GNMT provided by Zigmund Luka. Computational image analysis with FRIDA image analysis software was performed and the area of liver tissue covered by GNMT-positive cells was measured.

4.4. Statistical analysis

The numeric data obtained in the experiments are represented as mean ± SEM (Standard error of the mean).

The statistical analyses used to examine the statistical significance of the differences in the results depended on the group of results to be compared. The comparison between two groups was analysed using the unpaired Student's t-test or Mann-Whitney U test. For the examination of more than two groups of data the analysis of the variance (ANOVA) followed by Bonferroni test was applied.

Differences were considered significant when the probability of the null hypothesis (P) was <0.05. The statistical significant differences are stated with different symbols as explained in each figure caption, and the P value for ANOVAs is numerically reflected in the figures.

All analyses were performed using SPSS Version 15.0 software and GraphPad Version5.03.

5. Results

La auténtica ciencia enseña sobre todo a dudar y a saberse ignorante.

Miguel de Unamuno (1864-1936)

5. **RESULTS**

5.1. **Excess SAMe reroutes phosphatidylethanolamine towards phosphatidylcholine and triglyceride synthesis**

Non-alcoholic Fatty Liver Disease (NAFLD) is the most common cause of chronic liver disease in industrialised countries[142], it is generally linked to obesity, dyslipidemia and insulin resistance[118]. Its development has been associated with dysregulated levels of S-adenosylmethionine (SAMe) in mice[19, 20].

The deletion of Glycine N-methyltransferase (GNMT) protein in mice leads to a huge increase in hepatic SAMe[20]. This happens because GNMT is the main methyltransferase that regulates SAMe content in the liver[2]. On the other hand, Methionine Adenosyltransferase 1A (MAT1A) enzyme leads hepatic SAMe synthesis[2], and its absence produces a decrease in SAMe[19]. Low hepatic content in SAMe has been shown to reduce PC content leading to SREBP-1 activation and lipogenesis in *C. elegans* model; besides, the reduced PC quantity in HepG2 cells or in the liver of choline-phosphate cytidylyltransferase A knock out (KO) mice also leads to the activation of SREBP-1[59]. In addition, knocking out MAT1A in mice has been shown to disrupt Very Low Density Lipoproteins (VLDL) assembly, liver-secreted VLDL particles are small and triglyceride (TG)-poor[58]. MAT1A absence has also recently been shown to altered FA oxidation in the mitochondria[60]. The mentioned processes may prompt the development of hepatosteatosis in this animal model[58-60]. Fatty liver development also occurs in GNMT-KO mice[13] in which, as mentioned above, hepatic SAMe levels are markedly increased. But how can high levels of hepatic SAMe lead to the accumulation of fat in the liver? SAMe is the principal donor molecule of methyl groups[2], it is involved

in the synthesis of phosphatidylcholine (PC) from phosphatidylethanolamine (PE) via PE methyltransferase (PEMT) enzyme by three consecutive methylation reactions[119]. And it is by PEMT pathway that SAMe is related to glycerolipids metabolism. In this context, the aim of this part of the study was to unravel the mechanisms by which GNMT-KO mice develop NAFLD.

5.1.1. **GNMT deficiency in mice does not trigger liver triglyceride accumulation through the canonical pathways**

Primarily we analysed the usual pathways by which TG accumulates in the liver in order to know if any of them was being triggered by GNMT absence. Under physiological conditions TG liver levels are maintained in a low steady-state concentration thanks to a precise balance between acquisition and utilization[38].

Acquisition of TG is associated with free fatty acids (FFA) uptake and with *de novo* lipogenesis[38]. Increased *de novo* synthesis of TG and increased FFA uptake either from the diet or from those released into serum by the adipose tissue can lead to a imbalance and to TG accumulation[38]. GNMT-KO mice did not present any changes neither in the amount of food intake (Fig. R1a) nor in the serum circulating FFA (Fig. R1b) when compared to the wild-type (WT) animals, what correlates with glucose and insulin tolerance test that showed no insulin resistance in the KO in comparison with WT animals (Fig. R1c), indicating that FFA released from white adipose tissue (WAT) is not being stimulated[38]. What is more, their WAT was smaller than the WAT of their WT littermates (Fig. R1d), while their liver was bigger (Fig. R1e) and there was no change between genotypes in the body weight (Fig. R1f). *De novo* synthesis of TG was also assessed, in isolated hepatocytes the incorporation of [^{3}H]-acetate into TG was measured (Fig. R2a). Besides, the expression of genes involved in FA synthesis itself (*Fasn, Acaca*), in its regulation (*Srebf*) or in the production of the reducing power (NADPH) necessary for FA synthesis (*Cs, Me1, Pygl, G6pdx*) was analysed (Fig. R2b). Both results indicated that lipogenesis was not affected by GNMT ablation.
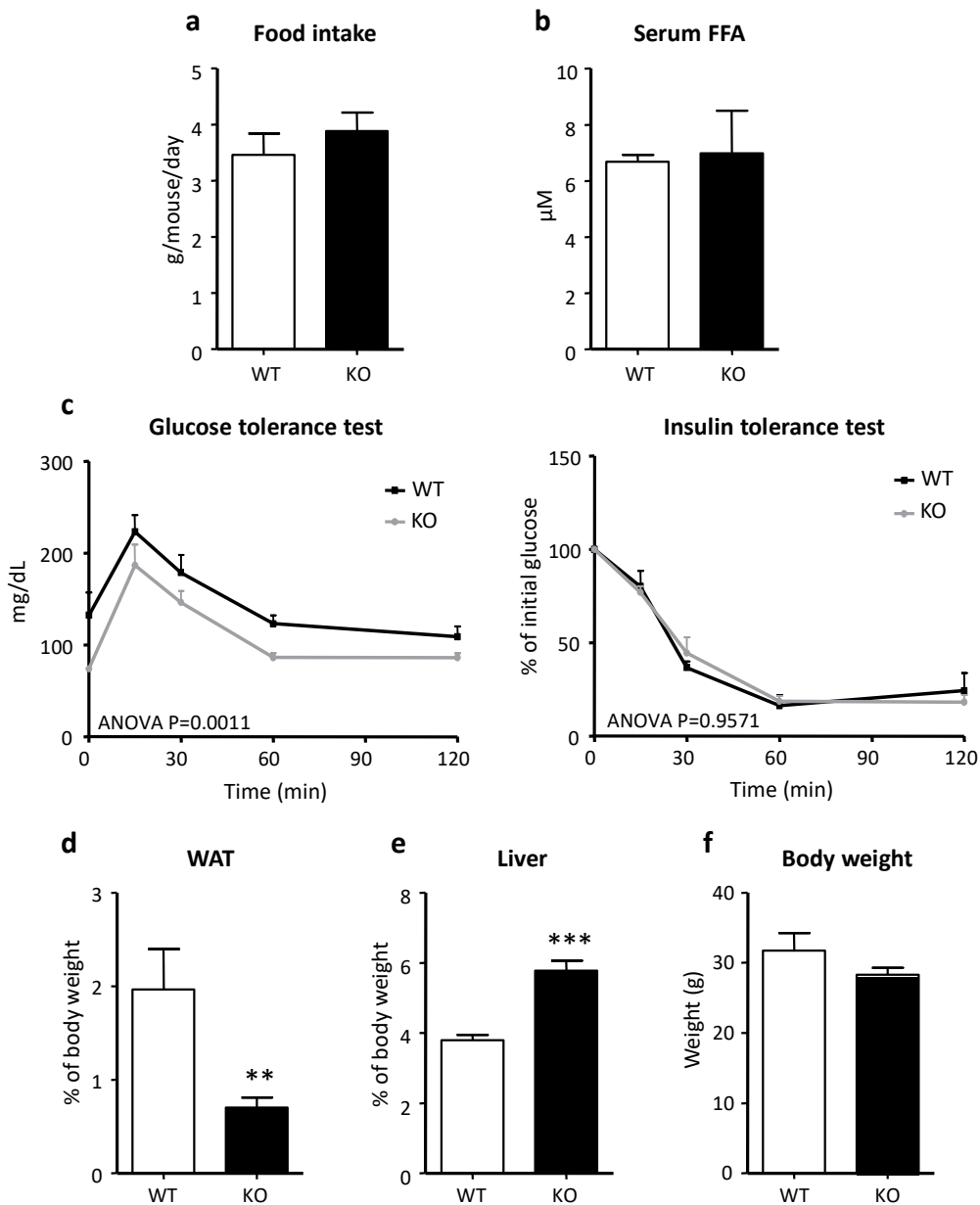
Figure R1. *Metabolic characterization of 3-month-old GNMT depleted mice.* 3-month-old wild type (WT) and GNMT-KO (KO) mice were fasted 3 hours before experiments were performed. (a) Food intake. (b) Serum fatty acid (FA) concentrations. (c) Glucose and insulin tolerance tests were assayed after oral administration of glucose (2mg/kg) or intraperitoneal injection of insulin (1U/kg). (d) Body weight. (e) Percentage of liver weight. (f) Percentage of white adipose tissue (WAT) weight. Values are mean±SEM of 4 animals per group. Statistical differences between KO and WT mice are denoted by **P<0.01; ***P<0.001 (Student's t test) and by two-way ANOVA.
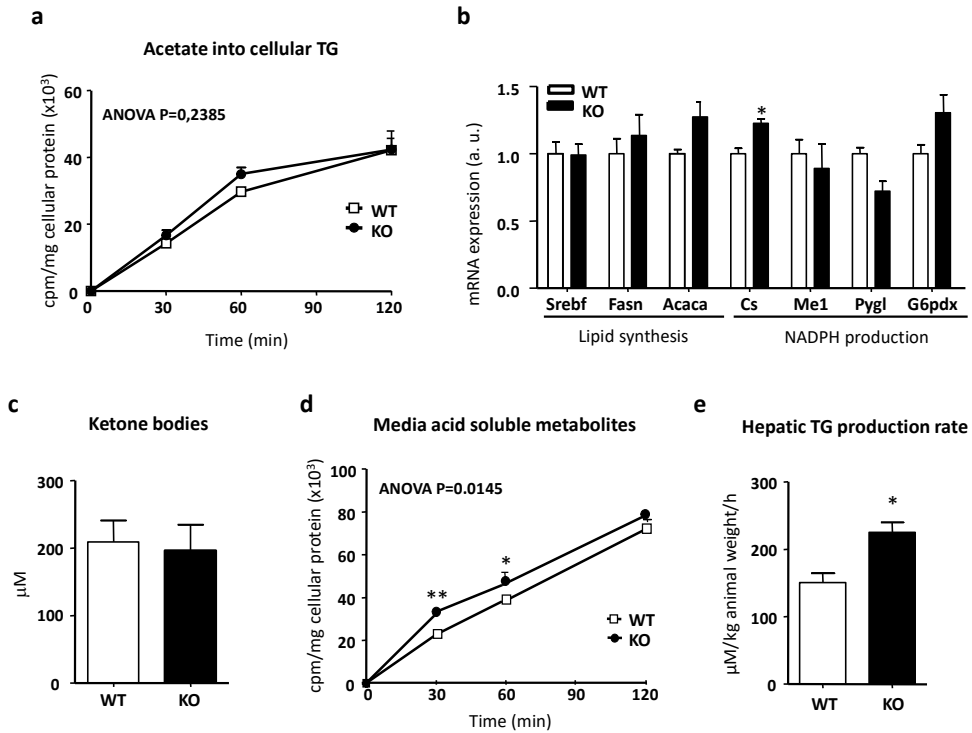
Figure R2. *GNMT ablation enhances TG secretion.* 3-month-old wild type (WT) and GNMT-KO (KO) were fasted 2 hours before experiments were performed. (a) Hepatocytes were isolated and incubated with [^{3}H]acetate for the time indicated. Radioactivity incorporated into TG was assessed with a scintillation counter. (b) Quantitative RT-PCR analysis of hepatic genes in WT and KO mice. (c) Hepatocytes were incubated with [^{3}H]oleate for the time indicated, the medium was harvested and the radiolabel in acid-soluble metabolites measured. (d) Serum was isolated and ketone bodies were quantified. (e) Hepatic TG secretion rate was measured after inhibition of VLDL metabolism with 1 g/kg poloxamer (P-407). *Acaca*, acetyl-CoA carboxylase; *Cs*, citrate synthase; *Fasn*, fatty acid synthase; *G6pdx*, glucose-6-phosphate dehydrogenase; *Me1*, malic enzyme 1; *Pygl*, glycogen phosphorylase; *Srebf*, sterol regulatory element-binding proteins. Values are means±SEM of 4-6 animals per group. Statistical differences between KO and WT mice are denoted by *P<0.05 and **P<0.01 (Student's t test) and by two-way ANOVA.

TGs in liver are utilised through β-oxidation to obtain energy or secreted to the blood stream in the form of VLDL particles[38]. FA β-oxidation was barely altered in the absence of GNMT, as it can be interpreted from serum ketone bodies (KB) (Fig. R2c) and the *in vitro* secretion of acid-soluble metabolites (Krebs cycle metabolites and KB) (Fig. R2d). Hepatic TG secretion was assessed *in vivo* after the inhibition of VLDL metabolism with poloxamer (P-407) (Fig. R2e), it was 55% elevated in GNMT-KO mice when compared to WT animals. According to these results, there is no imbalance between

acquisition and utilization of TG that can contribute to fatty liver in GNMT-depleted livers.

5.1.2. *Gnmt* ablation in mice activates the PEMT flux leading to the accumulation of diglyceride and triglyceride

The figures above demonstrate that none of the known pathways that lead to TG accumulation in the liver are contributing to fatty liver in the GNMT-KO mice animal model. Therefore we hypothesised that TG accumulation occurs as an adaptive response to the increased synthesis of PC through PEMT pathway induced by the elevated levels of SAMe (Fig. R3). SAMe is a substrate for PEMT enzyme[119], its excess in GNMT-KO mice livers would stimulate the flux from PE to PC, and that PC would be rerouted to DG and then TG production (Fig. R3).

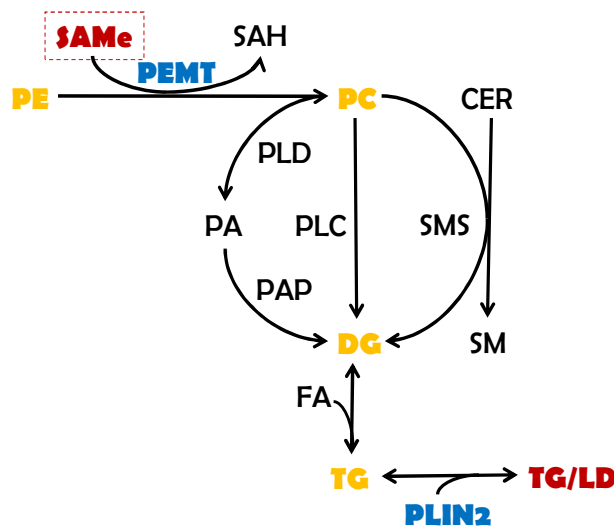**Figure R3.** *Schematic representation of SAMe role in mediating TG synthesis and accumulation via PEMT.* PE, phosphatidylethanolamine; PC, phosphatidylcholine; PA, phosphatidic acid; CER, ceramide; SM, sphingomyelin; DG, diglycerides; FA, fatty acids; TG, triglycerides; LD, lipid droplets; PEMT, PE N-methyltransferase; PLD, phospholipase D; PAP, PA phosphatase; PLC, phospholipase C; SMS, sphingomyelin synthase; PLIN2, perilipin2.
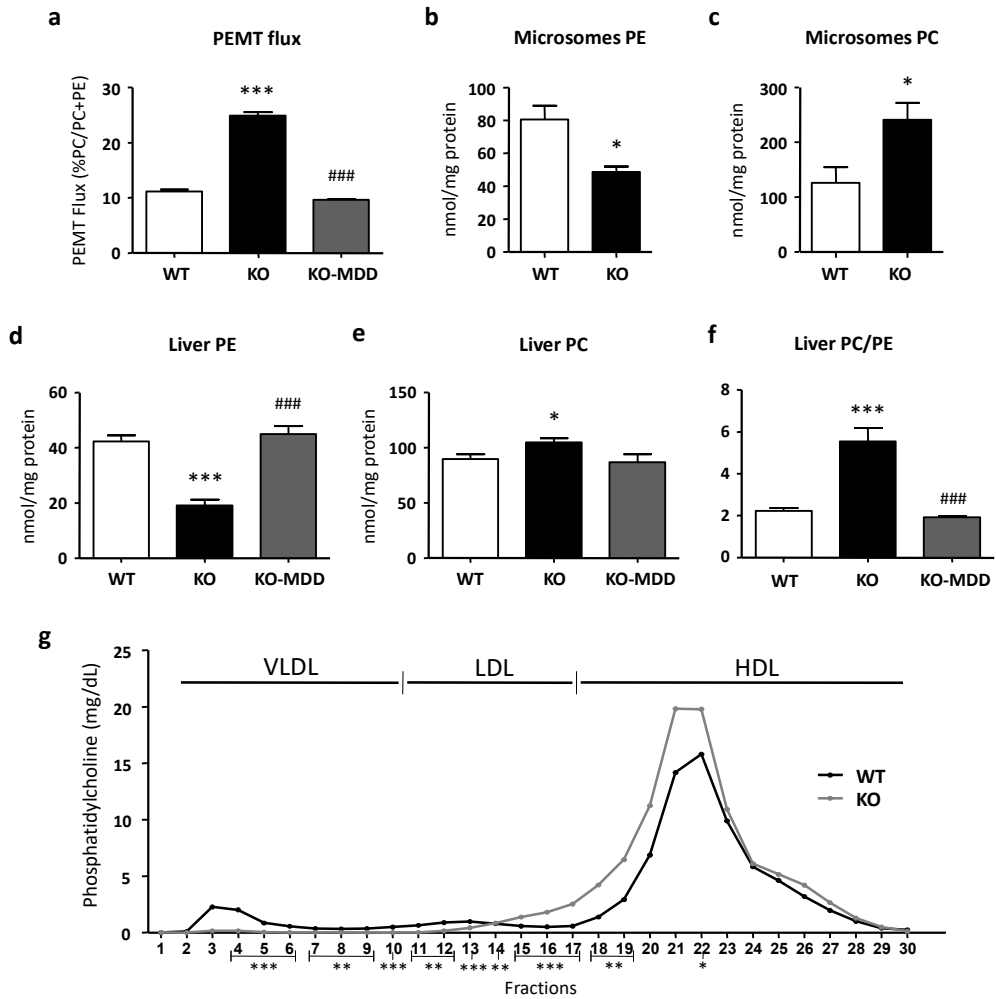
Figure R4. *Restoration of hepatic flux from PE to PC in GNMT-KO mice after feeding a methionine deficient diet.* 3-month-old wild type (WT), GNMT-KO (KO), and GNMT-KO mice fed a MDD (KO-MDD) for 3 weeks were fasted 2 hours before experiments were performed. (a) Hepatocytes were isolated and incubated with [^{3}H]ethanolamine for 4 hours, the radioactivity incorporated into PC was expressed as a percentage of the radiolabel incorporated into PC plus PE. (b-c) Microsomes were isolated from WT and GNMT-KO mice liver, and PE and PC levels quantified after lipid extraction and separation by TLC. (d) Liver PE and (e) PC were quantified after extraction and separation of lipids by TLC. (f) Liver PC/PE ratio. (g) PC content in serum lipoprotein fractions was quantified by a commercially available kit (Spinreact, Spain). Lipoprotein fractions were separated by ÄKTA fast-protein liquid chromatography using a Superose 6TM 10/300 column (GE Healthcare, Sweden). Values are means±SEM of 4-6 animals per group. Statistical differences between GNMT-KO and WT mice are denoted by *P<0.05, **P<0.01 and ***P<0.001 (Student's t test); between GNMT-KO and GNMT-KO fed a MDD are denoted by ### P<0.001 (Student's t test).

To prove the hypothesis we assessed PEMT flux by measuring the incorporation of [^{3}H]-ethanolamine into PE and PC in isolated hepatocytes and calculating the

radioactivity incorporated into PC as a percentage of the radiolabel incorporated into the sum of PC and PE (Fig. R4a). As predicted PEMT flux was increased, a 2.5-fold rise was observed in GNMT-KO hepatocytes (Fig. R4a). Since PEMT activity is mainly localised to the endoplasmic reticulum (ER)[119], the amount of PC and PE was analysed in whole liver microsomes (Fig. R4b,c). Consequently to PEMT overactivation a reduction of approximately 2-fold in the content of PE in microsomes and a 2-fold increase in microsomes PC content was observed in GNMT depleted livers (Fig. R4b,c). Whole liver quantity of PE and PC was also measured, the measurement revealed a 2-fold decrease in PE and a slight increase in PC in the KO animals when compared to WT (Fig. R4d,e). The fact that the increase in the whole liver PC did not resemble the increase in microsomes, suggests that once translocated from the ER to other membranes PC is being rapidly catabolised and/or secreted in high-density lipoproteins (HDL). Accordingly, HDL-PC levels were increased in GNMT deficient mice in comparison with their WT counterparts (Fig. R4g), and diglyceride (DG) and TG, which can be products of PC catabolisation, were also augmented in the liver (Fig. R5a,b).

Table R1

Hepatic SAMe content

Mouse Genotype	SAMe ± SE, pmol/mg liver tissue
WT-PLIN2	44.7 ± 18.6
WT-GNMT	65.1 ± 7.4
WT-GNMT + MDD	56.4 ± 7.8
WT-GNMT/WT-PLIN2	41.7 ± 4.3
PLIN2-KO	38.7 ± 5.8
GNMT-KO	2,452 ± 158
GNMT-KO + MDD	74.4 ± 12.6
GNMT-KO/PLIN2-KO	1,667 ± 408

The values in the table are from 3-month-old mice. Livers were collected and SAMe content determined as described (8). Data are from 4-6 animals per group. MDD, mice fed a methionine deficient diet for 3-weeks; WT, wild type mice.
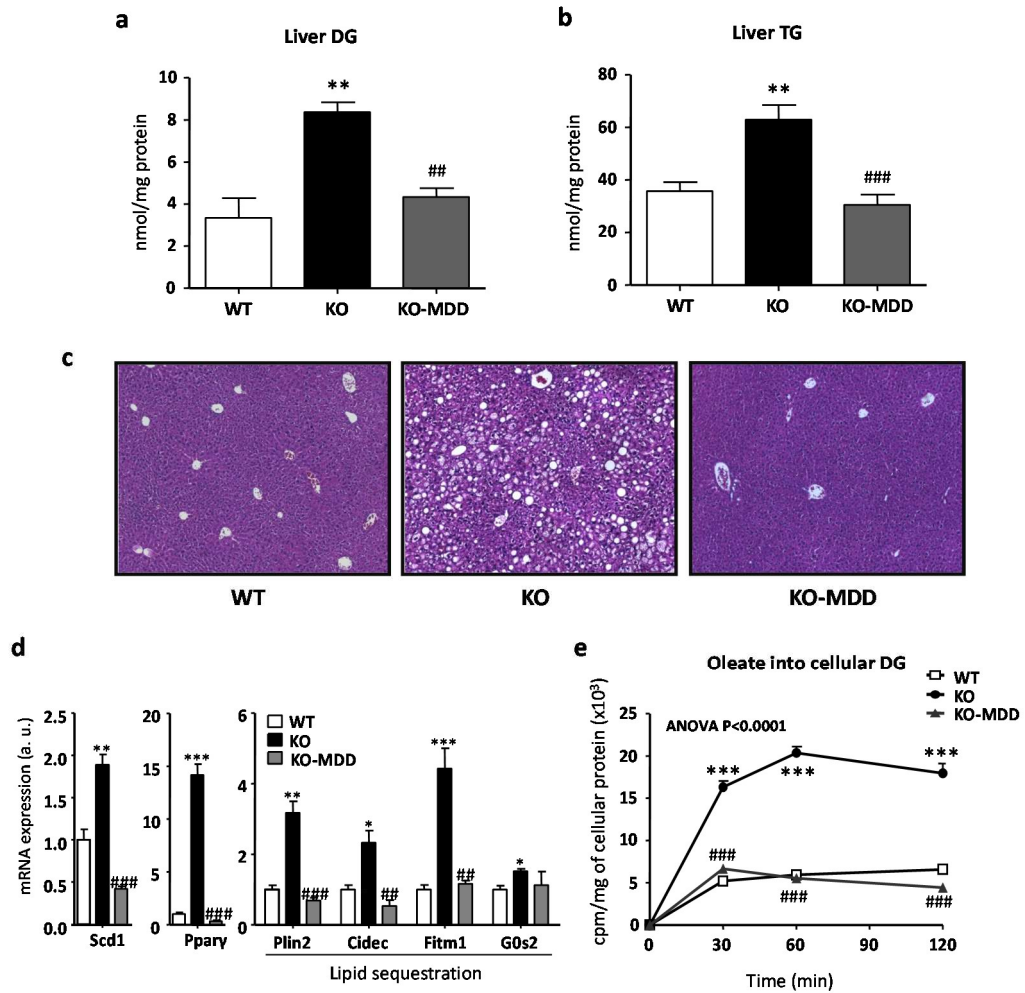
Figure R5. *Restoration of normal hepatic DG and TG content in GNMT-KO mice after feeding a methionine deficient diet.* 3-month-old wild type (WT), GNMT-KO (KO), and GNMT-KO mice fed a MDD (KO-MDD) for 3 weeks were fasted 2 hours before experiments were performed. (a) Liver DG and (b) TG were quantified after extraction and separation of lipids by TLC. (c) Representative hematoxylin and eosin staining. (d) Hepatocytes were isolated and incubated with [³H]oleate for the indicated time. Radioactivity incorporated into DG was assessed with a scintillation counter. (e) Quantitative RT-PCR analysis of genes in livers. *Cidec*, cell-death-inducing DFFA-like effector c; *Fitm1*, fat storage-inducing transmembrane protein 1; *G0s2*, G0/G1 switch gene; *Plin2*, perilipin 2; *Pparg*, peroxisome proliferator-activated receptor γ; *Scd1*, stearoyl-CoA desaturase 1. Values are means±SEM of 4-6 animals per group. Statistical differences between *GNMT-KO* and WT mice are denoted by *P<0.05; **P<0.01 and ***P<0.001 (Student's t test); between GNMT-KO and GNMT-KO fed a MDD are denoted by ##P<0.01 and ### P<0.001 (Student's t test). Multiple comparisons among groups were statistically evaluated by two-way ANOVA.

It should be considered that feeding GNMT-KO mice with a methionine-deficient-diet (MDD) in order to reduce hepatic SAMe levels (Table R1), restores not only SAMe in the liver but also PEMT flux and PE, PC, DG and TG liver levels. All those measurements went back to resemble WT values after MDD feeding (Fig. R4a,d,e,f, R5a,b), and steatosis, hence, was prevented (Fig. R5c), demonstrating that the observed changes were due to high SAMe levels.

Accordingly, *Plin2, Cidec, Fitm1* and *G0s2*, genes that encoded proteins involved in lipid sequestration, were upregulated in GNMT-deficient mice and restored to WT expression after feeding a MDD (Fig. R5d). Peroxisome proliferator-activated receptor γ (Pparγ), a prosteatotic transcription factor that regulates *Plin2, Cidec and G0s2*, was widely upregulated in mice with GNMT deficiency; *Scd1*, a FA desaturase, was also overexpressed; in both cases the level of expression recovered after the MDD. MDD feeding also reverted the incorporation of [^{3}H]-oleate into DG in GNMT-deficient hepatocytes that was 4-fold increased with respect to WT hepatocytes under the control diet (Fig. R5e).

To finally prove that PEMT overactivation is behind the accumulation of TG in GNMT-depleted livers we inhibited PEMT enzyme with 3-deazaadenosine (DZA)[128] in GNMT-deficient hepatocytes what resulted in decreased TG levels (Fig. R6). This result strongly supports the hypothesis that PEMT enhanced activity is leading hepatic TG accumulation through PC synthesis and catabolism to TG in the absence of GNMT.
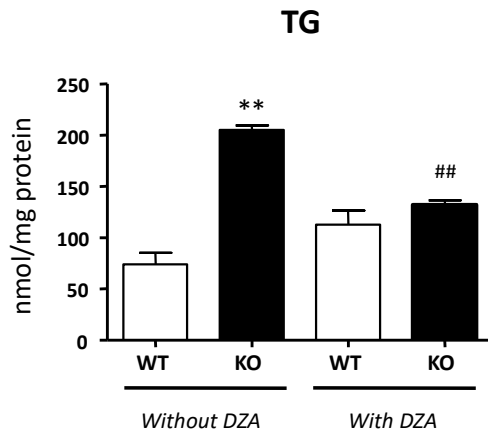
TG

Figure R6. *Inhibition of PEMT leads to a reduction in TG accumulation.* Hepatocytes of 3-month-old wild type (WT) and GNMT-KO (KO) were isolated and incubated with 3-deazaadenosine (DZA, 10 µM) for 4 hours and at the end of this period the content of TG quantified. Values are means±SEM of 4-6 animals per group. Statistical differences between *GNMT-KO* and WT mice are denoted by **P<0.01 and between GNMT-KO without DZA and with DZA by ##P<0.01 (Student's t test).

5.1.3. **Triglyceride accumulation through PEMT flux in GNMT-KO mice persists in 8 month-old mice.**

The already mentioned results were obtained from 3-month-old mice lacking GNMT enzyme. At this age the liver exhibits steatosis and fibrosis, which were more obvious in 8-month-old mice livers[13]. NAFLD progression even leads to hepatocarcinoma in the oldest animals[13].

To demonstrate that TG accumulation, through PEMT pathway, is not a transitory state in NAFLD development in 3-month-old GNMT-KO mice, we tested 8-month-old mice in the same terms. Food intake and body weight continued to be steady between the 2 genotypes (Fig. R7a,b). The presence of fat in the liver was still obvious because of the GNMT-KO liver overweight when compared to their WT littermates (Fig. R7c). The amount of WAT with respect to body weight was also less in the older GNMT-defective mice in comparison to their WT (Fig. R7d). Accordingly, FA in serum were unchanged (Fig. R7e), and completely in agreement the 8-month-old KO proven not to be insulin resistant but to have insulin sensitivity to a certain degree and to manage glucose more easily than the WT genotype (Fig. R7f). We continued analysing the canonical pathways

by which TG usually accumulates in the liver. We analysed the gene expression of *Fasn* and *Acaca*, the main enzymes involved in FA biosynthesis[38], and the protein levels of total acetyl-CoA carboxylase (ACC) and the phosphorylated form (pACC). *Fasn* and *Acaca* expression was unchanged (Fig. R7g) while ACC and pACC were augmented in the GNMT-depleted livers when compared to WT (Fig. R7h). The pACC/ACC ratio was also higher in the GNMT-KO (Fig. R7h), since the phosphorylated form of ACC is the inactive one[143], the larger pACC/ACC ratio in the KO implies that, concerning this enzyme, FA synthesis was not stimulated. The analysis of FA utilization revealed that β-oxidation was not stimulated, as KB quantity in serum remained unaltered (Fig. R7i). And finally, the secretion of TG from the liver was still augmented (Fig. R7j) as observed in the younger GNMT-KO animals. Altogether, these results indicate that the hepatosteatosis in 8-month-old as in 3-month-old mice is not being caused by the common TG accumulation pathways.
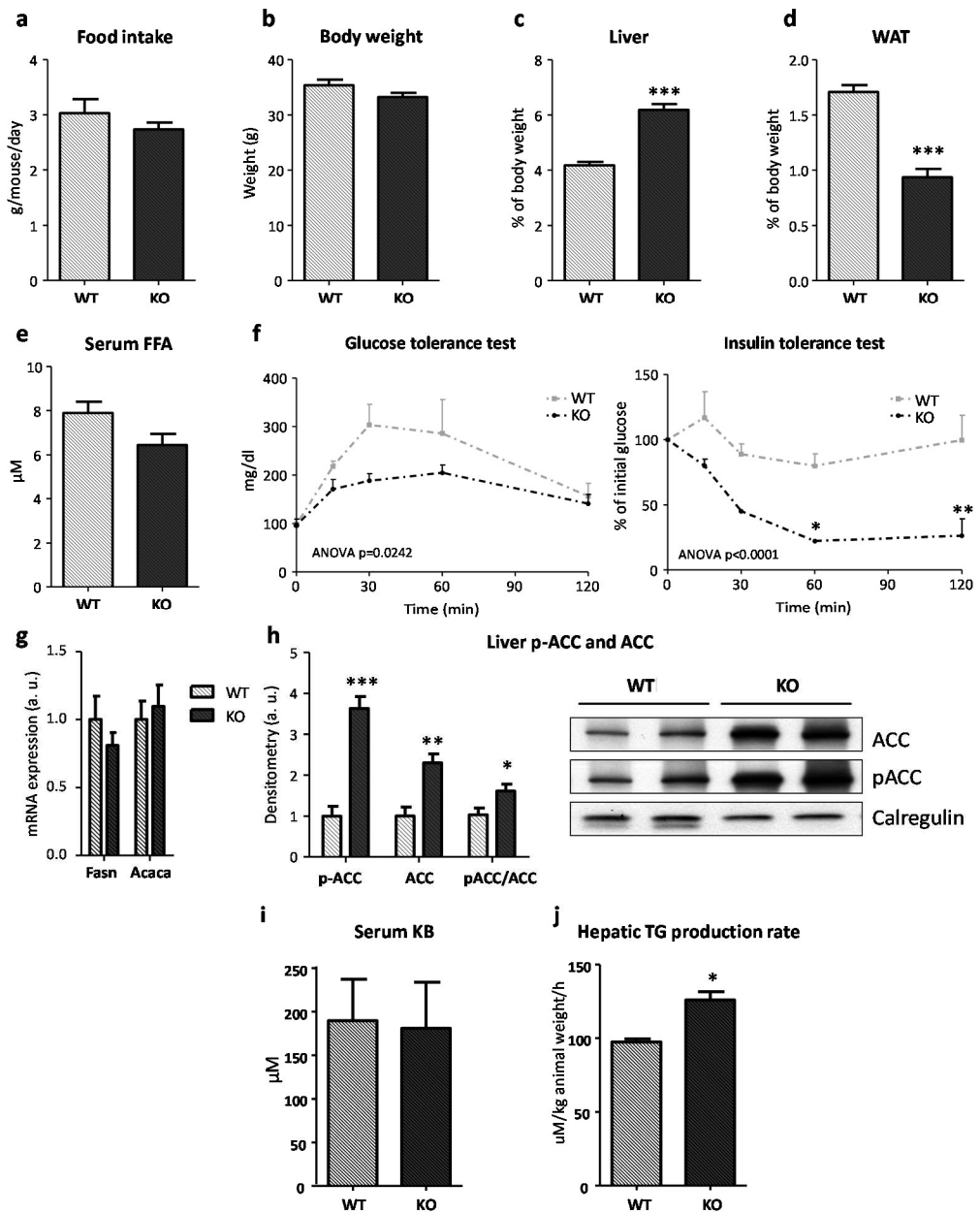
Even so, going backwards in the hypothesised pathway of liver TG accumulation, in the 8-month-old GNMT-KO mice we still found an increase of 42% in TG, of 54% in DG, a 2.3–fold decrease in PE and no changes in PC in the liver (Fig. R8a-d). Liver PC/PE ratio was still markedly augmented (Fig. R8e) in the KO animals as compared with the WT ones. The decrease in PE and the increase in PC in microsomes (Fig. R8f-g) also remained as in the younger animals.

In order to conclusively prove that the overactivation of the PEMT pathway is yet occurring in 8-month-old GNMT-depleted hepatocytes PEMT flux was measured as mentioned above showing a 1.6-fold increase in de KO mice when compared to their WT littermates (Fig. R8h).

Altogether, these data indicate that the older mice (8-month-old), which exhibit a more developed stage of liver disease, with higher degree of fibrosis and hepatocellular carcinoma, resemble the younger (3-month-old) in almost all the analysed parameters.

Figure R7. ***8-month-old metabolic state resembles 3-month-old GNMT-KO mice.*** 8-month-old wild type (WT) and GNMT-KO (KO) mice were fasted 2 or 3 hours before experiments were performed. (a) Food intake. (b) Body weight. (c) Percentage of liver weight. (d) Percentage of white adipose tissue (WAT). (e) Serum fatty acid (FA) concentrations. (f) Glucose and insulin tolerance tests were assayed after oral administration of glucose (2mg/kg) or intraperitoneal injection of insulin (1U/kg). (g) Quantitative RT-PCR analysis of hepatic genes in WT and KO mice. *Acaca*, Acetyl-CoA Carboxylase 1; *Fasn*, Fatty Acid Synthase. (h) Liver ACC (Acetyl-CoA Carboxylase) and p-ACC content was assessed by immunoblotting using calregulin as normaliser. (i) Serum was isolated and ketone bodies were quantified. (j) Hepatic TG secretion rate was measured after inhibition of VLDL metabolism with 1 g/kg poloxamer (P-407). Values are mean±SEM of 4 animals per group. Statistical differences between KO and WT mice are denoted by * $P<0.05$; **$P<0.01$ and ***$P<0.001$ (Student's t test) and multiple comparisons among groups were statistically evaluated by two-way ANOVA.
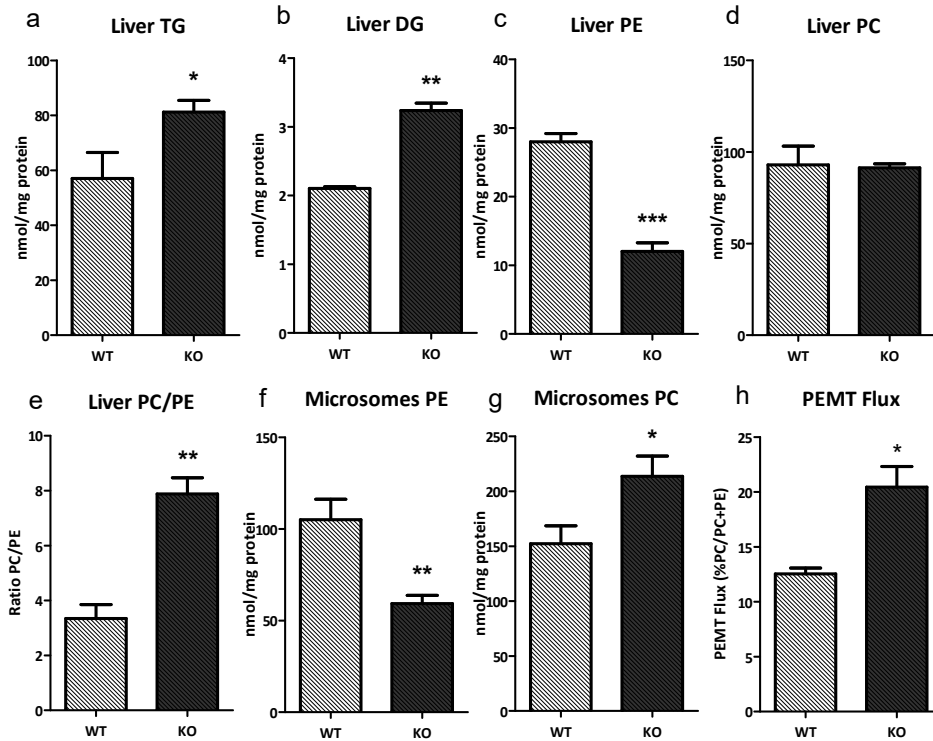
Figure R8. *GNMT ablation increases hepatic flux from PE to PC in 8-month-old mice.* 8-month-old wild type (WT) and GNMT-KO (KO) mice were fasted 2 hours before experiments were performed. (a) Liver TG, (b) DG, (c) PE and (d) PC were quantified after extraction and separation of lipids by TLC. (e) Liver PC/PE ratio. (f-g) Microsomes were isolated from WT and GNMT-KO mice liver, and PE and PC levels quantified after lipid extraction and separation by TLC. (h) Hepatocytes were isolated and incubated with [3H]ethanolamine for 4 hours, the radioactivity incorporated into PC was expressed as a percentage of the radiolabel incorporated into PC plus PE. Values are mean±SEM of 4 animals per group. Statistical differences between KO and WT mice are denoted by * P<0.05 and **P<0.01 (Student's t test).

5.1.4. **Deletion of PLIN2 in GNMT-KO mice inhibits lipid sequestration and promotes gluconeogenesis**

TG excessive accumulation in the form of Lipid Droplets (LD) is a key feature for fatty liver development[45]. LD are dynamic cellular organelles that store neutral lipids (mostly TGs and sterol esters) constrained by a monolayer of phospholipids[42]. LD composition also comprises some proteins, such as perilipin family proteins, which are the most abundant structural proteins on LD. Perilipin proteins not only stabilise LD, but also regulate the lipolysis of the neutral lipids stored in them[144]. Perilipin 2 (PLIN2), a

perilipin family member, has been shown to protect against hepatic TG accumulation when deleted in mice, and to be increased in the fatty liver[45]. Accordingly, PLIN2 expression is increased in the liver of GNMT-KO mice. In adipocytes and adipose tissue, PE methylation via PEMT has been demonstrated to promote the formation and stability of LD[145]. We reasoned that increased PC synthesis via PEMT would promote LD biosynthesis and steatosis in GNMT-KO mice. To prove this, a double knockout mice was created by crossing PLIN2-KO mice with GNMT-KO to produce a novel GNMT-PLIN2 double knockout (dKO) mouse model, in which hepatic SAMe levels (Table 1), and PE, PC, DG and TG were determined in the liver (Fig. R9a-e).

SAMe levels in the dKO animals (Table 1) remained almost as elevated as they were only with GNMT absence, therefore PLIN2 deletion had scarce effect on its hepatic concentration. Consistent with the high SAMe levels was the finding that liver PE content was 2-fold reduced in GNMT-PLIN2-KO mice, while PC levels persisted normal (Fig. R9a,b), as it happened in GNMT-KO animals, therefore, PC/PE ratio was also increased in the dKO with respect to their WT counterparts (Fig. R9c). In contrast to GNMT deficient mice, DG levels augmentation in the dKO mice was not as high as it was in GNMT-KO mice (Fig. R9d), yet it was significantly increased; but the liver TG content not only was not augmented but it was 2-fold decreased in the GNMT-PLIN2-KO animals (Fig. R9e). Hence, as expected, dKO mice failed to develop hepatoesteatosis (Fig. R9f) in spite of the high levels of SAMe and the low levels of PE in the liver.
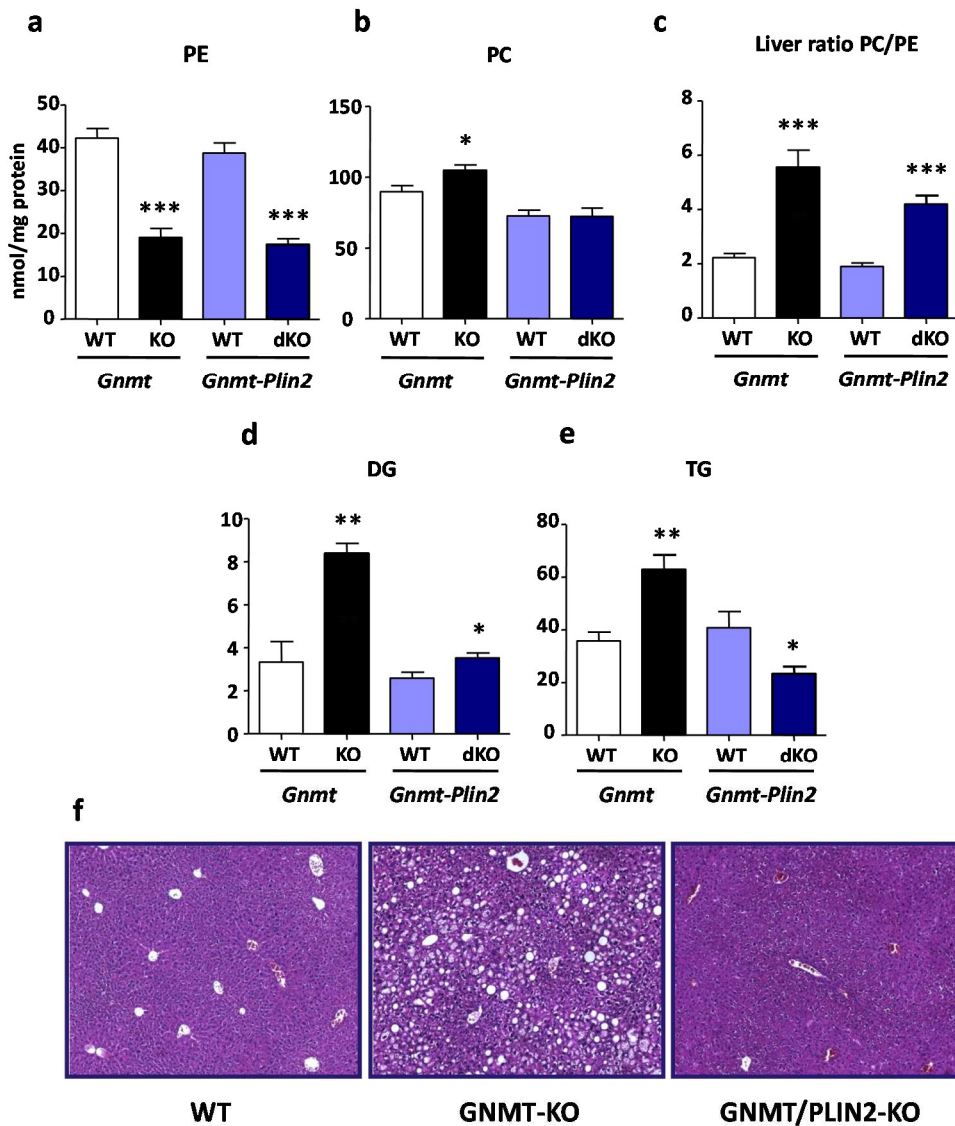
Figure R9. *Deletion of PLIN2 in GNMT-KO mice prevents liver steatosis.* 3-month-old GNMT-KO, GNMT/PLIN2-KO and their wildtypes (WT) were fasted 2 hours before experiments were performed. (a) PE, (b) PC, (c) DG, and (d) TG levels were quantified in liver after extraction and separation of lipids by TLC. (e) Liver PC/PE ratio. (f) Representative hematoxylin and eosin staining from 3-month-old wildtype (WT), GNMT-KO, and GNMT/PLIN2 mice. Values are means±SEM of 4-6 animals per group. Statistical differences between KO and WT mice are denoted by *$P<0.05$; **$P<0.01$; ***$P<0.001$ (Student t test).

The dKO animals were leaner than their counterparts (Fig. R10a), however they presented hepatomegaly (Fig. R10b) and they were more tolerant to glucose and to insulin (Fig. R10c,d). Under this metabolic context, despite the greater insulin sensitivity,

inhibition of lipid sequestration in GNMT-depleted mice induced a reduction in lipogenesis (Fig. R11a) while a higher hepatic TG secretion rate was maintained (Fig. R11b) as it occurred in single GNMT depletion. PLIN2 deletion in GNMT-KO mice also led to a reduction in serum KB (Fig. R11c) and had a minor positive effect on the production of acid-soluble metabolites (KB and Krebs cycle compounds) (Fig. R11d). This observation suggests that the acetyl-CoA generated through β-oxidation is being driven towards the Krebs cycle and gluconeogenesis. Accordingly, glucose production was increased in the double KO hepatocytes, both in the absence and in the presence of the precursors lactate/pyruvate and glycerol (Fig. R11e).
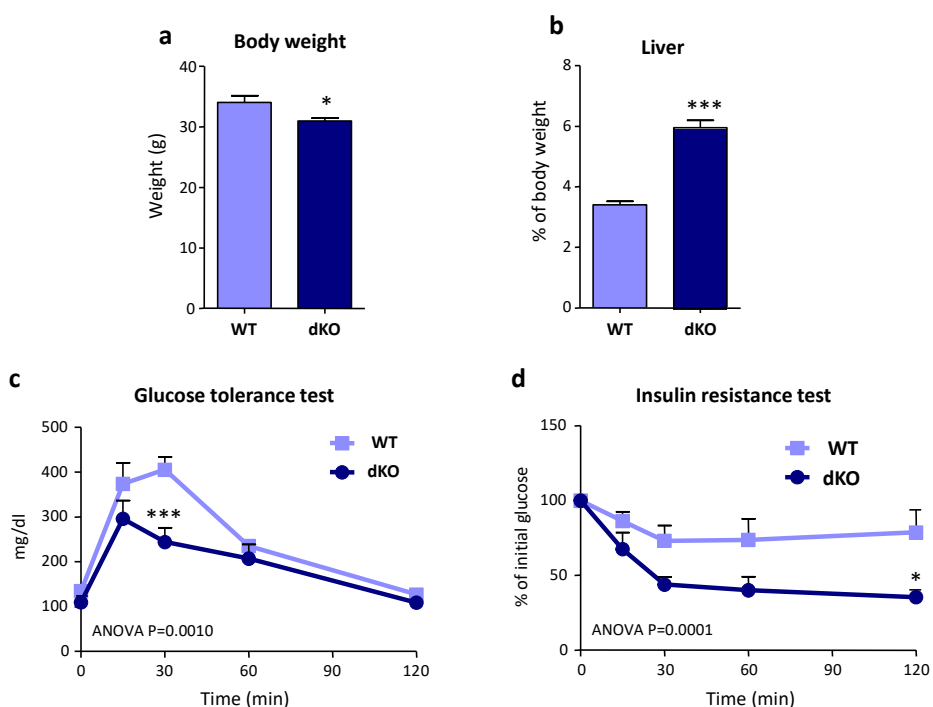
Figure R10. *Metabolic characterization of 3-month-old GNMT/PLIN2 depleted mice.* 3-month-old wild type (WT) and GNMT/PLIN2-KO (KO) mice were fasted 3 hours before experiments were performed. (a) Body weight. (b) Percentage of liver weight. Serum fatty acid (FA) concentrations. (c) Glucose tolerance test was assayed after oral administration of glucose (2mg/kg). (d) Insulin resistance test was assayed after intraperitoneal injection of insulin (1U/kg). Values are mean±SEM of 4-6 animals per group. Statistical differences between KO and WT mice are denoted by *P<0.05; ***P<0.001 (Student's t test) and by two-way ANOVA.
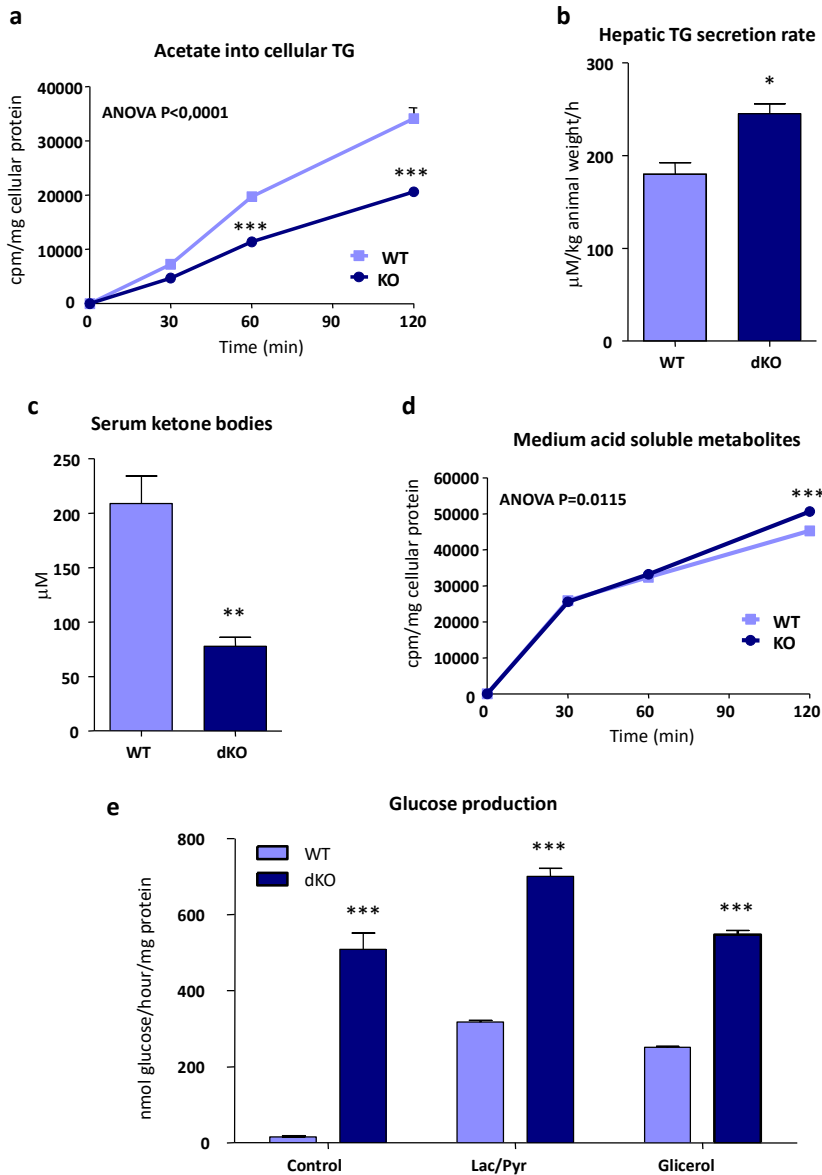
Figure R11. *Deletion of PLIN2 in GNMT-KO mice promotes gluconeogenesis.* 3-month-old wild type (WT) and GNMT/PLIN2-KO (KO) mice were fasted 2 hours before experiments were performed. (a) Hepatocytes were isolated and incubated with [^{3}H]acetate for the time indicated, radioactivity incorporated into TG was assessed with a scintillation counter. (b) Hepatocytes were incubated with [^{3}H]oleate for the time indicated, the medium was harvested and the radiolabel in acid-soluble metabolites measured. (c) Hepatic TG secretion rate was measured after inhibition of VLDL metabolism with 1 g/kg poloxamer (P-407). (d) Serum was isolated and ketone bodies quantified. (e) Hepatocytes were incubated in the absence or presence of lactate plus pyruvate (Lac/Pyr) at 30/3mM or 25mM glycerol, and glucose production determined. Values are means±SEM of 4-6 animals per group. Statistical differences between KO and WT mice are denoted by *P<0.05, **P<0.01, and ***P<0.001 (Student t test) and by two-way ANOVA.

5.2. **Altered levels of liver SAMe impair assembly and secretion of VLDL**

An essential feature of Non-Alcoholic Fatty Liver Disease (NAFLD) development is hepatic steatosis. The accumulation of triglycerides (TG) in the liver can occur after the impairment of lipid availability and metabolism in hepatocytes. Changes in the uptake of Fatty Acids (FA), in its de novo synthesis, in their catabolism or in their way out in the form of TGs into Very Low Density Lipoproteins (VLDL) can trigger hepatic fat accumulation[38]. As a matter of fact, an impairment in the secretion of VLDL has been described as a key factor in human NAFLD development[75].

VLDL assembly and secretion is controlled by numerous factors that ensure the output of adequate amounts of TGs from the liver. Apolipoprotein B (ApoB) translocation into the lumen of the endoplasmic reticulum (ER) during its translation while being lipidated by means of microsomal TG transfer protein (MTP) activity is the main process that determines VLDL secretion in the liver[78]. Another potentially regulated step in VLDL production and secretion is the mobilization of lipids from cytosolic lipid droplets towards the ER[92, 93], in this sense, factors that regulate cytosolic lipid storage, for instance perilipin 2 (PLIN2), can also impact VLDL secretion[95]. It has been described as well a requirement for Phosphatidylethanolamine (PE) Methyltransferase (PEMT) activity in the liver to ensure normal VLDL secretion[120], PEMT enzyme utilises S-adenosylmethionine (SAMe) as substrate.

Chronic changes in liver SAMe availability have shown to induce the spontaneous development of NAFLD in animal models[13, 19]. MAT1A-KO mice exhibit SAMe hepatic deficiency and a decrease of TG secretion into VLDL, what may be contributing to

hepatic steatosis. On the other hand, GNMT deficient mice have an increased availability of hepatic SAMe and likewise develop different stages of NAFLD[13].

We had previously observed that GNMT absence in mice altered hepatic TG secretion, as it has been shown in Part 1 of Results (Fig. R2e). Considering all the mentioned facts, we hypothesised that SAMe levels can control VLDL features, assembly and secretion. To prove it we have used both, MAT1A-KO and GNMT-KO mice administered SAMe for seven days and fed a Methionine-deficient-diet (MDD) for 3 weeks, respectively, in order to see the effects of normal hepatic SAMe levels recovery on VLDL assembly and secretion (Fig. R12).
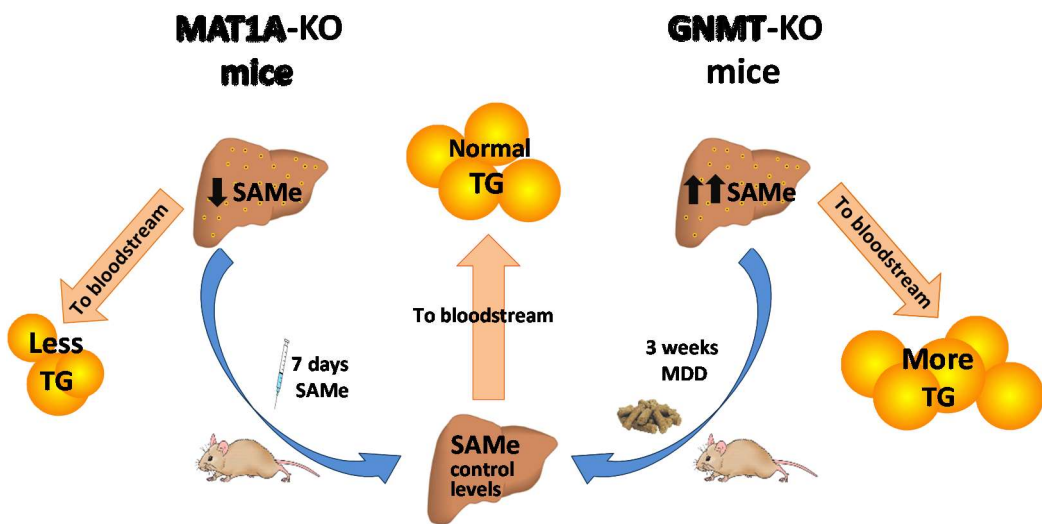
Figure R12. *Schematic representation of SAMe hypothesised influence on hepatic TG secretion.* MAT1A, Methionine Adenosyltransferase 1A; GNMT, Glycine N-Methyltransferase; SAMe, S-Adenosylmethionine; TG, Triglyceride; MDD, Methionine Deficient Diet.

5.2.1. **Low levels of liver SAMe reduce VLDL secretion in MAT1A-KO mice**

The 3-month-old MAT1A-KO mice have low levels of hepatic SAMe and present no signs of liver injury, yet they are more prone to develop NAFLD when fed a choline-

deficient diet than control animals, and the 8-month-old mice develop spontaneously non-alcoholic steatohepatitis (NASH)[19].

We already knew that assembly and secretion of VLDL is altered in MAT1A deficient mice at 3 months of age, what could be triggering the development of NASH at 8 months. The younger animals secrete VLDL enriched in ApoB and cholesterol (Cho) and poor in TG, what corresponds with smaller particle size, in comparison to wild-type (WT) animals. Besides, PEMT, Diacylglycerol (DG) acyltransferase (DGAT) and TG lipase activities, which are involved in the correct assembly of VLDL[78, 99], are diminished in mice lacking MAT1A[58].
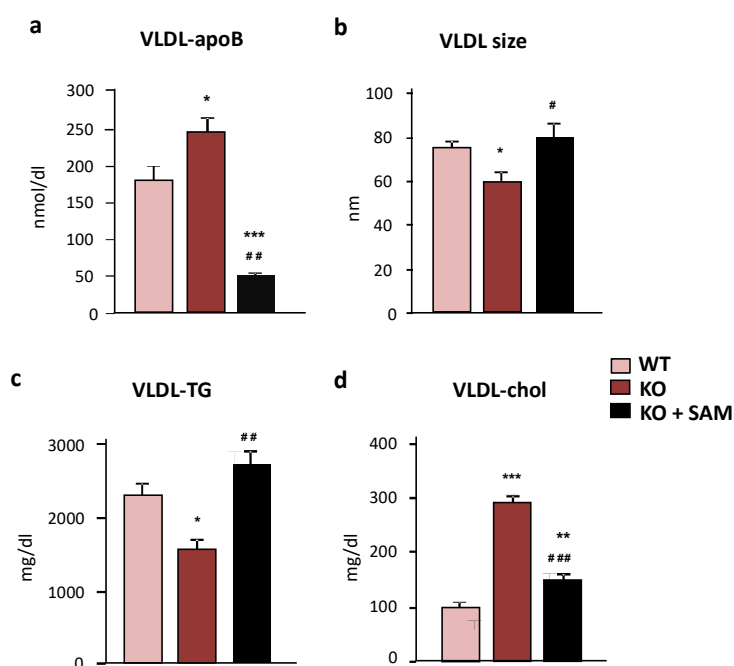
Figure R13. *SAMe administration recovers VLDL features in 3-month-old MAT1A-KO mice.* The 3-month-old wild-type (WT), MAT1A-knockout (MAT1A-KO) (KO) and SAMe treated MAT1A-KO (KO + SAMe) mice were fasted 2 hours prior to the injection of 1 mg/g poloxamer (P-407) in saline to inhibit VLDL metabolism. Before P-407 injection and 6 hours later blood was collected and VLDL (d < 1.02 g/mL) were isolated from serum by ultracentrifugation and characterised. (a) VLDL-ApoB was determined after being resolved by SDS-PAGE, stained with Gelcode Blue Stain reagent and quantified by optical densitometry using Quantity One software and phosphorylase b as a standard. (b) VLDL size. (c) VLDL-triglyceride (TG) and (d) VLDL-cholesterol (chol) content. Values are means 6±SEM of 4-8 animals per group. Statistical differences versus WT mice are denoted by *P < 0.05 and ***P < 0.001 and versus MAT1A-KO mice are denoted by #P < 0.05, ##P < 0.01, and ###P< 0.001 (Student's t test).
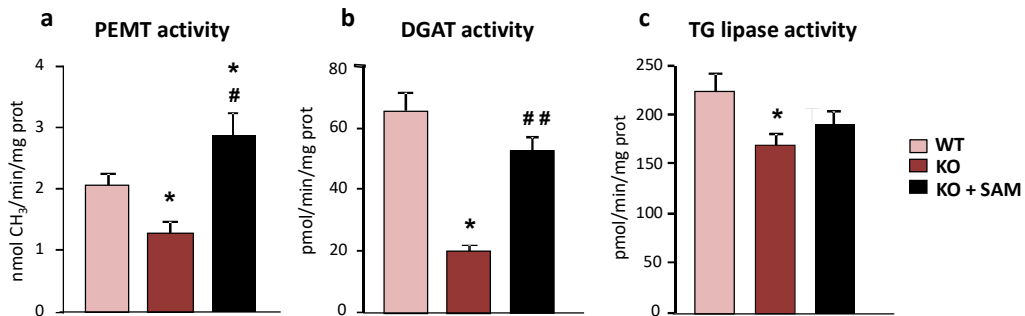
Figure R14. *SAMe recovers the activity of crucial enzymes involved in VLDL assembly in 3-month-old MAT1A-KO mice.* The 3-month-old wild-type (WT), MAT1A-knockout (MAT1A-KO) (KO) and SAMe treated MAT1A-KO (KO + SAMe) mice were fasted 2 hours before experiments were performed. Liver microsomes were prepared and microsomal (a) phosphatidylethanolamine N-methyltransferase (PEMT), (b) diacylglycerol acyltransferase (DGAT) and (c) TG lipase activities were determined as described in experimental procedures. Values are means 6±SEM of 4-8 animals per group. Statistical differences versus WT mice are denoted by *P < 0.05 and versus MAT1A-KO mice are denoted by #P < 0.05 and ##P < 0.01 (Student's t test).

To analyse if the aforementioned changes in MAT1A-KO mice VLDL assembly and secretion are linked to SAMe deficiency, we administered 3-month-old mice SAMe for seven days in order to normalised hepatic SAMe levels[122]. After the seven days of SAMe administration we found that VLDL-ApoB secretion decreased to be even lower than WT values (Fig. R13a) and VLDL size and TG and Cho content recovered to nearly resemble WT values (Fig. R13b-d) in mice lacking MAT1A. Furthermore, the administration of SAMe to MAT1A-KO animals recovered DGAT activity (Fig. R14b) and even stimulated PEMT activity over the WT values (Fig. R14a), while TG lipase activity did not recuperate (Fig. R14c). All together, these results show that SAMe levels are controlling VLDL assembly and secretion in MAT1A-KO mice.

5.2.2. Chronic high levels of SAMe in the liver disrupt VLDL assembly and features

At 3-months of age the liver of GNMT-KO mice exhibits steatosis and fibrosis[13] in the absence of insulin resistance (see Results Part 1 Fig. R1). They also show increased

TG secretion and augmented PEMT flux due to excess SAMe (see Results Part 1). To further understand the stimulated secretion of TG in GNMT deficient mice we performed an analysis of lipid storage mobilization and of the main enzymes involved in VLDL assembly. As expected, an increased turnover of TG lipid stores was observed in the hepatocytes of mice lacking GNMT enzyme (Fig. R15a). Moreover, MTP and DGAT activities were as well found to be increased (Fig. R15b,c) while TG lipase activity showed no change with respect to the WT animals (Fig. R15d). Besides, when PEMT activity was inhibited with 3-deazaadenosine (DZA) the increased TG secretion was also supressed in GNMT-KO mice hepatocytes (Fig. R15e), this points toward an involvement of PEMT in the secretion of VLDL in mice with hepatic high levels of SAMe lacking GNMT enzyme.

We further investigated VLDL features, and after inhibition of their catabolism, we found that the VLDL fraction secreted by GNMT-KO mice livers was 25% enriched in TG (Fig. R16a), whereas the amount of VLDL-PE was 75% less when compared with their WT counterparts values (Fig. R16b) and no changes were found in VLDL-PC secretion (Fig. R16c). VLDL-ApoB-100 content was reduced in the KO animals (Fig. R16d), and accordingly with it and with VLDL-TG increased secretion, VLDL-size was found to be also increased when GNMT was absent (Fig. R16e). All the described features of VLDL in GNMT-KO mice were restored to WT levels after feeding a MDD for 3 weeks (Fig. R16a-e); considering that MDD re-establish SAMe values, these results confirm that SAMe is involved in the correct assembly and secretion of VLDL in GNMT-KO mice.
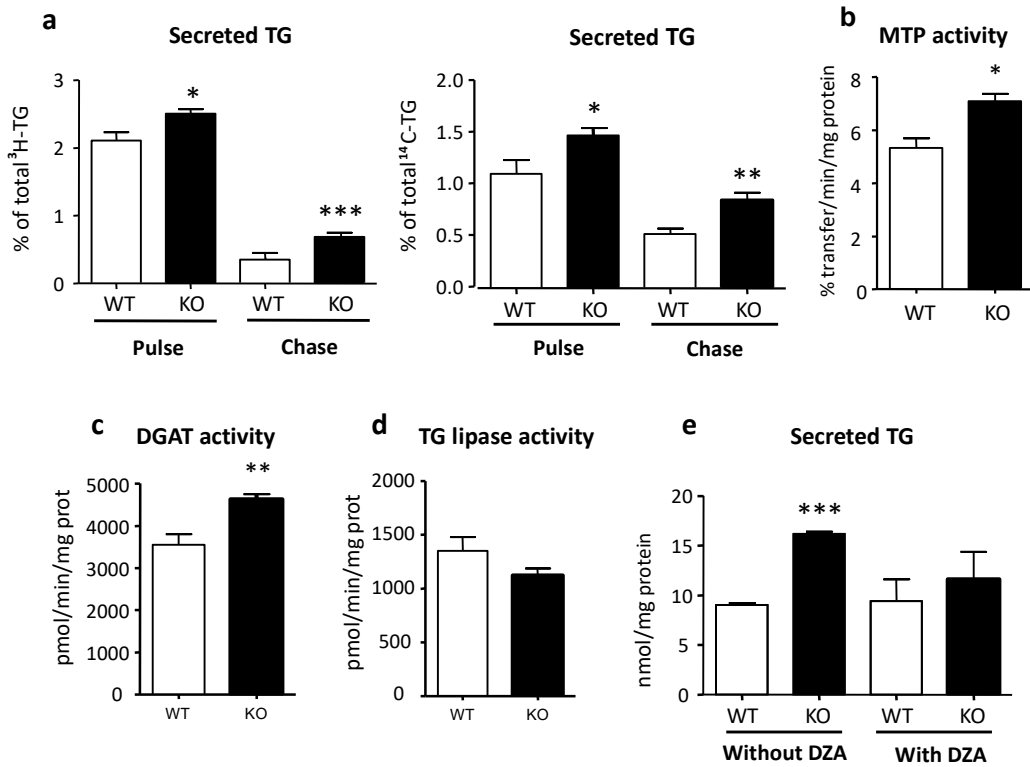
Figure R15. *GNMT deficiency increases triglyceride mobilization and assembly into VLDL particles.* 3-month-old wild type (WT) and *GNMT*-KO (KO) mice were fasted 2 hours before the experiments were performed. (a) Hepatocytes were incubated for 4 hours with 0.4 mM [^{3}H]oleic acid (5 µCi/dish) complexed with 0.5% fatty acid-free BSA and [^{14}C]glycerol (0.5 µCi/dish) (pulse), after a 1-hour wash in DMEM, cells were incubated for 4 hours (chase). The percentage of total [^{3}H]-TG and [^{14}C]-TG secreted into the media after both pulse and chase periods was calculated. (b) Hepatocytes were incubated with 3-deazaadenosine (DZA, 10 µM) for 4 h and TG secretion into the medium was determined. (c) MTP TG transfer activity was measured using a fluorescence assay. (d) Diacylglycerol acyltransferase (DGAT) and (e) triglyceride (TG) lipase activities were determined by radiometric assays, all as described in experimental procedures. Values are mean ± SEM of 5-6 animals per group. Statistical differences between GNMT-KO and WT mice are denoted by *P<0.05; **P<0.01 and ***P<0.001 (Student's t test).
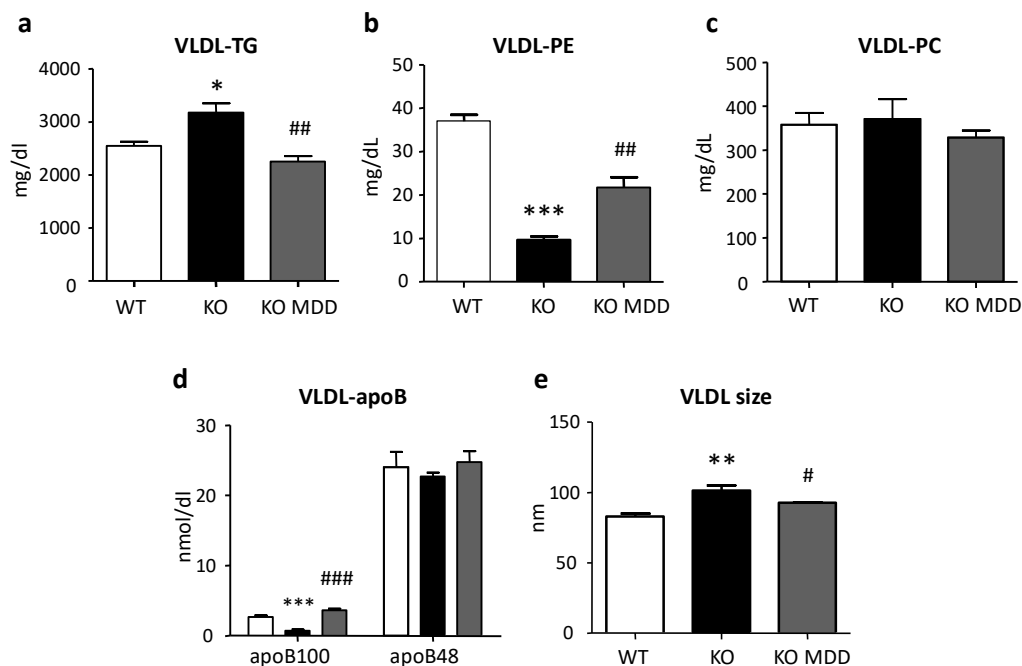
Figure R16. *VLDL features are restored after feeding a methionine deficient diet (MDD) to GNMT-KO mice.* Wild type (WT), GNMT-KO (KO) and GNMT-KO mice fed a MDD (KO MDD) were fasted for 2 h. Before the injection of 1 g/kg poloxamer (P-407) and 6 h later, VLDLs were isolated from the serum and characterised for (a) triglyceride (TG), (b) phosphatidylethanolamine (PE) and (c) phosphatidylcholine (PC) content after lipid extraction and separation by TLC. (d) VLDL-ApoB was determined after being resolved by SDS-PAGE, stained with Gelcode Blue Stain reagent and quantified by optical densitometry using Quantity One software and phosphorylase b as a standard. (e) VLDL size. Values are mean ± SEM of 5–6 animals per group. Statistical differences between GNMT-KO and WT mice are denoted by *P <0.05; **P <0.01 and ***P <0.001; and differences between GNMT-KO and GNMT-KO fed a MDD are denoted by #P <0.05; ##P <0.01 and ###P <0.001 (Student's t test).

Figure R17. *Liver ApoB content is reduced when SAMe levels are increased.* Wild type (WT), GNMT-KO (KO) and GNMT-KO mice fed a MDD (KO MDD) mice were fasted for 2 h. (a) Liver ApoB content in the liver from mice was assessed by immunoblotting using transferrin as loading control. (b) Quantitative RT-PCR analysis of Apob mRNA. (c) Binding of Apob mRNA to HuR was evaluated in livers by immunoprecipitation followed by quantitative real-time PCR. (d) The % of methylation of CpG sites within the Apob promoter was assessed by bisulfite pyrosequencing. Values are mean ± SEM of 4–6 animals per group. Statistical differences between GNMT-KO and WT mice are denoted by *P <0.05; **P <0.01 and ***P <0.001; and differences between GNMT-KO and GNMT-KO fed a MDD are denoted by #P <0.05; ##P <0.01 and ###P <0.001 (Student's t test).

The decrease in VLDL-ApoB-100 raised up the question whether it may be related to SAMe elevated levels. Liver *Apob* mRNA expression, ApoB content and some potential mechanisms that could affect mRNA expression and stability were analysed. Liver ApoB-100 content along with *Apob* mRNA expression were found to be decreased in GNMT-KO mice, and both recovered after MDD restoration of SAMe levels (Fig. R17a,b). *Apob* mRNA binding to the stabilizing HuR protein was also reduced and

restored after MDD feeding (Fig. R17c). Given that global DNA hypermethylation is a major characteristic of GNMT-KO mice[13], we wondered whether *Apob* promoter could also be methylated inducing a reduced expression of this gene. In the analysis of the promoter region of *Apob* we found a CpG rich region and six CpG sites, possible methylation sites, within this region, 3 of which were significantly hypermethylated in the KO mice in comparison with their WT littermates (Fig. R17d). Both, HuR-*Apob* binding and *Apob* promoter methylation levels recovered in GNMT-lacking mice after SAMe hepatic values were re-established feeding a MDD, indicating a role for SAMe in these processes (Fig. R17a-d).

5.2.3. **PLIN2 deficiency in GNMT-KO animals leads to an increase in VLDL-phosphatidylcholine secretion**

VLDL secretion is also influenced by factors that regulate lipid storage in hepatocytes cytosol, such as lipid droplets protein PLIN2[95]. We have already shown that deletion of PLIN2 in a GNMT-KO background results in the protection against hepatosteatosis and in the reduction of hepatic TG levels (see Results Part 1 Fig. R9). We wanted to know if PLIN2 absence in GNMT-KO mice also disturbs VLDL assembly and secretion, to achieve the aim mobilization of TG lipid stores and VLDL features were assessed. Accordingly with the lack of TG accumulation the turnover of TG lipid stores for secretion into VLDL was reduced in the double KO mice (dKO) when compared to WT (Fig. R18a). PLIN2 additional deletion led to an augmentation of VLDL-TG and size and to a reduction of VLDL-ApoB-100 and VLDL-PE (Fig. R18b-e), characteristics already observed in GNMT deficient mice. However, VLDL-PC secretion was found increased in the dKO when compared to WT animals (Fig. R18f), this was an unexpected finding, a novel feature not found in GNMT-KO mice that supports the role of PLIN2 in binding PC[147, 148]. In PLIN2-KO mice VLDL secretion analysis revealed no changes in the content of VLDL-PC, -PE and –ApoB (Fig. R19a-c) between KO and WT animals. Nonetheless,

PLIN2 deficient mice showed an increase in VLDL-TG secretion and in VLDL size (Fig. R19d,e), coincidentally with what has already been described[48]. For what is related to VLDL secretion, GNMT deficiency phenotype is maintained in spite of PLIN2 absence.
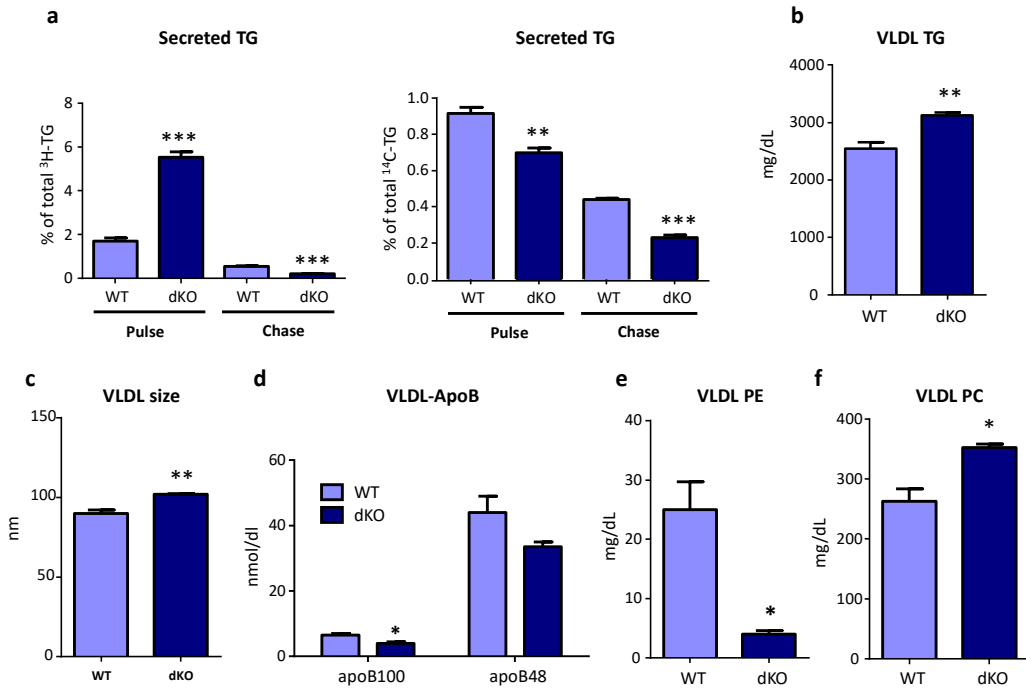
Figure R18. *PLIN2 deletion in GNMT-KO mice results in increased VLDL-PC secretion and decreased turnover of TG lipid stores for secretion into VLDL.* 3-month-old *GNMT-PLIN2*-KO (dKO) and their wild-types (WT) were fasted 2 hours before the experiments were performed. (a) Hepatocytes were incubated for 4 hours with 0.4 mM [³H]oleic acid (5 μCi/dish) complexed with 0.5% fatty acid-free BSA and [¹⁴C]glycerol (0.5 μCi/dish) (pulse), after a 1-hour wash in DMEM, cells were incubated for 4 hours (chase). The percentage of total [³H]-TG and [¹⁴C]-TG secreted into the media after both pulse and chase periods was calculated. (b) Before 1 g/kg poloxamer (P-407) injection and 6 hours later, blood was collected and VLDL (d<1.02 g/ml) were isolated from serum by ultracentrifugation and characterised for triglyceride (TG), (c) phosphatidylethanolamine (PE) and (d) phosphatidylcholine (PC) content after lipid extraction and separation by TLC. (e) VLDL-ApoB was determined after being resolved by SDS-PAGE, stained with Gelcode Blue Stain reagent and quantified by optical densitometry using Quantity One software and phosphorylase b as a standard. (f) VLDL size. Values are mean±SEM of 4-6 animals per group. Statistical differences between dKO and their WT mice are denoted by *P<0.05; **P<0.01 and ***P<0.001 (Student's t test).
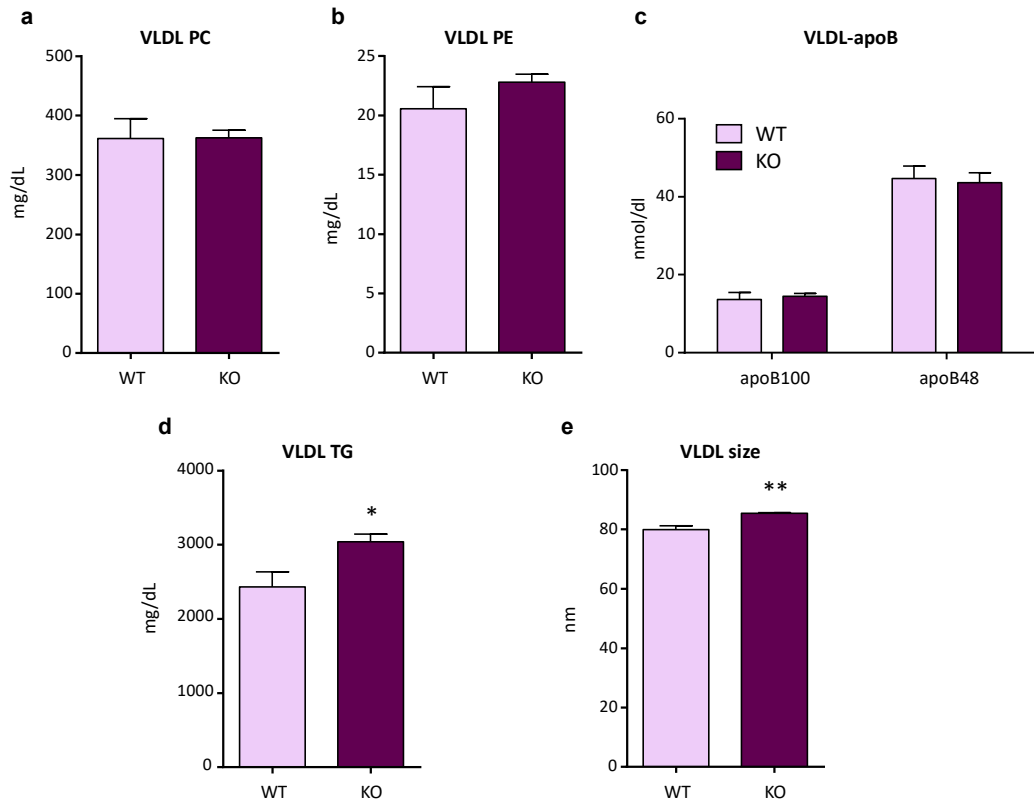
Figure R19. *VLDL secretion in PLIN2-KO mice.* 3- month-old wild type (WT) and PLIN2-KO (KO) were fasted 2 hours before the experiments were performed. Before 1 g/kg poloxamer (P-407) injection and 6 hours later, blood was collected and VLDL (d <1.02 g/ml) were isolated from serum by ultracentrifugation and characterised for (a) triglyceride (TG), (b) phosphatidylethanolamine (PE) and (c) phosphatidylcholine (PC) content after lipid extraction and separation by TLC. (d) VLDL-ApoB was determined after being resolved by SDS-PAGE, stained with Gelcode Blue Stain reagent and quantified by optical densitometry using Quantity One software and phosphorylase b as a standard. (e) VLDL size. Values are mean ± SEM of 4-5 animals per group. Statistical differences between PLIN2-KO and WT mice are denoted by *P <0.05; **P <0.01 (Student's t test).

5.3. **Elevated levels of liver SAMe increases VLDL clearance in NAFLD**

Based on[146] *Journal of Hepatology*, 2015; vol. 62:673-681

The liver develops a central role in the whole body lipid homeostasis. One of its many functions is to synthesise and secrete Very Low Density Lipoproteins (VLDL) into the bloodstream to deliver triglycerides, which serve as an energy source, to peripheral tissues. In plasma, VLDL levels respond to a steady-state between the hepatic secretion rate and the plasma rate clearance. Any imbalance between those two processes could lead to dyslipidemia and the consequent risk of cardiovascular disease[79, 121], which has been suggested to be one of the extrahepatic complications of Non-Alcoholic Fatty Liver Disease (NAFLD)[23].

Several factors, such as Triglycerides (TG) and apolipoprotein B (ApoB) availability and microsomal TG transfer protein (MTP) activity, regulate the hepatic secretion rate of VLDL[78]. Other factors, such as apolipoprotein E (ApoE) participate not only in VLDL secretion but also in VLDL clearance[149]. ApoE is a structural protein of VLDL which in the inside of hepatocytes facilitates ApoB maturation and subsequently VLDL assembly, and in the outside, in the circulation, it interacts with different receptors to mediate the cellular uptake of several lipoproteins[103].

We have already demonstrated in Part 2 of the Results that VLDL secretion is impaired in GNMT-KO mice; they secrete enlarged, ApoB- and phosphatidylethanolamine (PE)-poor and TG-enriched VLDL particles. Since high levels of hepatic S-adenosylmethionine (SAMe) disrupt VLDL assembly and features, we propose that VLDL clearance from the blood stream will also be affected.

5.3.1. **Serum triglyceride levels decrease along with GNMT expression**

In spite of the accumulation of TG in the liver GNMT-KO animals showed increased secretion of VLDL-TG along with other changes in VLDL features (Results Part 2 section 5.2.2). We wondered if changes in VLDL secretion were also disturbing VLDL clearance. Since one of the factors that define TG circulating levels in the bloodstream is the hepatic TG secretion rate, we first analysed serum TG levels. We found, unexpectedly, that GNMT deletion in mice resulted in a decrease of serum TG (Fig. R20a) due mostly to all VLDL and to some Low-density lipoproteins (LDL) sub-fractions (Fig. R20b), VLDLs that become smaller LDLs in the GNMT-KO when compared to WT mice (Fig. R20c). The analysis of serum ApoB, the apolipoprotein secreted by the liver into VLDL and LDL, paralleled the decrease of these lipoproteins since it was also diminished in GNMT-KO mice when compared to their WT littermates (Fig. R20d). The restoration of hepatic SAMe levels after feeding the animals with a Methionine-deficient-diet (MDD) restored both serum TG and ApoB levels in GNMT-KO mice (Fig. R20a,d) proving that SAMe must be playing a role in circulating VLDL metabolism.
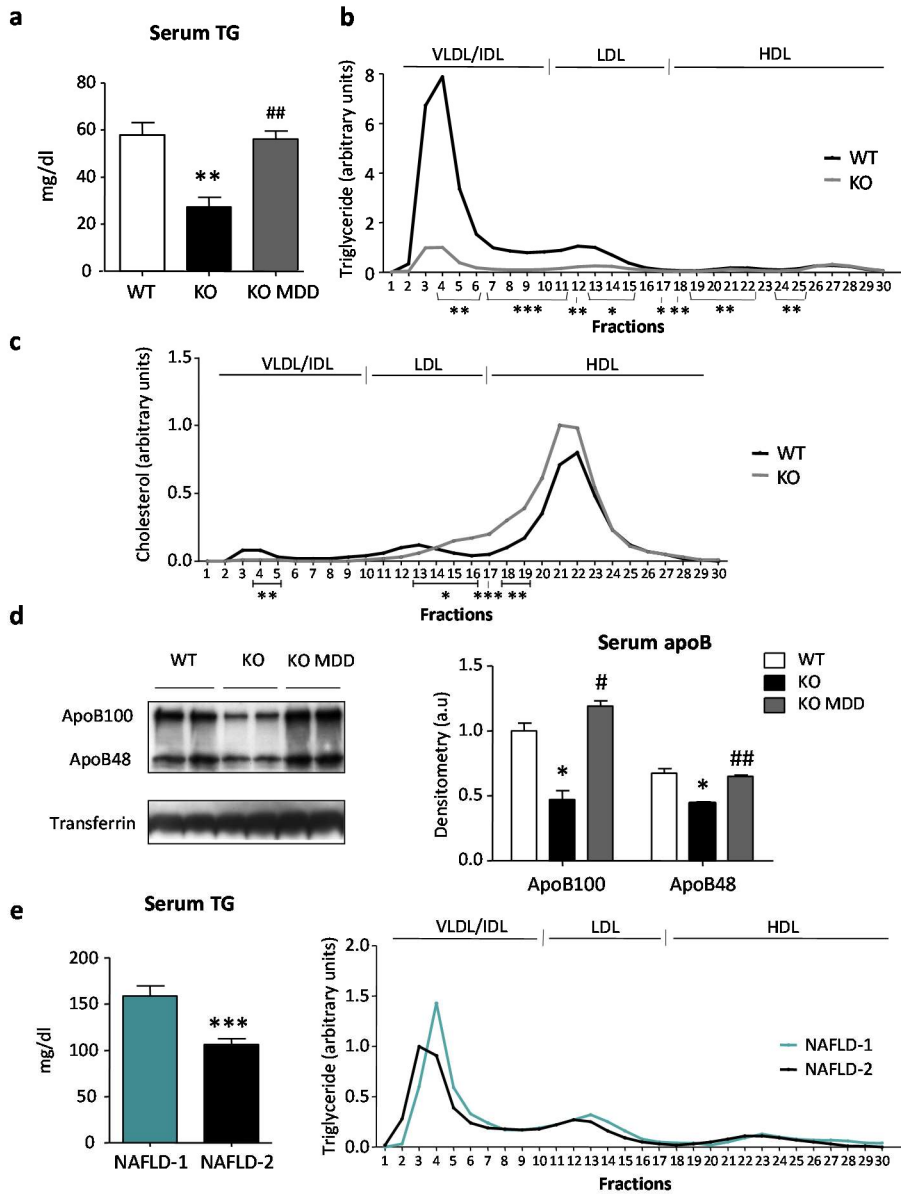
Figure R20. *Serum VLDL clearance is disrupted when GNMT is absent.* Wild type (WT), GNMT-KO (KO) and GNMT-KO mice fed a MDD (KO MDD) were fasted for 2 h. (a) TG levels were measured in serum. (b) TG and (c) Cho levels in serum lipoprotein subfractions of mice fed a control diet. (d) Serum apolipoprotein B (ApoB) content was assessed by immunoblotting using transferrin as normaliser. (e) Serum samples from NAFLD patients were obtained after a 12 h overnight fast. Serum samples from NAFLD-1 and NAFLD-2 patients were pooled and TG content in serum lipoprotein subfractions was quantified. Values are mean ± SEM of 5–6 animals per group and of the previously indicated patients. Statistical differences between GNMT-KO and WT mice or NAFLD-1 and NAFLD-2 patients are denoted by *P <0.05; **P <0.01 and ***P <0.001 and differences between GNMT-KO and GNMT-KO fed a MDD are denoted by #P <0.05 and ##P <0.01 (Student's t test).

Table R2. Demographic, metabolic, biochemical and histological characteristics of patients with normal liver and those with non-alcoholic fatty liver disease.

Characteristics	NL (n=36)		NAFLD (n=33)	
Age (years)	50.9	(31-83)	52.5	(21-81)
Male Gender	7	(19.4%)	12	(36.4%)
Triglycerides (mg/dl)	91.83	(54-153)	130.1	(54-317)***
BMI (kg/m^2)	26.42	(18.8-32.7)	28.64	(21.4-37.5)
Glucose (mg/dl)	92.14	(73-128)	100.0	(74-177)
Cholesterol (mg/dl)	178.28	(85-246)	209.9	(93-302)***
Cholesterol-HDL (mg/dl)	47.36	(29-84)	50.5	(33-97)
ALT (IU/l)	15.97	(6-30)	25.4	(9-93)***
AST (IU/l)	17.92	(11-33)	20.8	(12-43)
Alkaline Phosphatase	67.31	(35-138)	78.3	(37-124)*
Insulin (mU/ml)	6.5	(2.2-14.7)	8.5	(2.7-18.6)*
HOMA-IR	1.41	(0.3-4.3)	2.0	(0.7-5.2)**
Steatosis (%)				
Grade 0	36	(100%)		
Grade 1			27	(81.8%)
Grade 2			5	(15.2%)
Grade 3			1	(3.0%)

Data are shown as median (range) or n (%)

*p≤0.05, **p≤0.01 ***, p≤0.001 vs NL group

ALT, alanine aminotransferase; AST, aspartate aminotransferase; BMI, Body mass index; HDL, high density lipoprotein; HOMA-IR, homeostatic model assessment-insulin resistance; NAFLD, non-alcoholic fatty liver disease; NL, normal liver.

In a cohort of 33 NAFLD patients serum TG levels range from 54 to 317 mg/dl showing a wide heterogeneity among subjects (Table R2). With the aim of investigating whether altered SAMe metabolism could be linked to increased VLDL clearance in patients with NAFLD, the unhealthy individuals were classified into two groups according to their serum TG levels (Table R3). The first group, NAFLD-1 (n=11), was composed of those subjects whose serum TG levels were higher than the mean of TGs of the NAFLD patients as a whole (130.1 mg/dl); and in the second group, NAFLD-2 (n=22), the patients included were those with serum TG levels below 130.1 mg/dl. When separated, a significant difference in serum TG between NAFLD-1 and NAFLD-2 was found (Fig. R20e), and the examination of TG distribution in serum lipoproteins of the two groups revealed that the decrease in serum TG levels corresponded mostly with all VLDL and some LDL sub-fractions (Fig. R20e), resembling NAFLD-2 group GNMT-KO

animals' phenotype. The lipoproteinogram analysis also exposed a shift to the left of the maximum peak of VLDL sub-fractions in NAFLD-2 patients, what indicates that VLDL particles are enlarged in the subgroup of patients with lower values of serum TG (Fig. R20e). We have shown that VLDL enlargement in GNMT-KO mice is linked to high hepatic SAMe levels, while decreased hepatic SAMe levels have the opposite effect. MAT1A-KO mice secrete smaller VLDL particles, so we hypothesised that SAMe content could also be increased in NAFLD-2 patients as a consequence of a reduced expression of GNMT in the liver. A decreased expression of *Gnmt* and *Mat1a* genes has recently been described in patients with severe NAFLD[150, 151]. Therefore, we measured GNMT protein levels in liver samples of 17 NAFLD patients (6 from NAFLD-1 group and 11 from NAFLD-2 group) and we observed that GNMT protein levels were lower in NAFLD-2 liver samples when compared to NAFLD-1 patients (Fig. R21a,b). If the comparison was made against samples of healthy patients with normal livers (NL), NAFLD-1 subjects showed no changes in GNMT quantity while the decrease in NAFLD-2 patients was overtly patent (Fig. R21a,b). We have previously demonstrated that the SAMe increased availability in mice lacking GNMT lead to a persistent reduction in phosphatidylethanolamine (PE) content in the liver due to an increased PE methyltransferase (PEMT) flux (Results Part 1). Thus, we analysed lipid content in the liver of healthy and unhealthy individuals and found that PE content in NAFLD-2 patients was diminished (Fig. R21d) and consequently, since no significant changes were found in phosphatidylcholine (PC) content (Fig. R21e), PC to PE ratio was higher in those patients (Fig. R21f). These results suggest increased PEMT flux and probably VLDL secretion in NAFLD-2 patients. Hence, it seems possible that NAFLD-2 patients present increased hepatic SAMe levels that could be behind the decrease in serum TG levels due to increased VLDL clearance, resembling what occurs in GNMT-KO mice. In contrast, NAFLD-1 patients presented a lower PC to PE ratio due to lower levels of PC in the liver (Fig. R21e, f).

Table R3. Demographic, metabolic, biochemical and histological characteristics of patients with NAFLD.

Characteristics	NAFLD-1 (n=11)		NAFLD-2 (n=22)	
Age (years)	55.6	(30-77)	51.0	(21-81)
Male Gender	4	(36.4%)	8	(36.4%)
Triglycerides (mg/dl)	182.7	(134-317) ###	103.77	(54-130)***
BMI (kg/m^2)	28.40	(22.3-35.4)	28.76	(21.4-37.5)#
Glucose (mg/dl)	108.8	(791-177)##	95.55	(74-146)*
Cholesterol (mg/dl)	231.8	(166-302)###	198.95	(93-272)*#
Cholesterol-HDL (mg/dl)	50.6	(33-97)	50.50	(33-74)
ALT (IU/l)	29.3	(10-93)##	23.50	(9-53)##
AST (IU/l)	22.4	(12-43)	19.95	(13-40)
Alkaline Phosphatase	82.1	(37-116)	76.36	(48-124)
Insulin (mU/ml)	8.2	(4.4-13.4)	8.6	(2.7-18.6)#
HOMA-IR	2.1	(1.1-4.0)#	2.0	(0.7-5.2)#
Steatosis (%)				
Grade 0				
Grade 1	10	(90.9%)	17	(77.3%)
Grade 2	1	(9.1%)	4	(18.2%)
Grade 3			1	(4.5%)

Data are shown as media (range) or n (%)

*p≤0.05, **p≤0.01 ***, p≤0.001 vs NAFLD-1 group

#p≤0.05, ##p≤0.01, ###p≤0.001 vs NL group

ALT, alanine aminotransferase; AST, aspartate aminotransferase; BMI, Body mass index; HDL, high density lipoprotein; HOMA-IR, homeostatic model assessment-insulin resistance; NAFLD-1, non-alcoholic fatty liver patients with serum TG>130.1 (median in NAFLD patients); NAFLD-2, non-alcoholic fatty liver patients with serum TG<130.1.
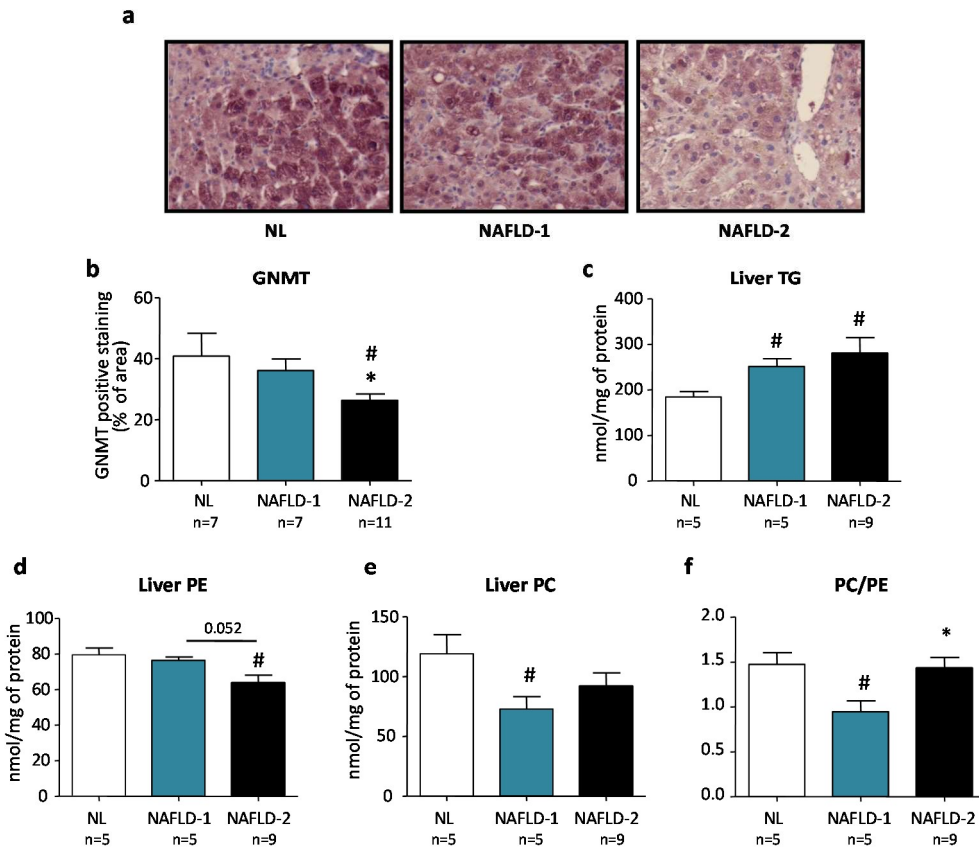
Figure R21. *A little cohort of NAFLD patients show lower expression of GNMT concomitantly with an increased PC/PE ratio.* Liver samples from patients with NAFLD (n = 17) (6 from NAFLD-1 and 11 from NAFLD-2) and normal livers (NL) (n = 7) were obtained by liver biopsy. (a) GNMT immunohistochemistry. Magnification 40x. (b) Quantitative assessments of IHC staining were performed using *FRIDA* image analysis software. Expressed in % of positive staining per area. (c) Triglycerides (TG), (d) Phosphatidylethanolamine (PE), (e) phosphatidylcholine (PC) content and (f) PC/PE ratio in liver samples from NAFLD-1 (n = 5), NAFLD-2 (n=9) and NL (n=5) patients after lipids were extracted and separated by thin layer chromatography. The values obtained from studies with NAFLD patients are mean ± SEM. Statistical differences are denoted by *P <0.05 *vs.* NAFLD-1 group; and by #P<0.05 *vs.* NL (Student's *t* test).

5.3.2. **A High Fat Diet induces VLDL clearance and triglyceride storage in the livers of GNMT-KO mice**

We had previously observed that in GNMT deficient mice excess SAMe in the liver induced increased secretion of VLDL-TG due to increased PEMT flux, MTP activity and turnover of TG lipid stores (see Results Part 2). Besides, augmented levels of hepatic SAMe prompted some transformations in VLDL features (see Results Part 2) and increased VLDL clearance from bloodstream (Fig. R20a-d). Under this context we wondered whether a High Fat Diet (HFD) challenge for six weeks could affect in a different way WT and GNMT-KO mice in VLDL handling, exacerbating both VLDL secretion and clearance in the mice lacking GNMT.

The HFD stimulation of VLDL-TG secretion was only observed in GNMT-KO mice (Fig. R22a), if compared with the mice fed the control diet (CD) GNMT deficient mice fed the HFD experienced an increase of 62% in VLDL-TG secretion (Fig. R22a vs. Results Part 2 Fig. R16a) while no changes were observed in WT mice. VLDL-PE, VLDL-PC and VLDL-size changes in HFD fed animals (Fig. R22b-d) maintained the same direction as in CD fed mice; VLDL-PE was decreased (Fig. R22b), VLDL-size was increased (Fig. R22d) and no changes were found in VLDL-PC (Fig. R22c)when compared to WT mice fed the HFD. Even though the HFD increased even more VLDL-TG secretion, serum TG levels were still nearly half of those in WT mice (Fig. R22e), which suggests a higher clearance of VLDL in GNMT-KO mice fed the HFD than in the KO fed the CD. The decreased serum TG levels also respond to lower levels of all VLDL and some LDL subfractions (Fig. R22f) as seen before in GNMT- KO mice fed the control diet and in human serum samples of individuals with low expression of GNMT (NAFLD-2 group). Accordingly, serum ApoB levels, both B-48 and B-100 were diminished in mice lacking GNMT when compared to their WT littermates (Fig. R22g).
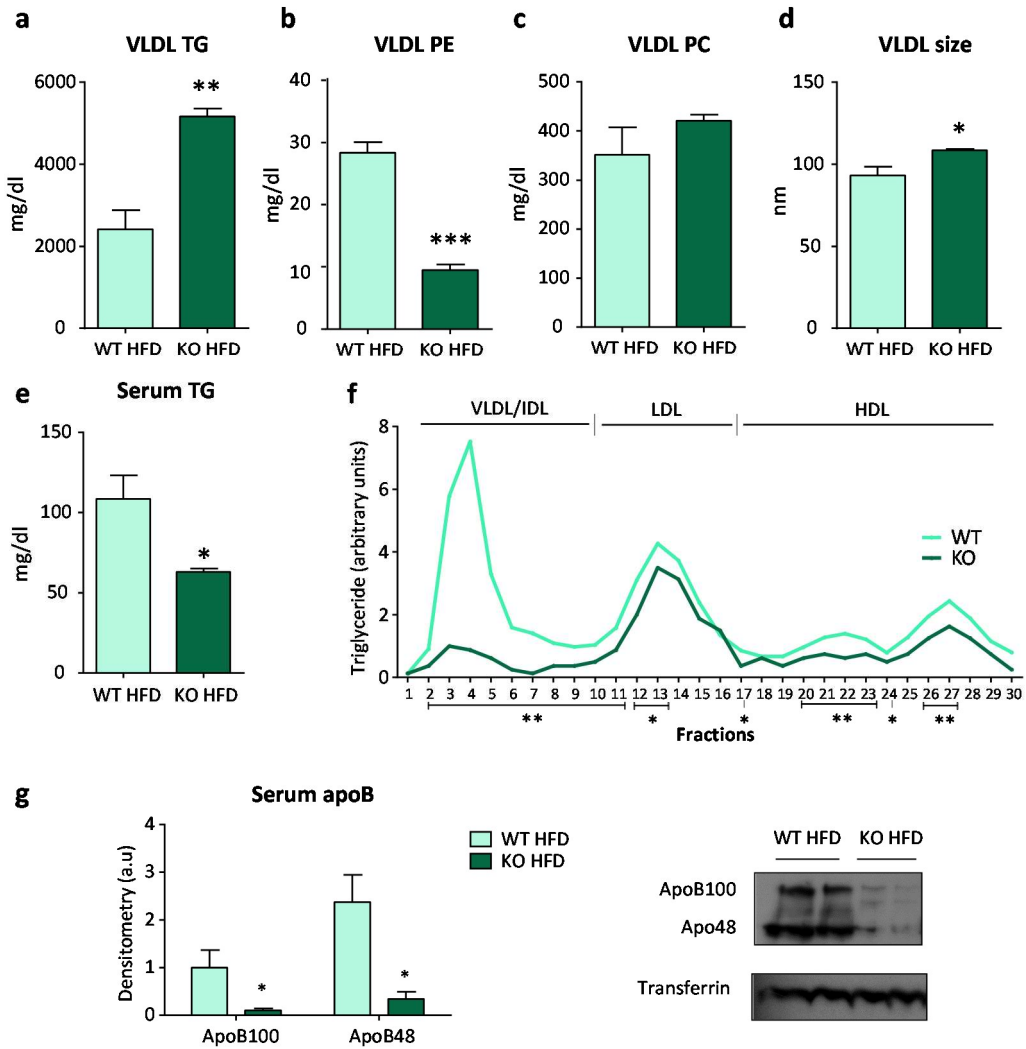
Figure R22. *HFD induces VLDL clearance in GNMT-KO mice.* Wild type mice fed a high fat diet (WT HFD) and GNMT-KO mice fed a HFD (KO HFD) were fasted for 2 h. (a) Before the 1 g/kg poloxamer (P-407) injection and 6 h later, VLDL particles were isolated from the serum and characterised for triglyceride (TG), (b) phosphatidylethanolamine (PE) and (c) phosphatidylcholine (PC) content and (d) VLDL size. (e) TG levels in serum and (f) in lipoprotein subfractions were measured. (g) Serum apolipoprotein B (ApoB) content was assessed by immunoblotting using transferrin as normaliser. Values are mean ± SEM of 4–5 animals per group. Statistical differences between KO and WT mice are denoted by *P <0.05; **P <0.01 and ***P <0.001 (Student's t test).
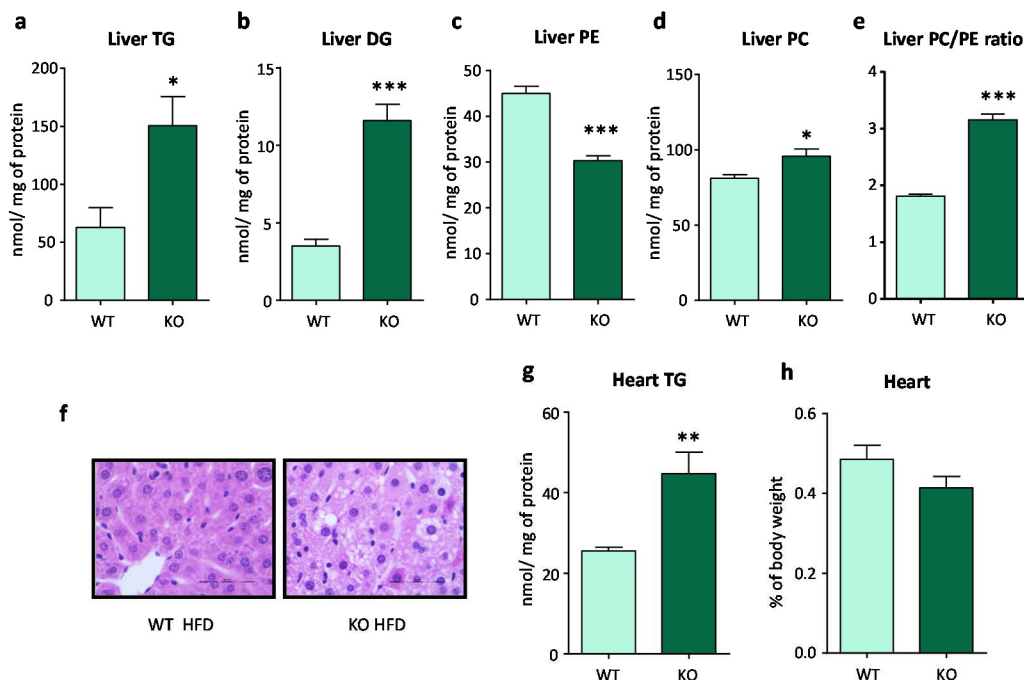
Figure R23. *HFD prompts liver and heart TG storage in GNMT-KO animals.* Wild type mice fed a high fat diet (WT HFD) and GNMT-KO mice fed a HFD (KO HFD) were fasted for 2 h. (a) Liver triglyceride (TG), (b) diglyceride (DG), (c) phosphatidylethanolamine (PE), (d) phosphatidylcholine (PC) levels and (e) PC/PE ratio from WT and KO mice fed the HFD were quantified. (f) Representative liver haematoxylin and eosin staining. (g) Heart TG levels were quantified after lipid extraction and (h) percentage of heart weight. Values are mean ± SEM of 4–5 animals per group. Statistical differences between KO and WT mice are denoted by *P <0.05; **P <0.01 and ***P <0.001 (Student's t test).

In a condition where VLDL clearance is increased, as shown in GNMT-KO mice fed HFD, VLDL lipid supply to tissues might as well be increased. After the HFD feeding liver TG content was 2.4 fold greater in GNMT-KO mice than in their WT counterparts (Fig. R23a) making the hepatosteatosis evident (Fig. R23f), whereas when feeding the CD the TG liver content increase was 1.75 fold when compared to WT mice (see Results Part 1 Fig. R5b). Hepatic DG, PE and PC content were also found altered in GNMT-KO mice fed the HFD when compared to WT animals; DG and PC were increased and PE was decreased (Fig. R23b-d), consequently, PC/PE ratio was increased (Fig. R23e) likewise CD fed animals (see Results Part 1 section 5.1.2.). Besides TG storage was found increased in the heart of mice lacking GNMT fed the HFD when compared to their

control animals (Fig. R23g), whereas when fed the CD it was not increased (data not shown) and no changes were found between genotypes in heart weight (Fig. R23h).

All of the above mentioned alterations took place in a metabolic context in which GNMT-KO mice food intake was slightly decreased in comparison to WT animals (Fig. R24a), and no changes were found in body weight nor in the % of body weight of White Adipose Tissue (WAT) (Fig. R24b,c), yet, accordingly with TG accumulation the % of liver weight was augmented (Fig. R23d). GNMT deficient mice fed the HFD presented no signs of insulin resistance, what is more they showed more glucose tolerance and to some extent more insulin tolerance when compared to their WT counterparts (Fig. R24e). Despite liver TG accumulation, the HFD did not modify mRNA expression of proteins involved in lipid synthesis and NADPH production if compared to control mice (Fig. R24g). Serum ketone bodies and fatty acids were not found altered either (Fig. R24f,h). And the hepatic content of CD36, a protein commonly increased in NAFLD context, was not increased but decreased in GNMT-KO fed the HFD when compared to WT mice (Fig. R24i).
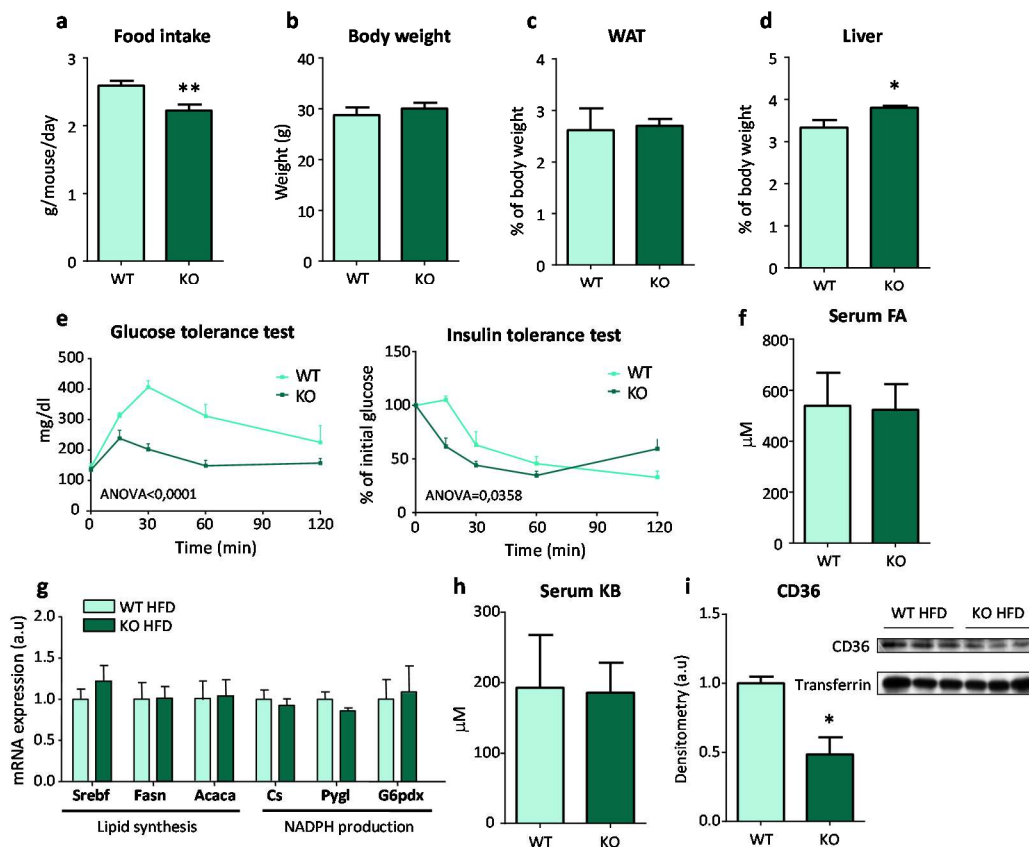
Figure R24. *Metabolic characterization of GNMT-KO fed a HFD for six weeks.* 3-month-old wild type mice fed a high fat diet (WT HFD) and *GNMT*-KO mice fed a HFD (KO HFD) for 6 weeks were fasted 2 or 4 hours before experiments were performed. (a) Food intake. (b) Body weight. (c) Percentage of white adipose tissue (WAT) weight. (d) Percentage of liver weight. (e) After a 4 hours fast, glucose and insulin tolerance tests were assayed after oral administration of glucose (2 mg/kg) or intraperitoneal injection of insulin (1 U/kg) (f) After 8 hours fasting fatty acids (FA) were determined in mice serum using a commercially available kit. (g) Quantitative RT-PCR analysis of hepatic genes in WT HFD and KO HFD mice. (h) After 8 hours fasting ketone bodies (KB) were determined in mice serum using a commercially available kit. (i) Liver CD36 content was assessed by immunoblotting using transferrin as normaliser. *Acaca*, acetyl-CoA carboxylase; *Cs*, citrate synthase; *Fasn*, fatty acid synthase; *G6pdx*, glucose-6-phosphate dehydrogenase; *Pygl*, glycogen phosphorylase; *Srebf*, sterol regulatory element-binding proteins. Values are means ± SEM of 4-6 animals per group. Statistical differences between KO and WT mice are denoted by *P <0.05 and **P <0.01 (Student's *t* test) and by two-way ANOVA.

5.3.3. **VLDL specific features of GNMT-KO mice are linked with increased VLDL clearance**

As it has been stated before, GNMT-KO VLDL particles secreted by liver are altered, presenting some specific features (see Results Part2 Section 5.2.2.). VLDL clearance can be mediated by interactions of ApoE with different receptors in different tissues[152]. Hence, in an effort to analyse the reasons behind the increased clearance of VLDL in GNMT-KO mice we further characterised VLDL features of mice lacking GNMT and we studied VLDL-ApoE secretion. The results showed a 1.48 fold increase in VLDL-ApoE secretion of mice fed the CD when compared to WT mice (Fig. R25a), and the VLDL-ApoE augmentation was even higher, 1.66 fold, in mice fed the HFD (Fig. R25a). What is more, the increase in ApoE responded to hepatic SAMe levels given that it reversed when GNMT deficient mice were fed a MDD (Fig. R25a). Each VLDL particle contains a single ApoB protein but several copies of ApoE, consequently ApoE/ApoB ratio was increased in GNMT-KO mice both when fed the CD and after HFD feeding (Fig. R25b), and it recovered after MDD feeding to GNMT deficient animals. Thus, VLDL particles were ApoE enriched in GNMT-KO mice. The rise in VLDL-ApoE responded to changes in ApoE protein availability, hepatic ApoE content was increased in the KO fed the CD (Fig. R25c) and ApoE hepatic levels were even higher when fed the HFD if compared to WT animals (Fig. R25c); its content recovered after SAMe levels re-establishment in mice lacking GNMT with the MDD (Fig. R25c). However, increased ApoE liver content was not linked with Apoe mRNA changes neither in mice fed the CD nor in those fed the HFD (Fig. R25d).
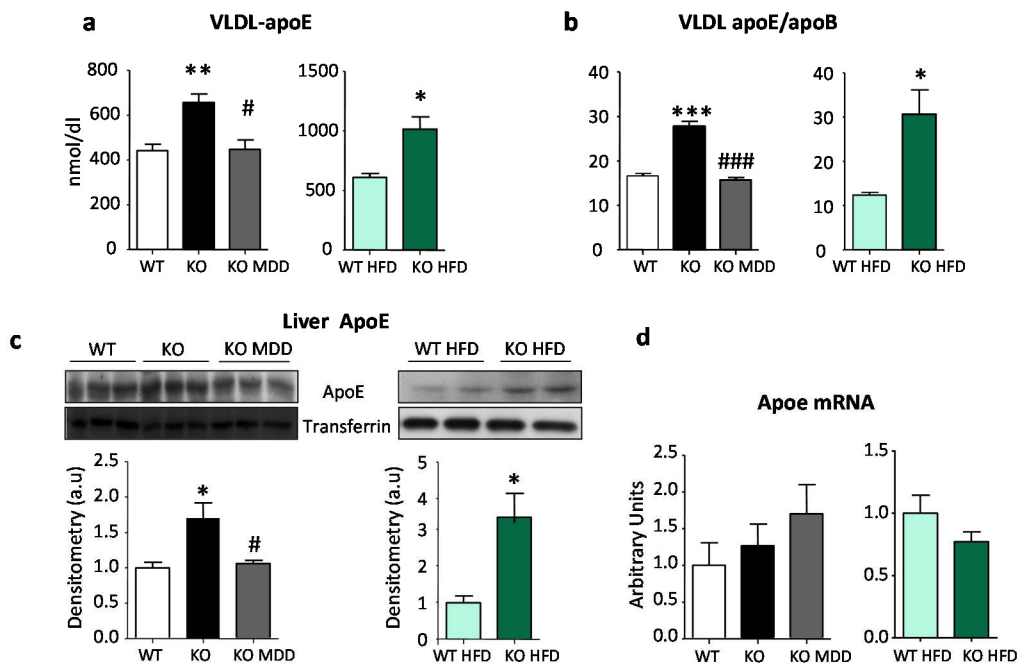
Figure R25. *ApoE enrichment in VLDL and in liver is a major characteristic of GNMT deficiency not linked with changes in Apoe gene expression.* 3-month-old wild type (WT), *GNMT*-KO (KO), *GNMT*-KO mice fed a MDD (KO MDD) for 3 weeks, WT mice fed a high fat diet (WT HFD) and *GNMT*-KO mice fed a HFD (KO HFD) for 6 weeks were fasted 2 hours before the experiments were performed. (a) Before 1 g/kg poloxamer (P-407) injection and 6 hours later, blood was collected and VLDL (d <1.02 g/ml) were isolated from serum by ultracentrifugation and VLDL-ApoE was determined after being resolved by SDS-PAGE, stained with Gelcode Blue Stain reagent and quantified by optical densitometry using Quantity One software and phosphorylase *b* as a standard. (b) The VLDL ratio ApoE/ApoB was calculated. (c) Quantitative RT-PCR analysis of Apoe mRNA in livers of WT, *GNMT*-KO (KO), *GNMT*-KO mice fed a MDD (KO MDD) and fed a HFD (WT HFD, KO HFD). (d) ApoE content in the liver was assessed by immunoblotting using transferrin as loading control. Values are mean ± SEM of 4-6 animals per group. Statistical differences between *GNMT*-KO and WT mice are denoted by *P <0.05; **P <0.01 and ***P <0.001; and between *GNMT*-KO and *GNMT*-KO fed a MDD are denoted by #P <0.05 and ###P <0.001 (Student's *t* test).

Going forward, if GNMT-KO mice were challenged with PLIN2 absence as well, as seen before, TG liver accumulation was inhibited (see Results Part 1 section 5.1.4.) while VLDL-TG was still augmented (see Results Part 1 section 5.2.3.), nevertheless, serum TG analysis revealed that VLDL clearance was also increased in GNMT-PLIN2-KO mice when compared to their WT counterparts (Fig. R26a). Moreover, the double KO (dKO) VLDL features resembled those of the single GNMT-KO mice (see Results Part 1 section 5.2.3.) and VLDL-ApoE secretion as well as VLDL-ApoE enrichment resulted to be increased in

dKO mice when compared to WTs (Fig. R26b,c) as shown for GNMT-KO. Therefore, TG storage in lipid droplets due to PLIN2 in GNMT-KO mice does not have any effect on VLDL-ApoE secretion. Instead, the increased ApoE availability seems to be directly related to excess SAMe levels.
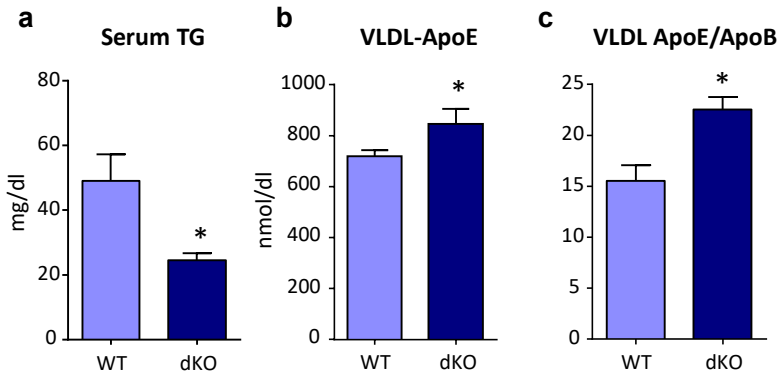
Figure R26. *PLIN2 deletion in GNMT-KO mice resembles GNMT deficiency phenotype.* 3-month-old *GNMT-PLIN2*-KO (dKO) and their wild-types (WT) were fasted 2 hours before the experiments were performed. (a) TG levels in serum of mice were measured. (b) Before 1 g/kg poloxamer (P-407) injection and 6 hours later, blood was collected and VLDL (d<1.02 g/ml) were isolated from serum by ultracentrifugation and VLDL-ApoE was determined after being resolved by SDS-PAGE, stained with Gelcode Blue Stain reagent and quantified by optical densitometry using Quantity One software and phosphorylase *b* as a standard. (c) The VLDL ratio ApoE/ApoB was calculated. Values are mean ± SEM of 4-6 animals per group. Statistical differences between dKO and their WT mice are denoted by *P <0.05; **P <0.01 and ***P <0.001 (Student's *t* test).
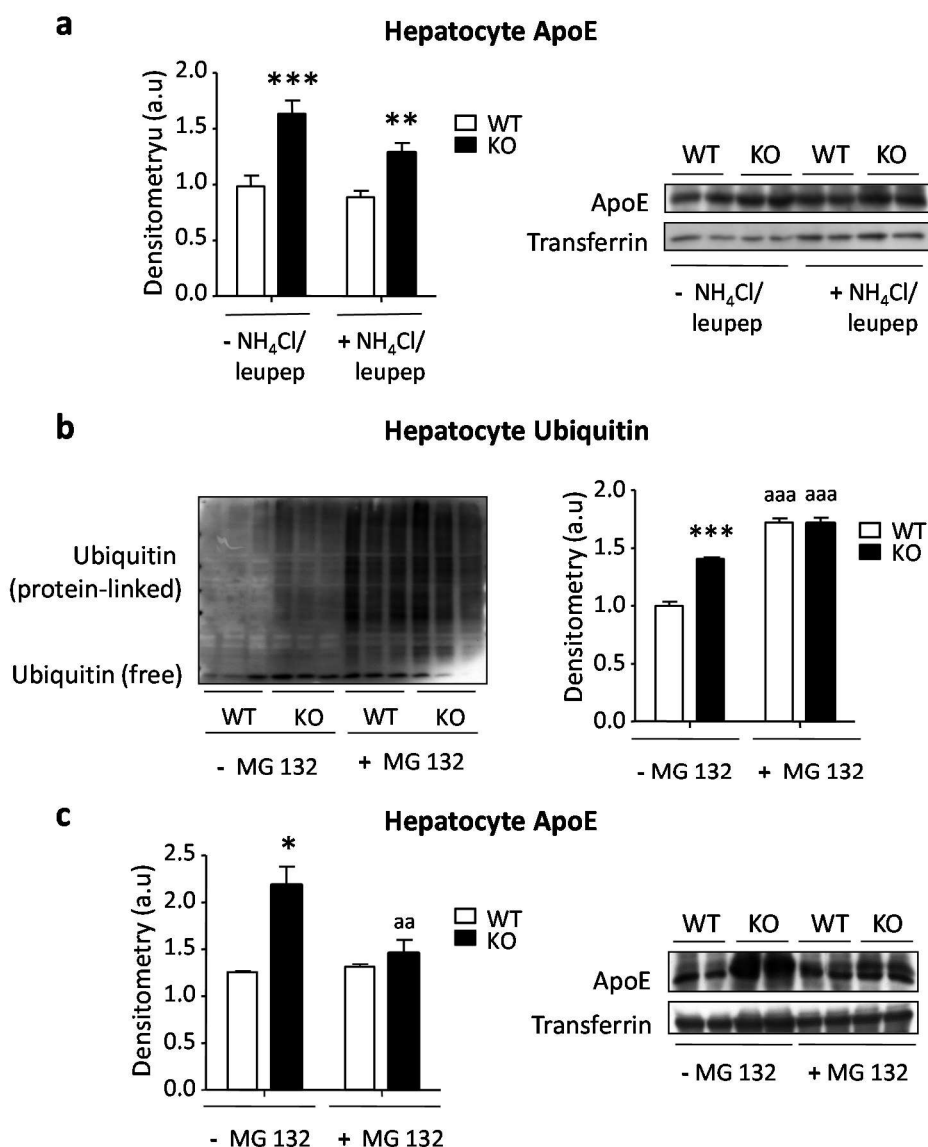
Figure R27. *Neither the proteasome nor the lysosomes are involved in ApoE liver enrichment.* 3-month-old wild type (WT) and GNMT-KO (KO) mice were fasted 2 hours before the experiments were performed. (a) Hepatocytes were incubated 24 hours in DMEM without or with a mixture of the lysosomal function inhibitors leupeptin (100 µM) and ammonium chloride (20 µM). Intracellular ApoE content was assessed by immunoblotting using transferrin as normaliser. (b) Hepatocytes were incubated 12 hours in DMEM without or with MG132, a proteasomal inhibitor (10 µM). Intracellular ubiquitin and ApoE content was assessed by immunoblotting using transferrin as normaliser. Values are mean±SEM of 5-6 animals per group. Statistical differences between *GNMT*-KO and WT mice are denoted by *P <0.05; **P <0.01 and ***P <0.001; and between KO hepatocytes and WT hepatocytes treated with MG132 [aa]P <0.01 and [aaa]P <0.001 (Student's *t* test).

To further investigate the increased hepatic content of ApoE in GNMT-KO mice, possible degradation routes were studied. It has been suggested that part of ApoE may degrade via lysosomal enzymes[153], so the effect of NH₄Cl/leupeptin inhibitors was investigated. The treatment did not induce any changes in hepatocytes ApoE levels nor in WT neither in GNMT-KO mice (Fig. R27a). The proteasome pathway was also analysed because part of ApoE is degraded through this path in HepG2 cells[154]. We observed that in GNMT-KO mice there is an accumulation of ubiquitinated proteins (Fig. R27b), and the inhibition of the proteasome function with MG132 did not increase ApoE levels in WT hepatocytes and they were decreased in GNMT-KO mice hepatocytes (Fig. R27c).

Finally, potential mechanisms that might explain the increased VLDL clearance were studied. First, since ApoE interacts with receptors such as VLDL receptor (VLDL-R), LDL receptor (LDL-R) or Prolow-density lipoprotein receptor-related protein 1 (LRP-1) in order to capture and internalise plasma lipoproteins[111], we analysed the mRNA expression of these receptors in the liver and found that both VLDL-R and LDL-R were increased in GNMT-KO fed the CD when compared to WT animals (Fig. R28a), and VLDL-R was greatly augmented in the KO mice after HFD feeding (Fig. R28b). Later, VLDL clearance at a systemic level was investigated, to define if the increased clearance of VLDL in GNMT-KO mice depended on the specific features of the VLDL particles of these animals, human VLDL particles were labelled with radioactivity and administered intravenously to GNMT-KO and WT mice. We found that the kinetic of the clearance of labelled human VLDL was similar in WT and in GNMT-KO mice (Fig. R29a), and that the % of injected dose per gram of tissue after 30 min of injection (the normalised amount of radioactivity received by each tissue) was not altered in GNMT-KO mice (Fig. R29b). Taken together these results indicate that the augmented expression of VLDL-R and LDL-R is not enough to explain the increased clearance of VLDL in GNMT-KO mice and that the specific features of the VLDL secreted by these animals might be contributing to that

increase.

a

VLDL uptake

b

VLDL uptake
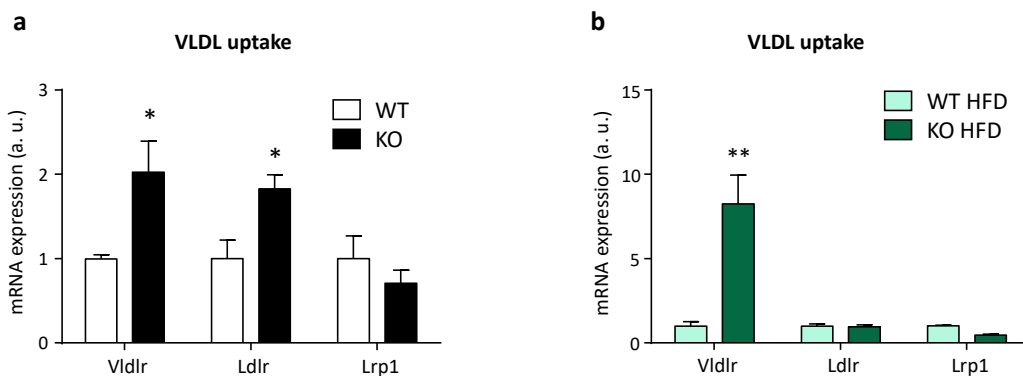
Figure R28. *VLDL receptor (Vldlr) is overexpressed in GNMT-KO mice liver when fed a Control Diet and a High Fat Diet.* (a) Quantitative RT-PCR analysis of *Vldlr, Ldlr* and *Lrp1* mRNA in livers of WT and *GNMT*-KO (KO) fed a control diet and of (b) WT (WT HFD) and GNMT-KO (KO HFD) fed a HFD. *Vldlr*, Very low-density lipoprotein receptor; *Ldlr*, Low-density lipoprotein receptor; *Lrp1*, Prolow-density lipoprotein receptor-related protein 1.

a

Rate of VLDL clearance

b
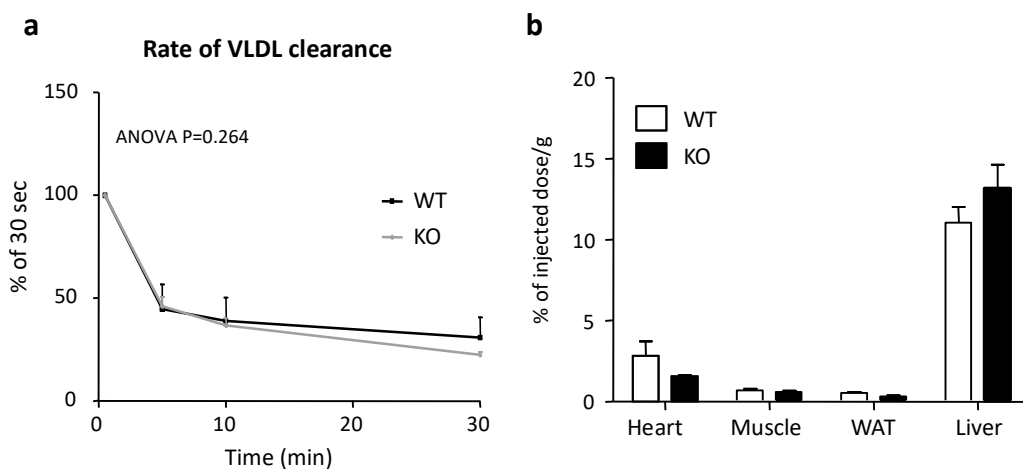
Figure R29. *Human VLDL clearance in GNMT-KO mice show no changes.* Wild type (WT) and GNMT-KO (KO) were fasted for 2 h. (a) VLDL clearance rate was measured after intravenous administration of radiolabeled VLDL particles. (b) The percentage of injected radiolabel dose per gram of tissue was calculated. Values are mean ± SEM of 4–6 animals per group. Statistical differences between GNMT-KO and WT mice are denoted by two-way ANOVA.

6. Discussion

Nada me inspira mas veneración y asombro que un anciano que sabe cambiar de opinión.

Santiago Ramón y Cajal (1852-1934)

6. **DISCUSSION**

6.1. **Excess SAMe induces hepatosteatosis through PEMT pathway**

S-Adenosylmethionine (SAMe) chronic excess and chronic deficiency have shown to be related with the development of liver damage, both in humans and in mice[2]. MAT1A-KO and GNMT-KO mice, animal models with chronic impairment of SAMe metabolism, develop spontaneously with age different stages of non-Alcoholic Fatty Liver Disease (NAFLD)[2].

The chronic deficiency of SAMe is caused by reduced or absent *Mat1a* gene expression, given that its products: MATI and MATIII, are the main actors in SAMe synthesis in the adult[4]. The causes by which low levels of SAMe induce NAFLD development have already been studied[58-60]. On one hand, it has been shown that low liver SAMe content reduces phosphatidylcholine (PC) amount leading to Sterol regulatory element-binding protein 1 (SREBP-1) activation and inducing lipogenesis in *C. elegans* model; besides, the reduced PC quantity in HepG2 cells or in the liver of choline-phosphate cytidylyltransferase A knock out (KO) mice also leads to the activation of SREBP-1[59]. And on the other hand, low hepatic SAMe in MAT1A-KO mice impairs VLDL assembly in a way that the secreted lipoproteins are small and lipid-poor particles so the secretion of triglycerides (TG) is diminished[58]. What is more, MAT1A absence has also recently been shown to altered FA oxidation in the mitochondria[60]. The aforementioned mechanisms can lead to the abnormal accumulation of TG in the liver, a prerequisite for NAFLD diagnosis[26].

Chronic excess of SAMe takes place when GNMT protein is reduced or absent[2]. And the mechanisms accountable for TG accumulation, NAFLD onset, when hepatic SAMe levels are high have not yet been stablished, so here we aimed to investigated

the mechanisms involved in the development of hepatosteatosis in GNMT deficient mice with high levels of liver SAMe.

GNMT catabolises SAMe and it is the main methyltransferase (MT) in charge for maintaining SAMe homeostasis in the liver[2]. Consequently, when GNMT is absent in GNMT-KO mice, SAMe accumulates in plasma and in the liver[20] since no other MTs are capable of compensating the lack of GNMT. In any case, MTs are activated by SAMe excess in GNMT-KO mice as it can be understood by the fact that they show global DNA hypermethylation[13]. There is another relevant MT in the liver that is related to lipid metabolism and that could be stimulated and behind TG accumulation, phosphatidylethanolamine (PE) MT (PEMT)[119]. PEMT synthesises PC through three consecutive methylations in which SAMe acts as the methyl donor[119], and it has already been suggested that PC synthesized via PEMT may be an important source of hepatic TG[155].

In this part of the study the role of SAMe in liver lipid homeostasis has been investigated and we have found that the overactivation of PEMT directed by excess SAMe leads to increased synthesis of TG and to the subsequent hepatic steatosis.

The studies were performed in GNMT-KO mice, animals characterised by high hepatic levels of SAMe and methionine that develop hepatic steatosis rapidly[20]. Initially we observed that NAFLD development in GNMT-KO mice occurs under a favourable metabolic condition in both 3- and 8- month-old mice, from the onset of the disease to the worsening of it. We also observed that, accordingly with the lipid accumulation in the liver they present hepatomegaly, commonly the sole physical finding in NAFLD[156]. Later, the study of the usual pathways for TG accumulation revealed that none of them was accountable for the hepatic steatosis in GNMT-KO mice, under a control diet GNMT deficient hepatocytes showed normal *de novo* lipogenesis and Fatty Acid (FA) β-oxidation but increased TG secretion, features that persist when mice get older. The fact that TG secretion is increased when SAMe levels are elevated in GNMT-KO mice is consistent with our previous finding that low SAMe levels also impair TG secretion[58]. Subsequently, we observed that PEMT flux was considerably increased in GNMT-KO

hepatocytes. This correlates with the fact that because of GNMT lack SAMe excess cannot be eliminated, consequently the 40-fold increase in SAMe stimulates other MTs, such as PEMT, in an effort to maintain SAMe homeostasis. In agreement with PEMT cellular localization[119] and with its activation, a reduction in microsomal PE concomitant with a 2-fold increase in PC was observed in the liver of GNMT-KO mice. However, in the whole liver the amount of PE was 2-fold reduced while PC content was only slightly increased. Given that all PC biosynthesis takes place in ER[107], the minor increase in the whole liver suggests that there is a higher catabolism and/or secretion in high density lipoproteins (HDL) of PC in the mutant mice. Accordingly, both the amount of DG and TG in the liver and serum HDL-PC levels were increased in GNMT-KO mice when compared to WT animals. These results are in agreement with the finding that shows that approximately 65% of the hepatic pool of TG is derived from hepatic PC[155]. Therefore, in GNMT-KO mice liver both biosynthesis of PC and its catabolism are stimulated.

SAMe hepatic content restored after the administration of a methionine deficient diet (MDD) to GNMT-KO mice, what is consistent with the role of GNMT in the cycle of methionine[7]. But more importantly, MDD not only lowered SAMe levels but also re-established control lipid hepatic metabolism, this reflects that SAMe is the rate-limiting substrate that links PE to TG through PC and DG. Additionally, the finding that PEMT inhibition with DZA in GNMT-KO hepatocytes resulted in a reduction of TG levels gave definitive support to the role of PEMT in TG accumulation in the liver of GNMT lacking mice. And the fact that 8-month-old GNMT-KO mice hepatic lipid metabolism resembled the one observed in 3-month-old animals shows that TG accumulation via PEMT is not a transitory state but a useless attempt to unceasingly try to maintain SAMe homeostasis.

These results demonstrate for the first time that in cases of SAMe excess PEMT is an unexpected source of TG. Thus, we conclude that stimulation of PEMT pathway induced by SAMe excess can explain the steatosis in GNMT deficient mice. The relevance of this finding to human disease resides in the notion that children with GNMT

mutations have been identified to suffer from liver injury[16, 62]. What remains to know is if PC synthesized via PEMT could be a quantitatively important source of hepatic TG under physiological conditions. Nevertheless, there are other situations besides GNMT ablation that can rise SAMe content in the liver, such as an increase of dietary methionine because of high protein diet[157] or cystathionine β-synthase (CBS) deletion[2]. Interestingly, CBS-KO mice also exhibit liver injury, steatosis and fibrosis.

In a similar manner, the role of PLIN2 on the background of high SAMe was investigated. PLIN2 increases in hepatocytes along with TG accumulation[46], accordingly it was augmented in the liver of GNMT-KO mice. To understand the role of PLIN2 in the context of GNMT absence a novel double GNMT/PLIN2-KO mouse model was generated. These mice also present a favourable metabolic context and as GNMT-KO mice low levels of hepatic PE and high levels of SAMe, however they do not develop hepatic steatosis. This suggests that SAMe excess might be still inducing PEMT activity but due to the lack of PLIN2 TG cannot be stored, and it might be redirected to VLDL secretion in total agreement with previous findings[47, 48] that show a reduction in hepatic TG and an increase in VLDL secretion in PLIN2-KO mice. Also consistent with previous findings[44, 48] PLIN2 ablation in GNMT-depleted livers decreased lipogenesis and induced TG secretion. A remarkable characteristic of the double KO mice is the increased gluconeogenesis; this indicates that in the context of high SAMe there exists a crosstalk between lipid synthesis and sequestration and glucose metabolism. In the altered methionine cycle of these animals the excess methionine could be a precursor for glucose synthesis. And since plasma glucose was not altered in the double KO animals the excess glucose in the liver might accumulate in the form of glycogen stores as it has been shown to occur in GNMT single KO mice[158]. In this way the hepatomegaly in the absence of TG accumulation observed in PLIN2/GNMT-KO animals could be explained. The results observed in the double KO model along with the observation that PE methylation promotes lipid droplet (LD) formation[145] supports GNMT-KO model, in which increased PEMT activity induces both TG synthesis and its accumulation into newly formed LD.

Collectively, these observations demonstrate that the right balance of SAMe is needed in order to achieve an adequate liver lipid homeostasis; otherwise, activation of lipogenesis[59] and inhibition of TG secretion[58] at low SAMe levels, and activation of TG synthesis via PEMT at high SAMe levels would lead to a discrepancy in lipid homeostasis. This cascade of events goes a long way towards explaining why a chronic imbalance in hepatic SAMe synthesis[19] or catabolism[13] is capable of inducing NAFLD.

6.2. **SAMe regulates VLDL assembly and secretion**

VLDL synthesis and secretion are essential processes not only for liver lipid metabolism but also for the whole body lipid homeostasis. As it can be understood by the fact that abnormalities affecting them can lead to dyslipidaemias and to fatty liver development[74, 75, 78]. Hepatic steatosis is an essential stage for NAFLD to further progress, and NAFLD development has been related with animal models with altered *Mat1a* and *Gnmt* gene expression[19, 20, 150], both genes implicated in methionine and SAMe metabolism. *Mat1a* encodes for MATI and MATIII enzymes, which are involved in SAMe synthesis from methionine; while *Gnmt* encodes for the methyltransferase GNMT that catabolises SAMe to form sarcosine and SAH[2]. When either *Mat1a* or *Gnmt* are absent, mice develop different stages of NAFLD in spite of the fact that they present opposite values of SAMe[13, 19, 56]. MAT1A-KO mice present a 75% reduction of hepatic SAMe[19] while GNMT-KO mice have a 35-fold increase in liver SAMe[20].

Under this context, we aimed to investigate the relationship between low and high levels of hepatic SAMe and the assembly and secretion of VLDL. It is known that d*e novo* biosynthesis of PC strongly influences VLDL assembly and secretion[54, 107]. And, in the liver, two pathways are involved in PC synthesis: CDP-choline pathway and PEMT pathway; in animal models both of them are required for normal VLDL secretion[98, 99, 107]. SAMe is the substrate for the latter, the methyltransferase PEMT, which synthesizes PC from PE through three consecutive methylations. PEMT has been demonstrated to be involved in VLDL assembly and secretion[99, 159], its absence reduces VLDL-TG secretion by 50%[99]. Therefore, SAMe could be controlling VLDL assembly and secretion through PEMT pathway in the abovementioned animal models with chronic impairment of SAMe hepatic levels. In this part of the study, we found that low levels of hepatic SAMe are responsible for the reduction in VLDL-TG and the augmentation in VLDL-ApoB secretion; while elevated liver levels of SAMe, on the contrary, induce increase of VLDL-TG and reduction of VLDL-ApoB secretion.

For the research purpose, with the intention of understanding which processes were under the influence of SAMe metabolite, 3-month-old MAT1A-KO mice administered SAMe for 7 days and GNMT-KO animals fed a MDD for 3 weeks, in order to restore physiological hepatic SAMe levels, were used.

VLDL features, assembly and secretion were known to be altered in MAT1A deficient mice, they secrete an increased number of VLDL particles that are TG-poor, ApoB-enriched and subsequently small[58]. And the hepatic secretion rate of TG has been shown to be increase in GNMT-KO mice in Part 1 of the results of this work. Here we found that the loss of *Gnmt* gene, in contrast to MAT1A absence and as expected due to increased SAMe levels, induces the assembly and secretion of TG-enriched and ApoB-poor VLDL. Given that each VLDL is secreted with one molecule of ApoB, GNMT-KO mice secrete less but larger VLDL particles. Those altered characteristics of VLDL were restored to functional levels after SAMe values recovery in both animal models, demonstrating the implication of SAMe in the control of VLDL assembly and secrertion, and consequently in VLDL features.

A major determinant of VLDL secretion is TG mobilization from cytosolic LD stores through lipolysis and re-esterification processes[78, 93]. MAT1A-KO mice were previously shown to have diminished TG turnover and secretion[58]; in opposition, GNMT deficient mice are presented here to have an increased mobilization of TG lipid stores, in total agreement with its increased secretion of VLDL-TG. Besides, in the latter animals, microsomal re-esterification reactions are also increased, as seen by the increased DGAT activity, which, as expected is reduced in MAT1A-KO animals, as it is in these animals the lipolytic activity of microsomal TGH, both activities recovered along with SAMe physiological values. The increased activity of DGAT in GNMT-KO mice could represent an additional problem to NAFLD development given that inhibition of DGAT1 reduces liver fibrosis in mice with NASH[160] while inhibition of DGAT2 results in decreased hepatosteatosis but higher fibrosis and liver damage[161]. In 8-month-old GNMT-KO mice, liver fibrosis is more prominent[13], consequently, the increased activity of DGAT through DGAT1 or DGAT2 could be playing a role in the progression of NAFLD in GNMT-KO mice.

Thus far, 3-month-old MAT1A-KO and GNMT-KO mice present inverse characteristics for what is related to VLDL assembly and secretion, likewise they present contrary values of SAMe. Being the linking point between both individualities PEMT activity, it is reasonable to find it diminished in MAT1A-KO animals due to chronic deficiency of SAMe. Also coincident with the line of thinking is the reduction in TG secretion when PEMT is inhibited in GNMT deficient hepatocytes, what demonstrates that PEMT over-activation, the increased PEMT flux (see Part 1 of the Results), is behind VLDL-TG over-secretion in these animals. The increased PEMT flux also causes a reduction in hepatic and microsomal PE (see Part 1 of the Results), a decrease that is replicated in VLDL-PE secretion. Unpredictably, despite the fact that PC synthesis is increased in GNMT-KO mice, VLDL-PC secretion was found unaltered. However, the additional deletion of PLIN2 in GNMT-KO mice, in which PLIN2 expression is increased (see Part 1 of the Results), results in the secretion of VLDL that match those of GNMT-KO animals except for the augmentation of VLDL-PC secretion. This characteristic of the PLIN2-GNMT double KO mice suggests a role of PLIN2 in the retention and catabolism of PC; hypothesis that is supported by the knowledge that PLIN2 binds lipids such as PC or SM with high affinity[148, 162]. Accordingly to PLIN2 role in lipid storage and in LD biogenesis, the double KO mice present not only less TG in the liver (see Part 1 of the Results) but also a decreased turnover of TG lipid stores. However, and as it happens when PLIN2 is knocked out[48], the mice lacking both genes, PLIN2 and GNMT, show increased secretion of VLDL-TG. This fact suggests that the increased secretion of VLDL-TG might be influenced by mechanisms other than TG mobilization such as increased PEMT activity or even augmented expression of proteins that may act as replacements for PLIN2, such as CIDE-B, which are also involved in VLDL secretion[163].

All of these results, together, corroborate the relevance of PEMT pathway in VLDL secretion[99, 107], and present its substrate, SAMe, as a modulator of VLDL assembly and secretion. Yet, the decreased secretion of VLDL-ApoB in GNMT-KO animals found no explanation in PEMT pathway. For the adequate VLDL assembly and secretion, ApoB while being translated should be translocated into the lumen of the ER where it interacts

with MTP for lipid binding[83]. In GNMT-KO mice, *Apob* is translated in a lower degree as both *Apob* mRNA levels and hepatic ApoB content, as a reflection, are decreased. Therefore this could be the limiting step in VLDL secretion that could explain why even being increased, VLDL-TG secretion is not enough to compensate the increased TG storage in GNMT-KO mice. ApoB secretion regulation is believed to be for the most part co- and post-transcriptionally[101], yet here we demonstrated for the first time that its reduced expression through epigenetic mechanisms can affect its secretion. The reduced expression of *Apob* mRNA in GNMT deficient mice challenges the largely believed idea of its expression to be constitutive[81], and its recovery after the MDD confirms the implication of SAMe in this process. SAMe is a methyl donor that can methylate the DNA modulating the expression of proteins[2]. The promoter region of *Apob* presents a CpG rich region predisposed to methylation that is hypermethylated in GNMT-KO mice, what could decrease the transcription of *Apob*, and that re-establishes its methylation status along with SAMe hepatic values. Besides, SAMe has been proven to be involved in the stability of some proteins through HuR protein regulation[164], and here we proof that it might be implicated in the stability of *Apob* mRNA, which is also challenged in the absence of GNMT by the lack of *Apob* mRNA-HuR binding.

Conclusively, herein it is shown that mice can develop NAFLD under contrasting circumstances. The finding that MAT1A-KO and GNMT-KO mice secrete contrary amounts of VLDL-TG and yet both develop NAFLD might seem controversial; however, the same fact has been found in humans with NAFLD[43, 165]. NAFLD patients can present both, increased[166, 167] and decreased[75] secretion of VLDL-TG, showing the heterogeneity of NAFLD pathogenesis as it is shown in our animal models.

The data collected in this part of the study makes it noticeable that SAMe homeostasis must be strictly controlled for the right functioning of VLDL secretory machinery. The mechanism by which SAMe controls VLDL secretion is mainly PEMT pathway; however, SAMe metabolite is also involved in other mechanisms, such as *Apob* gene expression control. What is more, VLDL-TG and -ApoB are not the only VLDL features that change under the influence of SAMe chronic impairment, VLDL-PE content

and VLDL size are also altered, which is another demonstration of NAFLD heterogeneity in the studied models. If those changes in VLDL characteristics can disturb VLDL metabolism deserves further attention given that there is a growing body of evidence suggesting that abnormalities in the size of VLDL particles secreted by the liver result in major disturbances of plasma lipoproteins metabolism[78, 168].

It is worth mentioning that SAMe levels can be modified not only by genetic causes[2] but also by external factors. For instance, SAMe plasma levels, hence liver levels[169], can be increased by oral administration of SAMe[170], by excess dietary methionine[171, 172], by diet supplementation with choline[173] and folic acid[174], or even by overfeeding in humans[175]. On the contrary, SAMe levels are negatively modified with methionine and/or choline deficient diets[176] or by deficiency of vitamins B6[177] and B12[178]. Therefore, the modulation of VLDL secretion via SAMe could have some clinical implications given that VLDL could be externally modulated through SAMe modulation and consequently the development of dyslipidaemias or NAFLD could be possible.

6.3. **SAMe increases VLDL clearance in NAFLD**

VLDLs are secreted by the liver to supply peripheral tissues with energy in the form of TG[82, 103]. VLDL secretion has already been proven to be modulated by SAMe levels in the liver (Part 2 of the Results). We have shown that in the background of elevated SAMe levels several features of VLDL are modified, GNMT-KO mice secrete enlarged VLDL, enriched in TG and poor in PE and ApoB. Given that VLDL clearance can be conditioned to the particles composition[73, 82, 106, 109], it would not be surprising to find it modified in GNMT-KO context. Whether VLDL catabolism is modified and if it is due to the mentioned characteristics or other changes taking place in the setting of elevated SAMe and NAFLD was the aim of this part of the work.

In spite of the increase in VLDL-TG secretion we found it striking that TG serum was diminished in the absence of GNMT, and provided that the MDD administration recovered serum TG levels, the elevated levels of SAMe must be playing a role in the augmented VLDL clearance.

NAFLD patients usually present hypertriglyceridemia[82], however serum TG values might be heterogeneous. Here we present a group of NAFLD patients with low levels of serum TG and increased VLDL size. The same patients presented low levels of GNMT in the liver, a feature that could be related with severe NAFLD given that a downregulation of *Mat1a* and *Gnmt* genes expression has been related with it[150] . What is more, *Gnmt* has been found hypermethylated and with reduced expression in patients with advanced NAFLD[151], and genome hypermethylation has been found to be an important characteristic of GNMT-KO mice[13] due to SAMe elevated levels[64]. In our group of patients we do not know the MAT protein status, however, the enlarged VLDL size, the reduction in hepatic PE and the increased levels of PC/PE ratio, distinctive features of GNMT-KO mouse model, suggest that the balance between GNMT and MAT activities tends toward increased hepatic SAMe levels which may enhance PEMT flux, what may possibly lead to a combination of pathophysiological mechanisms in glycerolipid

metabolism[179]. The pattern observed in VLDL in these NAFLD patients may also resemble that of GNMT-KO mice not only in size but also in the content of VLDL-PE considering that the phospholipid composition of secreted VLDL reflects that of the liver[179].

On another hand, an increased clearance of VLDL could imply an excessive supply to peripheral tissues and even to the liver, the principal actor in VLDL remnants clearance[82, 106]. The administration of a short-term HFD to GNMT-KO mice revealed an increased TG storage both in heart and in liver in the setting of higher rates of VLDL-TG secretion and clearance in comparison with animals that were fed the CD. The fact that no changes in serum FA nor in KB, along with the lack of an increase in CD36 protein levels or in genes related with lipogenesis in mice fed the HFD supports the involvement of an increased VLDL clearance in the augmentation of TG depots. Besides, from PC/PE ratio we can extract that PEMT flux is not as overactivated as it is in mice fed the CD (Results part 1), consequently this pathway is neither contributing to the increased hepatosteatosis in GNMT-KO mice fed the HFD. CD36 is usually elevated in the context of NAFLD or lipid-rich diets[180], thus its diminished levels in GNMT-KO mice fed the HFD were not predictable. However, it has been shown that mTOR selectively regulates its expression at a translational level[181], and mTOR activation is blocked in GNMT-KO animals[158], therefore, downregulation of mTOR pathway in this model could be suppressing, at least in part, CD36 translation.

The accumulation of TG in the heart deserves special attention given that cardiac dysfunction and even heart failure, a condition independently related with NAFLD[24], can be induced by the accumulation of TG in the heart both in mice and in humans[182]. ApoE-KO mice develop an age-dependent cardiomyopathy as a result of cardiac lipid accumulation due to hypertriglyceridemia[100]; cardiomyopathy that is accelerated under HFD effect[183] and attenuated in the absence of PEMT, likely due to the reduction in plasma lipid levels[100]. Conversely, GNMT-KO animals fed with the HFD develop cardiac lipid accumulation with an increased content of hepatic and VLDL-ApoE along with hepatic PEMT overactivation and reduced levels of plasma TG. The 3-month-old mice

fed the CD presented the same changes except for the increased TG in the heart, however, as it occurs in ApoE-KO mice they might develop it with age[100] and since TG serum is also diminished in 8-month-old mice fed both a CD and a HFD (data not shown), the increased lipid supply to peripheral tissues could suppose a long-term problem. Hence here we present a model with NAFLD and low levels of plasma TG that can potentially develop some of the known extrahepatic consequences of NAFLD, such as cardiovascular disease[23, 29].

PEMT overactivation in the case of GNMT-KO mice is due to high levels of SAMe (Results Part 1), and so seems the case for ApoE protein elevated levels considering that the MDD diet, aim at restoring SAMe concentrations, return ApoE to its physiological levels. ApoE increased hepatic content correlates with its increased secretion into VLDL, however, it is not linked to changes in its genetic expression. ApoE can be degraded through the proteasome[154] and through lysosomal enzymes[153], as it has been shown in HepG2 cells[153, 154], nevertheless, neither in GNMT-KO mice nor in their WT counterparts those mechanisms seem to be leading ApoE degradation. A plausible explanation for the increased ApoE hepatic content in the KO model relies on a recycling pathway. It has been demonstrated that following LDL-R family proteins-mediated internalization by the liver, ApoE can escape degradation and be resecreted[184, 185] in a quantitative significant fashion[186] that is accelerated by the presence of HDL[184, 187]. In concordance with this possibility we had previously demonstrated that HDL-PC was increased in GNMT-KO plasma (Results part 1. Fig. R4g). And by these mechanisms, overactivation of PEMT pathway, hence SAMe, could be related with ApoE increased levels, both in liver and in VLDL.

Increased ApoE content in VLDL is also a major feature in mice lacking GNMT fed the CD as well as in those fed the HFD. Under the HFD the VLDL enrichment in ApoE was even higher, along with TG storage. Consequently, since factors that regulate cytosolic lipid storage such as PLIN2 or CIDE-B can influence VLDL secretion[48, 95, 97], we thought that in this case, cytosolic lipid storage might as well be influencing ApoE secretion into VLDL particles. However, when liver TG accumulation is inhibited in GNMT-KO mice due

to the additional deletion of PLIN2 (Results Part 1), the VLDL enrichment in ApoE is still increased, therefore, the increased levels of SAMe must be playing a role in this enrichment.

ApoE plays a crucial role in VLDL catabolism[106, 110], so changes in its content, as it occurs with VLDL-ApoE increased content in GNMT-KO animals, could affect VLDL clearance. Increased content of ApoE in ApoB-containing lipoproteins have the potential to increase the deposition in the arterial wall, resulting in atherosclerosis[188]. Smaller dense LDL particles are proatherogenic either in mice or humans[189, 190]; and that small dense LDL originate from large TG-rich VLDL, such as those secreted by GNMT-KO mice liver, has long been known[191, 192]. Therefore, the finding of increased content of cholesterol in the fraction of smaller LDLs is not surprising in this model, yet it suggests an increased risk for atherosclerosis development in these animals, a condition that has been associated with NAFLD in humans[193]. ApoE plays the main role in clearance of TG-rich lipoproteins[188], so given the high content in ApoE in the secreted VLDL of GNMT-KO mice, it seems logical to find low levels of plasma TG in these mice. However, hypertriglyceridemia (HTG) has been described both in the case of ApoE deficiency[188, 194, 195] and during its overexpression[188, 196]. In the latter case, HTG can be explained through the inhibition of LPL and the stimulation of VLDL assembly[188, 196]; and in the first case by the lack of ApoE to serve as ligand for the LDL receptor family proteins[188, 194, 195]. Consequently, the increased content in ApoE in GNMT-KO VLDLs cannot explain only by itself the increased clearance, and other mechanisms might be taking place concomitantly.

The increased gene expression in the liver of *Vldlr* and *Ldlr*, both ApoE-binding receptors involved mainly in VLDL remnants clearance[82, 103] that can be regulated by PPARγ[197, 198], whose expression is hugely augmented in the liver under elevated levels of SAMe (Results Part 1), suggests that they could also be playing a role in the increased clearance of VLDL. However, the finding that human VLDLs were not catabolised faster from the GNMT-KO bloodstream suggests that other mechanisms, such as those related with the specific features of the GNMT-deficient mice VLDLs, might be involved in the

augmented VLDL clearance in the context of SAMe elevated levels. For instance, the larger size and increased content in TG of VLDL could influence their susceptibility to hydrolysis by LPL[106, 108]; or the fact that ApoB48-containing lipoproteins are removed faster from plasma than the ones-containing ApoB100 because ApoE associates with ApoB48[199], might also be influencing the rapid VLDL clearance in GNMT-KO given that in these mice the majority of the secreted VLDL contain ApoB48 instead of ApoB100 (Results Part 2).

Conclusively, SAMe plays an observable role in VLDL removal from the bloodstream, although the mechanisms involved are not evident at first sight and there might be various participating concomitantly. Besides, our results suggest that when excess SAMe couples with increased diet lipid supply, the enhanced VLDL clearance could lead to increased TG depots in the liver and heart, which could end in aggravation of NAFLD progression and the development of CVD. Accordingly, there is increasing evidence relating CVD with one-carbon metabolism pathophysiology[200]. However, lowering plasma VLDL has been suggested as a strategy to reduce CVD risk[110], but in the light of this work we could classify SAMe as a VLDL lowering agent nonetheless other mechanisms taking place at the same time could increase CVD risk or even low levels of VLDL in NAFLD context could be related with increased risk of CVD.

6.4. **General discussion**

The right amount of SAMe to provide an adequate supply of methyl groups is necessary to avoid liver injury[4]. However, the mechanisms linking SAMe with lipid homeostasis are not obvious at first glance. Nevertheless, we have demonstrated in this work that when at supraphysiological levels in the liver[20], SAMe greatly disturbs glycerolipid metabolism. Disturbance that is mainly led by the overactivation of PC biosynthesis through SAMe-dependent enzyme PEMT. In GNMT-KO mice liver the excess PC is redirected to the synthesis of TG, which is either accumulated in lipid droplets triggering steatosis or oversecreted into VLDL. The oversecretion of TG is not capable of compensating the increased TG accumulation probably due to the increased clearance of VLDL, which, as demonstrated in animals fed a HFD, induces the accumulation of TG in the liver and the heart. Consequently, dysregulated levels of SAMe can have consequences not only for liver lipid metabolism but also for systemic lipid metabolism through the secreted VLDL. By this way SAMe-induced NAFLD can be linked to extrahepatic consequences of this common disease. VLDL secretion is controlled by SAMe as well when SAMe hepatic levels are decreased, as it is the case for MAT1A mice[19], here again, the piece that links SAMe and VLDL secretion is PEMT, whose activity is diminished in this case.

In GNMT-KO case, the overactivation of PEMT presents a duality given that it is capable of inducing TG accumulation inducing NAFLD development through PC catabolism and at the same time it also induces an oversecretion of TG in the form of VLDL (Fig. D1). By contrast, PEMT-KO hepatocytes secrete approximately 50% less TG into VLDL[99] and develop hepatic steatosis due in part to the diminished secretion of VLDL[201]. Likewise, MAT1A-KO mice develop hepatosteatosis and secrete 25% less TG into their VLDL, besides, PEMT activity is diminished in these animals[58] . Accordingly, PC/PE ratio is reduced in the absence of MAT1A, as it occurs in PEMT-KO mice; on the

contrary, and in concordance with increased PEMT flux, PC/PE ratio is increased in GNMT-KO mice.
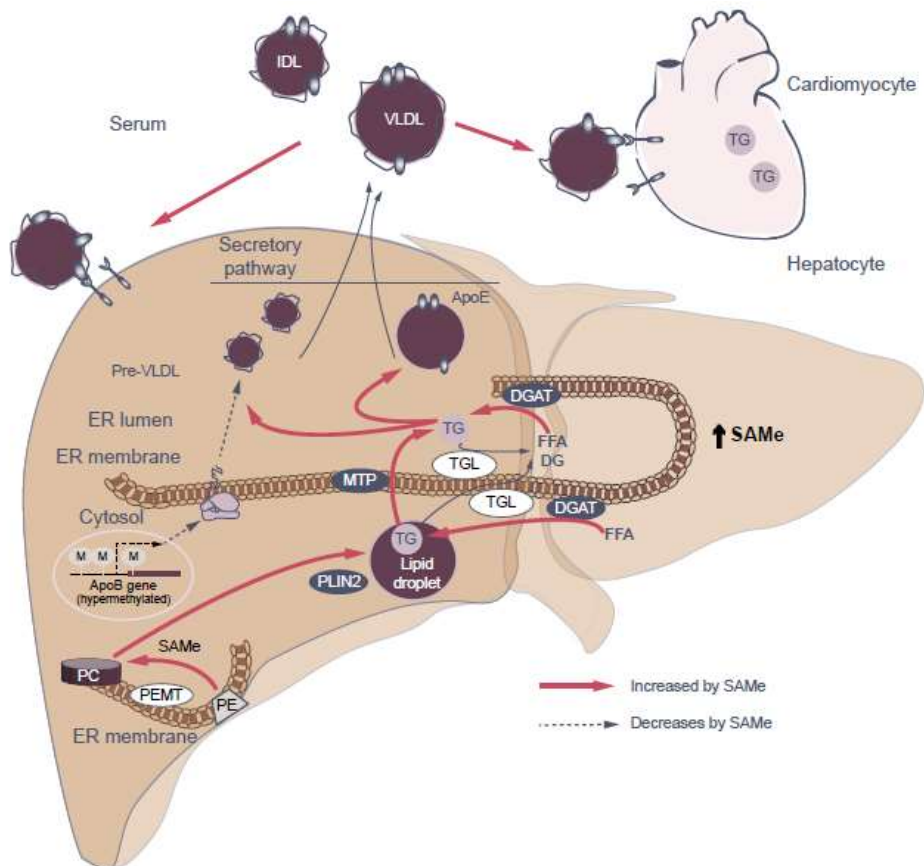
Figure D1. *Representation of the processes affected by high hepatic levels of SAMe.* Hepatic TG secretion is increased mainly due to a stimulated PEMT flux that also stimulates TG storage in lipid droplets. The rise in mobilization of TGs from cytoplasmic lipid droplet stores enhance the availability of TGs to be channelled towards VLDL secretion; and MTP and DGAT activities also promote the process. Excess levels of SAMe induce the secretion of less but enlarged, PE-poor and TG-enriched VLDL particles. ApoB availability is decreased in the liver due to lower mRNA synthesis and stability. The secreted VLDL particles are rapidly metabolized from the bloodstream due mainly to their specific VLDL features, leading to increased lipid supply to tissues such as liver and heart. Abbreviations: Apo, apolipoprotein; DGAT, diacylglycerol O-acyltransferase; ER, endoplasmic reticulum; MTP, microsomal triglyceride transfer protein; PE, phosphatidylethanolamine; PEMT, phosphatidylethanolamine N-methyltransferase; PLIN2, perilipin 2; SAMe, S-adenosylmethionine; TG, triglyceride; TGL, TG lipase; VLDL, very-low-density lipoprotein. Graphical abstract taken from Martinez-Uña, et al., 2015[146].

All the abovementioned goes a long way towards explaining why a chronic imbalance in hepatic SAMe synthesis[19] or catabolism[13] is capable of altering lipid liver

metabolism leading NAFLD development. And the subsequent decrease or increase, respectively, of PC/PE ratio, hence PEMT flux, seems to be of great importance for liver lipid homeostasis maintenance (Fig. D1).

On another hand, NAFLD is usually associated with insulin resistance in humans[25, 118] and in some animal models[66]. However, in spite of NAFLD development, GNMT-KO mice do not present systemic insulin resistance (Results Part 1). What is more, they present a not significant tendency to be more insulin sensitive than the WT animals. GNMT deficient mice have very high levels of DG content in the liver (Results Part 1), a feature that has widely been associated with hepatic insulin resistance[202]; nonetheless, it has also been shown that GNMT-KO mice accumulate glycogen in the liver[158, 203], hence its synthesis, that is stimulated by insulin, might be working. Therefore this suggests that hepatic insulin response might be functioning as well as systemic insulin response. Nevertheless, the increased insulin sensitivity found when NAFLD worsens in 8-month-old animals (Results Part 1) or in those fed with the HFD (Results Part 3) was a striking finding. On the contrary, the improvement on insulin sensitivity in GNMT-PLIN2-KO mice come without surprise because deletion of PLIN2 had already been proven to improve it in obesity-prone leptin deficient mice along with steatosis[48]. The relationship between insulin resistance and NAFLD is complex and they are not always associated neither in animal models nor in humans[165]. A positive association between PC/PE ratio and insulin sensitivity has recently been suggested in muscle[204]. Increased insulin sensitivity is also found in PEMT deficient mice[205], along with hepatostatosis and low levels of PC/PE ratio[206]. This, together with the finding of increased insulin sensitivity in our models with augmented PC/PE ratio suggests that the relation of PC to PE, which has been described as an indicator of membrane integrity[207], might be playing also a role in insulin response.

All in all, GNMT-KO mice model for NAFLD is a good model for studying the disease in the context of non-obese, non-insulin resistant subjects. And the whole study supports the hypothesis that administration of SAMe to improve liver disease and lipoprotein metabolism will have beneficial effects only in patients with low levels of

SAMe. And when SAMe levels are increased, a methionine deficient diet would be of major benefit.

7. Conclusions

7. **CONCLUSIONS**

1. **Excess SAMe induces TG accumulation in the liver of GNMT-KO mice.**

   1.1. GNMT-KO animals develop NAFLD although they present an increased rate of hepatic TG secretion without increased lipogenesis, FA uptake or altered β-oxidation. TG accumulates in the liver of GNMT-KO mice by a newly described pathway; excess SAMe increases PEMT flux, hence PC synthesis; excess PC is then mainly redirected towards DG and TG synthesis. PEMT overactivation is responsible for the TG accumulation in the liver of GNMT-KO mice.

   1.2. The additional deletion of PLIN2 in GNMT-KO mice protects them against hepatosteatosis although excess SAMe still induces PEMT activity. In this model hepatic TG secretion rate and gluconeogenesis are increased; in the context of elevated levels of SAMe there is a crosstalk between lipid synthesis and sequestration and glucose metabolism.

2. **Chronic impairment of SAMe levels results in dysregulation of VLDL assembly and secretion.**

   2.1. Low levels and high levels of SAMe present opposite effects over VLDL assembly and secretion. SAMe controls VLDL secretion mainly by PEMT pathway which activity is reduced when SAMe levels are low and increased when SAMe levels are high.

      2.1.1. Low hepatic levels of SAMe in MAT1A-KO mice reduce the enzymatic activities involve in VLDL assembly and impair the features of the secreted VLDL, VLDLs are small, TG-poor and ApoB-rich.

2.1.2. Elevated levels of hepatic SAMe in GNMT-KO animals increase VLDL-TG secretion due to increase mobilization of TG lipid stores and increase activity of VLDL assembly-related enzymes. VLDL-ApoB secretion is reduced when SAMe levels are elevated due to reduced presence of Apolipoprotein B mRNA because of the hypermethylation of its promoter region and of the lack of *Apob*-HuR binding.

3. SAMe plays a role over VLDL catabolism.

3.1. Increased levels of SAMe due to GNMT deficiency reduce bloodstream circulating levels of TG and ApoB. The augmented clearance of VLDL in GNMT-KO mice depend upon the specific features of the VLDLs secreted by the liver of these animals and upon the increased expression of VLDL and LDL receptors. VLDLs are poor in ApoB and PE, enriched in ApoE and TG and of a larger size. The increased ApoE content in VLDLs responds to elevated levels of this apoprotein in the liver as a consequence of excess SAMe.

3.2. In a context where there is an increased lipid supply, the increased clearance of VLDL in GNMT-KO mice induces the accumulation of TG in the liver and the heart.

3.3. A group of NAFLD patients with low levels of GNMT in the liver resemble the mice phenotype and present reduced serum TG levels and increased PC/PE ratio in the liver.

8. References

8. **REFERENCES**

1. Martinez-Lopez N, Varela-Rey M, Ariz U, Embade N, Vazquez-Chantada M, Fernandez-Ramos D, Gomez-Santos L, Lu SC, Mato JM, Martinez-Chantar ML. S-adenosylmethionine and proliferation: New pathways, new targets. Biochem Soc Trans 2008 Oct;36(Pt 5):848-52.

2. Lu SC, Mato JM. S-adenosylmethionine in liver health, injury, and cancer. Physiol Rev 2012 Oct;92(4):1515-42.

3. CATONI GL. S-adenosylmethionine; a new intermediate formed enzymatically from L-methionine and adenosinetriphosphate. J Biol Chem 1953 Sep;204(1):403-16.

4. Mato JM, Lu SC. Role of S-adenosyl-L-methionine in liver health and injury. Hepatology 2007 May;45(5):1306-12.

5. Fontecave M, Atta M, Mulliez E. S-adenosylmethionine: Nothing goes to waste. Trends Biochem Sci 2004 May;29(5):243-9.

6. Mudd SH, Brosnan JT, Brosnan ME, Jacobs RL, Stabler SP, Allen RH, Vance DE, Wagner C. Methyl balance and transmethylation fluxes in humans. Am J Clin Nutr 2007 Jan;85(1):19-25.

7. Luka Z, Mudd SH, Wagner C. Glycine N-methyltransferase and regulation of S-adenosylmethionine levels. J Biol Chem 2009 Aug 21;284(34):22507-11.

8. Vance DE. Phospholipid methylation in mammals: From biochemistry to physiological function. Biochim Biophys Acta 2014 Jun;1838(6):1477-87.

9. Bottiglieri T. S-adenosyl-L-methionine (SAMe): From the bench to the bedside--molecular basis of a pleiotrophic molecule. Am J Clin Nutr 2002 Nov;76(5):1151S-7S.

10. Li Z, Vance DE. Phosphatidylcholine and choline homeostasis. J Lipid Res 2008 Jun;49(6):1187-94.

11. Mato JM, Martinez-Chantar ML, Lu SC. S-adenosylmethionine metabolism and liver disease. Ann Hepatol 2013 Mar-Apr;12(2):183-9.

12. Williams KT, Schalinske KL. Homocysteine metabolism and its relation to health and disease. Biofactors 2010 Jan-Feb;36(1):19-24.

13. Martinez-Chantar ML, Vazquez-Chantada M, Ariz U, Martinez N, Varela M, Luka Z, Capdevila A, Rodriguez J, Aransay AM, Matthiesen R, et al. Loss of the glycine N-methyltransferase gene leads to steatosis and hepatocellular carcinoma in mice. Hepatology 2008 Apr;47(4):1191-9.

14. Kinsell LW, Harper HA, Barton HC, Hutchin ME, Hess JR. Studies in methionine and sulfur metabolism. I. the fate of intravenously administered methionine, in normal individuals and in patients with liver damage. J Clin Invest 1948 Sep;27(5):677-88.

15. Kalhan SC, Edmison J, Marczewski S, Dasarathy S, Gruca LL, Bennett C, Duenas C, Lopez R. Methionine and protein metabolism in non-alcoholic steatohepatitis: Evidence for lower rate of transmethylation of methionine. Clin Sci (Lond) 2011 Aug;121(4):179-89.

16. Mudd SH, Cerone R, Schiaffino MC, Fantasia AR, Minniti G, Caruso U, Lorini R, Watkins D, Matiaszuk N, Rosenblatt DS, et al. Glycine N-methyltransferase deficiency: A novel

inborn error causing persistent isolated hypermethioninaemia. J Inherit Metab Dis 2001 Aug;24(4):448-64.

17. Tseng TL, Shih YP, Huang YC, Wang CK, Chen PH, Chang JG, Yeh KT, Chen YM, Buetow KH. Genotypic and phenotypic characterization of a putative tumor susceptibility gene, GNMT, in liver cancer. Cancer Res 2003 Feb 1;63(3):647-54.

18. Anstee QM, Day CP. S-adenosylmethionine (SAMe) therapy in liver disease: A review of current evidence and clinical utility. J Hepatol 2012 Nov;57(5):1097-109.

19. Lu SC, Alvarez L, Huang ZZ, Chen L, An W, Corrales FJ, Avila MA, Kanel G, Mato JM. Methionine adenosyltransferase 1A knockout mice are predisposed to liver injury and exhibit increased expression of genes involved in proliferation. Proc Natl Acad Sci U S A 2001 May 8;98(10):5560-5.

20. Luka Z, Capdevila A, Mato JM, Wagner C. A glycine N-methyltransferase knockout mouse model for humans with deficiency of this enzyme. Transgenic Res 2006 Jun;15(3):393-7.

21. WGO Global Guidelines. Nonalcoholic Fatty Liver Disease and Nonalcoholic Steatohepatitis [Internet] [cited 2012 Junio]. Available from: http://www.worldgastroenterology.org/guidelines/global-guidelines/nafld-nash/nafld-nash-english.

22. Bellentani S, Scaglioni F, Marino M, Bedogni G. Epidemiology of non-alcoholic fatty liver disease. Dig Dis 2010;28(1):155-61.

23. Armstrong MJ, Adams LA, Canbay A, Syn WK. Extrahepatic complications of nonalcoholic fatty liver disease. Hepatology 2013 Sep 3.

24. Byrne CD, Targher G. NAFLD: A multisystem disease. J Hepatol 2015 Apr;62(1 Suppl):S47-64.

25. Younossi ZM, Koenig AB, Abdelatif D, Fazel Y, Henry L, Wymer M. Global epidemiology of nonalcoholic fatty liver disease-meta-analytic assessment of prevalence, incidence, and outcomes. Hepatology 2016 Jul;64(1):73-84.

26. Brunt EM, Wong VW, Nobili V, Day CP, Sookoian S, Maher JJ, Bugianesi E, Sirlin CB, Neuschwander-Tetri BA, Rinella ME. Nonalcoholic fatty liver disease. Nat Rev Dis Primers 2015 Dec 17;1:15080.

27. Anderson EL, Howe LD, Jones HE, Higgins JP, Lawlor DA, Fraser A. The prevalence of non-alcoholic fatty liver disease in children and adolescents: A systematic review and meta-analysis. PLoS One 2015 Oct 29;10(10):e0140908.

28. Angulo P. Long-term mortality in nonalcoholic fatty liver disease: Is liver histology of any prognostic significance? Hepatology 2010 Feb;51(2):373-5.

29. Chacko KR, Reinus J. Extrahepatic complications of nonalcoholic fatty liver disease. Clin Liver Dis 2016 May;20(2):387-401.

30. Yu J, Marsh S, Hu J, Feng W, Wu C. The pathogenesis of nonalcoholic fatty liver disease: Interplay between diet, gut microbiota, and genetic background. Gastroenterol Res Pract 2016;2016:2862173.

31. NCD Risk Factor Collaboration (NCD-RisC). Trends in adult body-mass index in 200 countries from 1975 to 2014: A pooled analysis of 1698 population-based

measurement studies with 19.2 million participants. Lancet 2016 Apr 2;387(10026):1377-96.

32. NCD Risk Factor Collaboration (NCD-RisC). Worldwide trends in diabetes since 1980: A pooled analysis of 751 population-based studies with 4.4 million participants. Lancet 2016 Apr 9;387(10027):1513-30.

33. Masarone M, Federico A, Abenavoli L, Loguercio C, Persico M. Non alcoholic fatty liver: Epidemiology and natural history. Rev Recent Clin Trials 2014;9(3):126-33.

34. Li L, Liu DW, Yan HY, Wang ZY, Zhao SH, Wang B. Obesity is an independent risk factor for non-alcoholic fatty liver disease: Evidence from a meta-analysis of 21 cohort studies. Obes Rev 2016 Jun;17(6):510-9.

35. Day CP, James OF. Steatohepatitis: A tale of two "hits"? Gastroenterology 1998 Apr;114(4):842-5.

36. Buzzetti E, Pinzani M, Tsochatzis EA. The multiple-hit pathogenesis of non-alcoholic fatty liver disease (NAFLD). Metabolism 2016 Aug;65(8):1038-48.

37. Tilg H, Moschen AR. Evolution of inflammation in nonalcoholic fatty liver disease: The multiple parallel hits hypothesis. Hepatology 2010 Nov;52(5):1836-46.

38. Kawano Y, Cohen DE. Mechanisms of hepatic triglyceride accumulation in non-alcoholic fatty liver disease. J Gastroenterol 2013 Apr;48(4):434-41.

39. Donnelly KL, Smith CI, Schwarzenberg SJ, Jessurun J, Boldt MD, Parks EJ. Sources of fatty acids stored in liver and secreted via lipoproteins in patients with nonalcoholic fatty liver disease. J Clin Invest 2005 May;115(5):1343-51.

40. Fabbrini E, Magkos F. Hepatic steatosis as a marker of metabolic dysfunction. Nutrients 2015 Jun 19;7(6):4995-5019.

41. Fon Tacer K, Rozman D. Nonalcoholic fatty liver disease: Focus on lipoprotein and lipid deregulation. J Lipids 2011;2011:783976.

42. Guo Y, Cordes KR, Farese RV,Jr, Walther TC. Lipid droplets at a glance. J Cell Sci 2009 Mar 15;122(Pt 6):749-52.

43. Carr RM, Ahima RS. Pathophysiology of lipid droplet proteins in liver diseases. Exp Cell Res 2016 Jan 15;340(2):187-92.

44. Chang BH, Chan L. Regulation of triglyceride metabolism. III. emerging role of lipid droplet protein ADFP in health and disease. Am J Physiol Gastrointest Liver Physiol 2007 Jun;292(6):G1465-8.

45. Okumura T. Role of lipid droplet proteins in liver steatosis. J Physiol Biochem 2011 Dec;67(4):629-36.

46. Sahini N, Borlak J. Recent insights into the molecular pathophysiology of lipid droplet formation in hepatocytes. Prog Lipid Res 2014 Apr;54:86-112.

47. Chang BH, Li L, Paul A, Taniguchi S, Nannegari V, Heird WC, Chan L. Protection against fatty liver but normal adipogenesis in mice lacking adipose differentiation-related protein. Mol Cell Biol 2006 Feb;26(3):1063-76.

48. Chang BH, Li L, Saha P, Chan L. Absence of adipose differentiation related protein upregulates hepatic VLDL secretion, relieves hepatosteatosis, and improves whole body insulin resistance in leptin-deficient mice. J Lipid Res 2010 Aug;51(8):2132-42.

49. Lonardo A, Ballestri S, Marchesini G, Angulo P, Loria P. Nonalcoholic fatty liver disease: A precursor of the metabolic syndrome. Dig Liver Dis 2015 Mar;47(3):181-90.

50. Ratziu V, Goodman Z, Sanyal A. Current efforts and trends in the treatment of NASH. J Hepatol 2015 Apr;62(1 Suppl):S65-75.

51. Caballero F, Fernandez A, Matias N, Martinez L, Fucho R, Elena M, Caballeria J, Morales A, Fernandez-Checa JC, Garcia-Ruiz C. Specific contribution of methionine and choline in nutritional nonalcoholic steatohepatitis: Impact on mitochondrial S-adenosyl-L-methionine and glutathione. J Biol Chem 2010 Jun 11;285(24):18528-36.

52. Zeisel SH, Zola T, daCosta KA, Pomfret EA. Effect of choline deficiency on S-adenosylmethionine and methionine concentrations in rat liver. Biochem J 1989 May 1;259(3):725-9.

53. Obeid R, Herrmann W. Homocysteine and lipids: S-adenosyl methionine as a key intermediate. FEBS Lett 2009 Apr 17;583(8):1215-25.

54. Yao ZM, Vance DE. The active synthesis of phosphatidylcholine is required for very low density lipoprotein secretion from rat hepatocytes. J Biol Chem 1988 Feb 25;263(6):2998-3004.

55. Avila MA, Berasain C, Torres L, Martin-Duce A, Corrales FJ, Yang H, Prieto J, Lu SC, Caballeria J, Rodes J, et al. Reduced mRNA abundance of the main enzymes involved in methionine metabolism in human liver cirrhosis and hepatocellular carcinoma. J Hepatol 2000 Dec;33(6):907-14.

56. Martinez-Chantar ML, Corrales FJ, Martinez-Cruz LA, Garcia-Trevijano ER, Huang ZZ, Chen L, Kanel G, Avila MA, Mato JM, Lu SC. Spontaneous oxidative stress and liver tumors in mice lacking methionine adenosyltransferase 1A. Faseb J 2002 Aug;16(10):1292-4.

57. Rubio A, Guruceaga E, Vazquez-Chantada M, Sandoval J, Martinez-Cruz LA, Segura V, Sevilla JL, Podhorski A, Corrales FJ, Torres L, et al. Identification of a gene-pathway associated with non-alcoholic steatohepatitis. J Hepatol 2007 Apr;46(4):708-18.

58. Cano A, Buque X, Martinez-Una M, Aurrekoetxea I, Menor A, Garcia-Rodriguez JL, Lu SC, Martinez-Chantar ML, Mato JM, Ochoa B, et al. Methionine adenosyltransferase 1A gene deletion disrupts hepatic very low-density lipoprotein assembly in mice. Hepatology 2011 Dec;54(6):1975-86.

59. Walker AK, Jacobs RL, Watts JL, Rottiers V, Jiang K, Finnegan DM, Shioda T, Hansen M, Yang F, Niebergall LJ, et al. A conserved SREBP-1/phosphatidylcholine feedback circuit regulates lipogenesis in metazoans. Cell 2011 Nov 11;147(4):840-52.

60. Alonso C, Fernandez-Ramos D, Varela-Rey M, Martinez-Arranz I, Navasa N, Van Liempd SM, Lavin Trueba JL, Mayo R, Ilisso CP, de Juan VG, et al. Metabolomic identification of subtypes of nonalcoholic steatohepatitis. Gastroenterology 2017 May;152(6):1449,1461.e7.

61. Chen YM, Shiu JY, Tzeng SJ, Shih LS, Chen YJ, Lui WY, Chen PH. Characterization of glycine-N-methyltransferase-gene expression in human hepatocellular carcinoma. Int J Cancer 1998 Mar 2;75(5):787-93.

62. Augoustides-Savvopoulou P, Luka Z, Karyda S, Stabler SP, Allen RH, Patsiaoura K, Wagner C, Mudd SH. Glycine N -methyltransferase deficiency: A new patient with a novel mutation. J Inherit Metab Dis 2003;26(8):745-59.

63. Varela-Rey M, Embade N, Ariz U, Lu SC, Mato JM, Martinez-Chantar ML. Non-alcoholic steatohepatitis and animal models: Understanding the human disease. Int J Biochem Cell Biol 2009 May;41(5):969-76.

64. Varela-Rey M, Martinez-Lopez N, Fernandez-Ramos D, Embade N, Calvisi DF, Woodhoo A, Rodriguez J, Fraga MF, Julve J, Rodriguez-Millan E, et al. Fatty liver and fibrosis in glycine N-methyltransferase knockout mice is prevented by nicotinamide. Hepatology 2010 Jul;52(1):105-14.

65. Bray GA, Paeratakul S, Popkin BM. Dietary fat and obesity: A review of animal, clinical and epidemiological studies. Physiol Behav 2004 Dec 30;83(4):549-55.

66. Hebbard L, George J. Animal models of nonalcoholic fatty liver disease. Nat Rev Gastroenterol Hepatol 2011 Jan;8(1):35-44.

67. Anstee QM, Goldin RD. Mouse models in non-alcoholic fatty liver disease and steatohepatitis research. Int J Exp Pathol 2006 Feb;87(1):1-16.

68. Biddinger SB, Almind K, Miyazaki M, Kokkotou E, Ntambi JM, Kahn CR. Effects of diet and genetic background on sterol regulatory element-binding protein-1c, stearoyl-CoA desaturase 1, and the development of the metabolic syndrome. Diabetes 2005 May;54(5):1314-23.

69. Ito M, Suzuki J, Tsujioka S, Sasaki M, Gomori A, Shirakura T, Hirose H, Ito M, Ishihara A, Iwaasa H, et al. Longitudinal analysis of murine steatohepatitis model induced by chronic exposure to high-fat diet. Hepatol Res 2007 Jan;37(1):50-7.

70. Takahashi Y, Soejima Y, Fukusato T. Animal models of nonalcoholic fatty liver disease/nonalcoholic steatohepatitis. World J Gastroenterol 2012 May 21;18(19):2300-8.

71. Buettner R, Scholmerich J, Bollheimer LC. High-fat diets: Modeling the metabolic disorders of human obesity in rodents. Obesity (Silver Spring) 2007 Apr;15(4):798-808.

72. Kanuri G, Bergheim I. In vitro and in vivo models of non-alcoholic fatty liver disease (NAFLD). Int J Mol Sci 2013 Jun 5;14(6):11963-80.

73. Ramasamy I. Recent advances in physiological lipoprotein metabolism. Clin Chem Lab Med 2014 Dec;52(12):1695-727.

74. Minehira K, Young SG, Villanueva CJ, Yetukuri L, Oresic M, Hellerstein MK, Farese RV,Jr, Horton JD, Preitner F, Thorens B, et al. Blocking VLDL secretion causes hepatic steatosis but does not affect peripheral lipid stores or insulin sensitivity in mice. J Lipid Res 2008 Sep;49(9):2038-44.

75. Fujita K, Nozaki Y, Wada K, Yoneda M, Fujimoto Y, Fujitake M, Endo H, Takahashi H, Inamori M, Kobayashi N, et al. Dysfunctional very-low-density lipoprotein synthesis

and release is a key factor in nonalcoholic steatohepatitis pathogenesis. Hepatology 2009 Sep;50(3):772-80.

76. Fabbrini E, deHaseth D, Deivanayagam S, Mohammed BS, Vitola BE, Klein S. Alterations in fatty acid kinetics in obese adolescents with increased intrahepatic triglyceride content. Obesity (Silver Spring) 2009 Jan;17(1):25-9.

77. Jo H, Choe SS, Shin KC, Jang H, Lee JH, Seong JK, Back SH, Kim JB. Endoplasmic reticulum stress induces hepatic steatosis via increased expression of the hepatic very low-density lipoprotein receptor. Hepatology 2013 Apr;57(4):1366-77.

78. Gibbons GF, Wiggins D, Brown AM, Hebbachi AM. Synthesis and function of hepatic very-low-density lipoprotein. Biochem Soc Trans 2004 Feb;32(Pt 1):59-64.

79. Scott R, Donoghoe M, Watts GF, O'Brien R, Pardy C, Taskinen MR, Davis TM, Colman PG, Manning P, Fulcher G, et al. Impact of metabolic syndrome and its components on cardiovascular disease event rates in 4900 patients with type 2 diabetes assigned to placebo in the FIELD randomised trial. Cardiovasc Diabetol 2011 Nov 21;10:102,2840-10-102.

80. Sundaram M, Yao Z. Recent progress in understanding protein and lipid factors affecting hepatic VLDL assembly and secretion. Nutr Metab (Lond) 2010 Apr 27;7:35,7075-7-35.

81. Fazio S, Linton MF. Section I. basic mechanisms. chapter 2. regulation and clearance of apolipoprotein B-containing lipoproteins. In: Lipidología clínica. Barcelona: J&C; 2011. [Texto impreso]: complemento al Tratado de cardiología de Braunwald's Heart Disease Christie M. Ballantyne ; Josep Guindo i Soldevila, director de la edición española ; [traducido por Antonio Díez i Mercè Calvo]; Incluye referencias bibliográficas e índice; Título original: Clinical lipidology.

82. Cohen DE, Fisher EA. Lipoprotein metabolism, dyslipidemia, and nonalcoholic fatty liver disease. Semin Liver Dis 2013 Nov;33(4):380-8.

83. Tiwari S, Siddiqi SA. Intracellular trafficking and secretion of VLDL. Arterioscler Thromb Vasc Biol 2012 May;32(5):1079-86.

84. Wu X, Zhou M, Huang LS, Wetterau J, Ginsberg HN. Demonstration of a physical interaction between microsomal triglyceride transfer protein and apolipoprotein B during the assembly of ApoB-containing lipoproteins. J Biol Chem 1996 Apr 26;271(17):10277-81.

85. Patel SB, Grundy SM. Interactions between microsomal triglyceride transfer protein and apolipoprotein B within the endoplasmic reticulum in a heterologous expression system. J Biol Chem 1996 Aug 2;271(31):18686-94.

86. Hussain MM, Shi J, Dreizen P. Microsomal triglyceride transfer protein and its role in apoB-lipoprotein assembly. J Lipid Res 2003 Jan;44(1):22-32.

87. Powell LM, Wallis SC, Pease RJ, Edwards YH, Knott TJ, Scott J. A novel form of tissue-specific RNA processing produces apolipoprotein-B48 in intestine. Cell 1987 Sep 11;50(6):831-40.

88. Bartolome N, Aspichueta P, Martinez MJ, Vazquez-Chantada M, Martinez-Chantar ML, Ochoa B, Chico Y. Biphasic adaptative responses in VLDL metabolism and lipoprotein homeostasis during gram-negative endotoxemia. Innate Immun 2012 Feb;18(1):89-99.

89. Mohler PJ, Zhu MY, Blade AM, Ham AJ, Shelness GS, Swift LL. Identification of a novel isoform of microsomal triglyceride transfer protein. J Biol Chem 2007 Sep 14;282(37):26981-8.

90. Khatun I, Zeissig S, Iqbal J, Wang M, Curiel D, Shelness GS, Blumberg RS, Hussain MM. Phospholipid transfer activity of microsomal triglyceride transfer protein produces apolipoprotein B and reduces hepatosteatosis while maintaining low plasma lipids in mice. Hepatology 2012 May;55(5):1356-68.

91. Kulinski A, Rustaeus S, Vance JE. Microsomal triacylglycerol transfer protein is required for lumenal accretion of triacylglycerol not associated with ApoB, as well as for ApoB lipidation. J Biol Chem 2002 Aug 30;277(35):31516-25.

92. Gibbons GF, Khurana R, Odwell A, Seelaender MC. Lipid balance in HepG2 cells: Active synthesis and impaired mobilization. J Lipid Res 1994 Oct;35(10):1801-8.

93. Wiggins D, Gibbons GF. The lipolysis/esterification cycle of hepatic triacylglycerol. its role in the secretion of very-low-density lipoprotein and its response to hormones and sulphonylureas. Biochem J 1992 Jun 1;284 (Pt 2)(Pt 2):457-62.

94. Gilham D, Ho S, Rasouli M, Martres P, Vance DE, Lehner R. Inhibitors of hepatic microsomal triacylglycerol hydrolase decrease very low density lipoprotein secretion. Faseb J 2003 Sep;17(12):1685-7.

95. Magnusson B, Asp L, Bostrom P, Ruiz M, Stillemark-Billton P, Linden D, Boren J, Olofsson SO. Adipocyte differentiation-related protein promotes fatty acid storage in cytosolic triglycerides and inhibits secretion of very low-density lipoproteins. Arterioscler Thromb Vasc Biol 2006 Jul;26(7):1566-71.

96. Nourbakhsh M, Douglas DN, Pu CH, Lewis JT, Kawahara T, Lisboa LF, Wei E, Asthana S, Quiroga AD, Law LM, et al. Arylacetamide deacetylase: A novel host factor with important roles in the lipolysis of cellular triacylglycerol stores, VLDL assembly and HCV production. J Hepatol 2013 Aug;59(2):336-43.

97. Ye J, Li JZ, Liu Y, Li X, Yang T, Ma X, Li Q, Yao Z, Li P. Cideb, an ER- and lipid droplet-associated protein, mediates VLDL lipidation and maturation by interacting with apolipoprotein B. Cell Metab 2009 Feb;9(2):177-90.

98. Jacobs RL, Devlin C, Tabas I, Vance DE. Targeted deletion of hepatic CTP:Phosphocholine cytidylyltransferase alpha in mice decreases plasma high density and very low density lipoproteins. J Biol Chem 2004 Nov 5;279(45):47402-10.

99. Noga AA, Zhao Y, Vance DE. An unexpected requirement for phosphatidylethanolamine N-methyltransferase in the secretion of very low density lipoproteins. J Biol Chem 2002 Nov 1;277(44):42358-65.

100. Cole LK, Dolinsky VW, Dyck JR, Vance DE. Impaired phosphatidylcholine biosynthesis reduces atherosclerosis and prevents lipotoxic cardiac dysfunction in ApoE-/- mice. Circ Res 2011 Mar 18;108(6):686-94.

101. Vance JE, Adeli K. CHAPTER 18. assembly and secretion of triacylglycerol-rich lipoproteins. In: Biochemistry of lipids, lipoproteins and membranes. ; 2008. editors Dennis E. Vance and Jean E. Vance.

102. Liza M, Chico Y, Fresnedo O, Ochoa B. Dual action of neutral sphingomyelinase on rat hepatocytes: Activation of cholesteryl ester metabolism and biliary cholesterol secretion and inhibition of VLDL secretion. Lipids 2003 Jan;38(1):53-63.

103. Jiang ZG, Robson SC, Yao Z. Lipoprotein metabolism in nonalcoholic fatty liver disease. J Biomed Res 2013 Jan;27(1):1-13.

104. Tomiyasu K, Walsh BW, Ikewaki K, Judge H, Sacks FM. Differential metabolism of human VLDL according to content of ApoE and ApoC-III. Arterioscler Thromb Vasc Biol 2001 Sep;21(9):1494-500.

105. Wood RJ, Volek JS, Liu Y, Shachter NS, Contois JH, Fernandez ML. Carbohydrate restriction alters lipoprotein metabolism by modifying VLDL, LDL, and HDL subfraction distribution and size in overweight men. J Nutr 2006 Feb;136(2):384-9.

106. Morita SY. Metabolism and modification of apolipoprotein B-containing lipoproteins involved in dyslipidemia and atherosclerosis. Biol Pharm Bull 2016;39(1):1-24.

107. Cole LK, Vance JE, Vance DE. Phosphatidylcholine biosynthesis and lipoprotein metabolism. Biochim Biophys Acta 2012 May;1821(5):754-61.

108. Fisher RM, Coppack SW, Humphreys SM, Gibbons GF, Frayn KN. Human triacylglycerol-rich lipoprotein subfractions as substrates for lipoprotein lipase. Clin Chim Acta 1995 Apr 30;236(1):7-17.

109. Sacks FM. The crucial roles of apolipoproteins E and C-III in apoB lipoprotein metabolism in normolipidemia and hypertriglyceridemia. Curr Opin Lipidol 2015 Feb;26(1):56-63.

110. Pechlaner R, Tsimikas S, Yin X, Willeit P, Baig F, Santer P, Oberhollenzer F, Egger G, Witztum JL, Alexander VJ, et al. Very-low-density lipoprotein-associated apolipoproteins predict cardiovascular events and are lowered by inhibition of APOC-III. J Am Coll Cardiol 2017 Feb 21;69(7):789-800.

111. Hauser PS, Narayanaswami V, Ryan RO. Apolipoprotein E: From lipid transport to neurobiology. Prog Lipid Res 2011 Jan;50(1):62-74.

112. Go GW, Mani A. Low-density lipoprotein receptor (LDLR) family orchestrates cholesterol homeostasis. Yale J Biol Med 2012 Mar;85(1):19-28.

113. Multhaupt HA, Gafvels ME, Kariko K, Jin H, Arenas-Elliot C, Goldman BI, Strauss JF,3rd, Angelin B, Warhol MJ, McCrae KR. Expression of very low density lipoprotein receptor in the vascular wall. analysis of human tissues by in situ hybridization and immunohistochemistry. Am J Pathol 1996 Jun;148(6):1985-97.

114. Takahashi S, Sakai J, Fujino T, Hattori H, Zenimaru Y, Suzuki J, Miyamori I, Yamamoto TT. The very low-density lipoprotein (VLDL) receptor: Characterization and functions as a peripheral lipoprotein receptor. J Atheroscler Thromb 2004;11(4):200-8.

115. Gao Y, Shen W, Lu B, Zhang Q, Hu Y, Chen Y. Upregulation of hepatic VLDLR via PPARalpha is required for the triglyceride-lowering effect of fenofibrate. J Lipid Res 2014 Aug;55(8):1622-33.

116. Zheng C, Khoo C, Furtado J, Sacks FM. Apolipoprotein C-III and the metabolic basis for hypertriglyceridemia and the dense low-density lipoprotein phenotype. Circulation 2010 Apr 20;121(15):1722-34.

117. Yuan G, Al-Shali KZ, Hegele RA. Hypertriglyceridemia: Its etiology, effects and treatment. Cmaj 2007 Apr 10;176(8):1113-20.

118. Yilmaz Y. NAFLD in the absence of metabolic syndrome: Different epidemiology, pathogenetic mechanisms, risk factors for disease progression? Semin Liver Dis 2012 Feb;32(1):14-21.

119. Vance DE. Physiological roles of phosphatidylethanolamine N-methyltransferase. Biochim Biophys Acta 2013 Mar;1831(3):626-32.

120. Nishimaki-Mogami T, Suzuki K, Takahashi A. The role of phosphatidylethanolamine methylation in the secretion of very low density lipoproteins by cultured rat hepatocytes: Rapid inhibition of phosphatidylethanolamine methylation by bezafibrate increases the density of apolipoprotein B48-containing lipoproteins. Biochim Biophys Acta 1996 Nov 11;1304(1):21-31.

121. Smith SC,Jr. Multiple risk factors for cardiovascular disease and diabetes mellitus. Am J Med 2007 Mar;120(3 Suppl 1):S3-S11.

122. Tomasi ML, Ramani K, Lopitz-Otsoa F, Rodriguez MS, Li TW, Ko K, Yang H, Bardag-Gorce F, Iglesias-Ara A, Feo F, et al. S-adenosylmethionine regulates dual-specificity mitogen-activated protein kinase phosphatase expression in mouse and human hepatocytes. Hepatology 2010 Jun;51(6):2152-61.

123. Seglen PO. Preparation of isolated rat liver cells. In: Methods in cell biology. Prescott,David M.; ed. New York: Academic Press; 1976. Volume XIII [electronic resource] / edited by David M. Prescott.; 1 online resource; Includes bibliographical references and index.; Access restricted by licensing agreement.; Description based on print version record.; Access is available to the Yale community.; Methods in cell biology ; 13.

124. BLIGH EG, DYER WJ. A rapid method of total lipid extraction and purification. Can J Biochem Physiol 1959 Aug;37(8):911-7.

125. Ruiz JI, Ochoa B. Quantification in the subnanomolar range of phospholipids and neutral lipids by monodimensional thin-layer chromatography and image analysis. J Lipid Res 1997 Jul;38(7):1482-9.

126. Cole LK, Jacobs RL, Vance DE. Tamoxifen induces triacylglycerol accumulation in the mouse liver by activation of fatty acid synthesis. Hepatology 2010 Oct;52(4):1258-65.

127. Ko KW, Erickson B, Lehner R. Es-x/Ces1 prevents triacylglycerol accumulation in McArdle-RH7777 hepatocytes. Biochim Biophys Acta 2009 Dec;1791(12):1133-43.

128. Samborski RW, Ridgway ND, Vance DE. Metabolism of molecular species of phosphatidylethanolamine and phosphatidylcholine in rat hepatocytes during prolonged inhibition of phosphatidylethanolamine N-methyltransferase. J Lipid Res 1993 Jan;34(1):125-37.

129. Sun Z, Miller RA, Patel RT, Chen J, Dhir R, Wang H, Zhang D, Graham MJ, Unterman TG, Shulman GI, et al. Hepatic Hdac3 promotes gluconeogenesis by repressing lipid synthesis and sequestration. Nat Med 2012 Jun;18(6):934-42.

130. Millar JS, Cromley DA, McCoy MG, Rader DJ, Billheimer JT. Determining hepatic triglyceride production in mice: Comparison of poloxamer 407 with triton WR-1339. J Lipid Res 2005 Sep;46(9):2023-8.

131. Aspichueta P, Perez S, Ochoa B, Fresnedo O. Endotoxin promotes preferential periportal upregulation of VLDL secretion in the rat liver. J Lipid Res 2005 May;46(5):1017-26.

132. Laemmli UK. Cleavage of structural proteins during the assembly of the head of bacteriophage T4. Nature 1970 Aug 15;227(5259):680-5.

133. Bharadwaj KG, Hiyama Y, Hu Y, Huggins LA, Ramakrishnan R, Abumrad NA, Shulman GI, Blaner WS, Goldberg IJ. Chylomicron- and VLDL-derived lipids enter the heart through different pathways: In vivo evidence for receptor- and non-receptor-mediated fatty acid uptake. J Biol Chem 2010 Dec 3;285(49):37976-86.

134. Seo T, Al-Haideri M, Treskova E, Worgall TS, Kako Y, Goldberg IJ, Deckelbaum RJ. Lipoprotein lipase-mediated selective uptake from low density lipoprotein requires cell surface proteoglycans and is independent of scavenger receptor class B type 1. J Biol Chem 2000 Sep 29;275(39):30355-62.

135. Wang H, Gilham D, Lehner R. Proteomic and lipid characterization of apolipoprotein B-free luminal lipid droplets from mouse liver microsomes: Implications for very low density lipoprotein assembly. J Biol Chem 2007 Nov 9;282(45):33218-26.

136. Dolinsky VW, Douglas DN, Lehner R, Vance DE. Regulation of the enzymes of hepatic microsomal triacylglycerol lipolysis and re-esterification by the glucocorticoid dexamethasone. Biochem J 2004 Mar 15;378(Pt 3):967-74.

137. Cristobal S, Ochoa B, Fresnedo O. Purification and properties of a cholesteryl ester hydrolase from rat liver microsomes. J Lipid Res 1999 Apr;40(4):715-25.

138. Ridgway ND, Vance DE. Phosphatidylethanolamine N-methyltransferase from rat liver. Methods Enzymol 1992;209:366-74.

139. Matthews DR, Hosker JP, Rudenski AS, Naylor BA, Treacher DF, Turner RC. Homeostasis model assessment: Insulin resistance and beta-cell function from fasting plasma glucose and insulin concentrations in man. Diabetologia 1985 Jul;28(7):412-9.

140. Kleiner DE, Brunt EM, Van Natta M, Behling C, Contos MJ, Cummings OW, Ferrell LD, Liu YC, Torbenson MS, Unalp-Arida A, et al. Design and validation of a histological scoring system for nonalcoholic fatty liver disease. Hepatology 2005 Jun;41(6):1313-21.

141. Martinez-Una M, Varela-Rey M, Cano A, Fernandez-Ares L, Beraza N, Aurrekoetxea I, Martinez-Arranz I, Garcia-Rodriguez JL, Buque X, Mestre D, et al. Excess S-adenosylmethionine reroutes phosphatidylethanolamine towards phosphatidylcholine and triglyceride synthesis. Hepatology 2013 Oct;58(4):1296-305.

142. Vernon G, Baranova A, Younossi ZM. Systematic review: The epidemiology and natural history of non-alcoholic fatty liver disease and non-alcoholic steatohepatitis in adults. Aliment Pharmacol Ther 2011 Aug;34(3):274-85.

143. Ha J, Daniel S, Broyles SS, Kim KH. Critical phosphorylation sites for acetyl-CoA carboxylase activity. J Biol Chem 1994 Sep 2;269(35):22162-8.

144. Brasaemle DL. Thematic review series: Adipocyte biology. the perilipin family of structural lipid droplet proteins: Stabilization of lipid droplets and control of lipolysis. J Lipid Res 2007 Dec;48(12):2547-59.

145. Horl G, Wagner A, Cole LK, Malli R, Reicher H, Kotzbeck P, Kofeler H, Hofler G, Frank S, Bogner-Strauss JG, et al. Sequential synthesis and methylation of phosphatidylethanolamine promote lipid droplet biosynthesis and stability in tissue culture and in vivo. J Biol Chem 2011 May 13;286(19):17338-50.

146. Martinez-Una M, Varela-Rey M, Mestre D, Fernandez-Ares L, Fresnedo O, Fernandez-Ramos D, Gutierrez-de Juan V, Martin-Guerrero I, Garcia-Orad A, Luka Z, et al. S-adenosylmethionine increases circulating very-low density lipoprotein clearance in non-alcoholic fatty liver disease. J Hepatol 2015 Mar;62(3):673-81.

147. Senthivinayagam S, McIntosh AL, Moon KC, Atshaves BP. Plin2 inhibits cellular glucose uptake through interactions with SNAP23, a SNARE complex protein. PLoS One 2013 Sep 6;8(9):e73696.

148. McIntosh AL, Storey SM, Atshaves BP. Intracellular lipid droplets contain dynamic pools of sphingomyelin: ADRP binds phospholipids with high affinity. Lipids 2010 Jun;45(6):465-77.

149. Mensenkamp AR, Havekes LM, Romijn JA, Kuipers F. Hepatic steatosis and very low density lipoprotein secretion: The involvement of apolipoprotein E. J Hepatol 2001 Dec;35(6):816-22.

150. Moylan CA, Pang H, Dellinger A, Suzuki A, Garrett ME, Guy CD, Murphy SK, Ashley-Koch AE, Choi SS, Michelotti GA, et al. Hepatic gene expression profiles differentiate presymptomatic patients with mild versus severe nonalcoholic fatty liver disease. Hepatology 2014 Feb;59(2):471-82.

151. Murphy SK, Yang H, Moylan CA, Pang H, Dellinger A, Abdelmalek MF, Garrett ME, Ashley-Koch A, Suzuki A, Tillmann HL, et al. Relationship between methylome and transcriptome in patients with nonalcoholic fatty liver disease. Gastroenterology 2013 Nov;145(5):1076-87.

152. Huang Y, Mahley RW. Apolipoprotein E: Structure and function in lipid metabolism, neurobiology, and alzheimer's diseases. Neurobiol Dis 2014 Dec;72 Pt A:3-12.

153. Ye SQ, Reardon CA, Getz GS. Inhibition of apolipoprotein E degradation in a post-golgi compartment by a cysteine protease inhibitor. J Biol Chem 1993 Apr 25;268(12):8497-502.

154. Wenner C, Lorkowski S, Engel T, Cullen P. Apolipoprotein E in macrophages and hepatocytes is eegraded via the proteasomal pathway. Biochem Biophys Res Commun 2001 Mar 30;282(2):608-14.

155. van der Veen JN, Lingrell S, Vance DE. The membrane lipid phosphatidylcholine is an unexpected source of triacylglycerol in the liver. J Biol Chem 2012 Jul 6;287(28):23418-26.

156. Angulo P. Nonalcoholic fatty liver disease. N Engl J Med 2002 Apr 18;346(16):1221-31.

157. Finkelstein JD, Kyle WE, Harris BJ, Martin JJ. Methionine metabolism in mammals: Concentration of metabolites in rat tissues. J Nutr 1982 May;112(5):1011-8.

158. Zubiete-Franco I, Garcia-Rodriguez JL, Martinez-Una M, Martinez-Lopez N, Woodhoo A, Juan VG, Beraza N, Lage-Medina S, Andrade F, Fernandez ML, et al. Methionine and S-adenosylmethionine levels are critical regulators of PP2A activity modulating lipophagy during steatosis. J Hepatol 2016 Feb;64(2):409-18.

159. Kharbanda KK, Mailliard ME, Baldwin CR, Beckenhauer HC, Sorrell MF, Tuma DJ. Betaine attenuates alcoholic steatosis by restoring phosphatidylcholine generation via the phosphatidylethanolamine methyltransferase pathway. J Hepatol 2007 Feb;46(2):314-21.

160. Yamaguchi K, Yang L, McCall S, Huang J, Yu XX, Pandey SK, Bhanot S, Monia BP, Li YX, Diehl AM. Diacylglycerol acyltranferase 1 anti-sense oligonucleotides reduce hepatic fibrosis in mice with nonalcoholic steatohepatitis. Hepatology 2008 Feb;47(2):625-35.

161. Yamaguchi K, Yang L, McCall S, Huang J, Yu XX, Pandey SK, Bhanot S, Monia BP, Li YX, Diehl AM. Inhibiting triglyceride synthesis improves hepatic steatosis but exacerbates liver damage and fibrosis in obese mice with nonalcoholic steatohepatitis. Hepatology 2007 Jun;45(6):1366-74.

162. McIntosh AL, Senthivinayagam S, Moon KC, Gupta S, Lwande JS, Murphy CC, Storey SM, Atshaves BP. Direct interaction of Plin2 with lipids on the surface of lipid droplets: A live cell FRET analysis. Am J Physiol Cell Physiol 2012 Oct 1;303(7):C728-42.

163. Tiwari S, Siddiqi S, Siddiqi SA. CideB protein is required for the biogenesis of very low density lipoprotein (VLDL) transport vesicle. J Biol Chem 2013 Feb 15;288(7):5157-65.

164. Martinez-Chantar ML, Vazquez-Chantada M, Garnacho M, Latasa MU, Varela-Rey M, Dotor J, Santamaria M, Martinez-Cruz LA, Parada LA, Lu SC, et al. S-adenosylmethionine regulates cytoplasmic HuR via AMP-activated kinase. Gastroenterology 2006 Jul;131(1):223-32.

165. Fabbrini E, Sullivan S, Klein S. Obesity and nonalcoholic fatty liver disease: Biochemical, metabolic, and clinical implications. Hepatology 2010 Feb;51(2):679-89.

166. Fabbrini E, Mohammed BS, Magkos F, Korenblat KM, Patterson BW, Klein S. Alterations in adipose tissue and hepatic lipid kinetics in obese men and women with nonalcoholic fatty liver disease. Gastroenterology 2008 Feb;134(2):424-31.

167. Lambert JE, Ramos-Roman MA, Browning JD, Parks EJ. Increased de novo lipogenesis is a distinct characteristic of individuals with nonalcoholic fatty liver disease. Gastroenterology 2014 Mar;146(3):726-35.

168. Adiels M, Olofsson SO, Taskinen MR, Boren J. Overproduction of very low-density lipoproteins is the hallmark of the dyslipidemia in the metabolic syndrome. Arterioscler Thromb Vasc Biol 2008 Jul;28(7):1225-36.

169. Duncan TM, Reed MC, Nijhout HF. The relationship between intracellular and plasma levels of folate and metabolites in the methionine cycle: A model. Mol Nutr Food Res 2013 Apr;57(4):628-36.

170. Loehrer FM, Schwab R, Angst CP, Haefeli WE, Fowler B. Influence of oral S-adenosylmethionine on plasma 5-methyltetrahydrofolate, S-adenosylhomocysteine, homocysteine and methionine in healthy humans. J Pharmacol Exp Ther 1997 Aug;282(2):845-50.

171. Finkelstein JD, Martin JJ. Methionine metabolism in mammals. adaptation to methionine excess. J Biol Chem 1986 Feb 5;261(4):1582-7.

172. Regina M, Korhonen VP, Smith TK, Alakuijala L, Eloranta TO. Methionine toxicity in the rat in relation to hepatic accumulation of S-adenosylmethionine: Prevention by dietary stimulation of the hepatic transsulfuration pathway. Arch Biochem Biophys 1993 Feb 1;300(2):598-607.

173. Innis SM, Davidson AG, Melynk S, James SJ. Choline-related supplements improve abnormal plasma methionine-homocysteine metabolites and glutathione status in children with cystic fibrosis. Am J Clin Nutr 2007 Mar;85(3):702-8.

174. Pizzolo F, Blom HJ, Choi SW, Girelli D, Guarini P, Martinelli N, Stanzial AM, Corrocher R, Olivieri O, Friso S. Folic acid effects on s-adenosylmethionine, s-adenosylhomocysteine, and DNA methylation in patients with intermediate hyperhomocysteinemia. J Am Coll Nutr 2011 Feb;30(1):11-8.

175. Elshorbagy AK, Jerneren F, Samocha-Bonet D, Refsum H, Heilbronn LK. Serum S-adenosylmethionine, but not methionine, increases in response to overfeeding in humans. Nutr Diabetes 2016 Jan 25;6:e192.

176. Niculescu MD, Zeisel SH. Diet, methyl donors and DNA methylation: Interactions between dietary folate, methionine and choline. J Nutr 2002 Aug;132(8 Suppl):2333S-5S.

177. Nguyen TT, Hayakawa T, Tsuge H. Effect of vitamin B6 deficiency on the synthesis and accumulation of S-adenosylhomocysteine and S-adenosylmethionine in rat tissues. J Nutr Sci Vitaminol (Tokyo) 2001 Jun;47(3):188-94.

178. Doi T, Kawata T, Tadano N, Iijima T, Maekawa A. Effect of vitamin B12 deficiency on S-adenosylmethionine metabolism in rats. J Nutr Sci Vitaminol (Tokyo) 1989 Feb;35(1):1-9.

179. van der Veen JN, Kennelly JP, Wan S, Vance JE, Vance DE, Jacobs RL. The critical role of phosphatidylcholine and phosphatidylethanolamine metabolism in health and disease. Biochim Biophys Acta 2017 Apr 11.

180. Wilson CG, Tran JL, Erion DM, Vera NB, Febbraio M, Weiss EJ. Hepatocyte-specific disruption of CD36 attenuates fatty liver and improves insulin sensitivity in HFD-fed mice. Endocrinology 2016 Feb;157(2):570-85.

181. Wang C, Hu L, Zhao L, Yang P, Moorhead JF, Varghese Z, Chen Y, Ruan XZ. Inflammatory stress increases hepatic CD36 translational efficiency via activation of the mTOR signalling pathway. PLoS One 2014 Jul 21;9(7):e103071.

182. Brindley DN, Kok BP, Kienesberger PC, Lehner R, Dyck JR. Shedding light on the enigma of myocardial lipotoxicity: The involvement of known and putative regulators of fatty acid storage and mobilization. Am J Physiol Endocrinol Metab 2010 May;298(5):E897-908.

183. Ma KL, Liu J, Ni J, Zhang Y, Lv LL, Tang RN, Ni HF, Ruan XZ, Liu BC. Inflammatory stress exacerbates the progression of cardiac fibrosis in high-fat-fed apolipoprotein E knockout mice via endothelial-mesenchymal transition. Int J Med Sci 2013;10(4):420-6.

184. Rensen PC, Jong MC, van Vark LC, van der Boom H, Hendriks WL, van Berkel TJ, Biessen EA, Havekes LM. Apolipoprotein E is resistant to intracellular degradation in vitro and in vivo. evidence for retroendocytosis. J Biol Chem 2000 Mar 24;275(12):8564-71.

185. Fazio S, Linton MF, Hasty AH, Swift LL. Recycling of apolipoprotein E in mouse liver. J Biol Chem 1999 Mar 19;274(12):8247-53.

186. Swift LL, Farkas MH, Major AS, Valyi-Nagy K, Linton MF, Fazio S. A recycling pathway for resecretion of internalized apolipoprotein E in liver cells. J Biol Chem 2001 Jun 22;276(25):22965-70.

187. Heeren J, Grewal T, Jackle S, Beisiegel U. Recycling of apolipoprotein E and lipoprotein lipase through endosomal compartments in vivo. J Biol Chem 2001 Nov 9;276(45):42333-8.

188. Rasmussen KL. Plasma levels of apolipoprotein E, APOE genotype and risk of dementia and ischemic heart disease: A review. Atherosclerosis 2016 Dec;255:145-55.

189. Packard CJ, Shepherd J. Lipoprotein heterogeneity and apolipoprotein B metabolism. Arterioscler Thromb Vasc Biol 1997 Dec;17(12):3542-56.

190. Veniant MM, Withycombe S, Young SG. Lipoprotein size and atherosclerosis susceptibility in apoe(-/-) and ldlr(-/-) mice. Arterioscler Thromb Vasc Biol 2001 Oct;21(10):1567-70.

191. Millar JS, Packard CJ. Heterogeneity of apolipoprotein B-100-containing lipoproteins: What we have learnt from kinetic studies. Curr Opin Lipidol 1998 Jun;9(3):197-202.

192. Demant T, Packard C. In vivo studies of VLDL metabolism and LDL heterogeneity. Eur Heart J 1998 Jul;19 Suppl H:H7-10.

193. Ampuero J, Gallego-Duran R, Romero-Gomez M. Association of NAFLD with subclinical atherosclerosis and coronary-artery disease: Meta-analysis. Rev Esp Enferm Dig 2015 Jan;107(1):10-6.

194. Zhang SH, Reddick RL, Piedrahita JA, Maeda N. Spontaneous hypercholesterolemia and arterial lesions in mice lacking apolipoprotein E. Science 1992 Oct 16;258(5081):468-71.

195. Mak AC, Pullinger CR, Tang LF, Wong JS, Deo RC, Schwarz JM, Gugliucci A, Movsesyan I, Ishida BY, Chu C, et al. Effects of the absence of apolipoprotein e on lipoproteins, neurocognitive function, and retinal function. JAMA Neurol 2014 Oct;71(10):1228-36.

196. Huang Y, Liu XQ, Rall SC,Jr, Taylor JM, von Eckardstein A, Assmann G, Mahley RW. Overexpression and accumulation of apolipoprotein E as a cause of hypertriglyceridemia. J Biol Chem 1998 Oct 9;273(41):26388-93.

197. Duan Y, Chen Y, Hu W, Li X, Yang X, Zhou X, Yin Z, Kong D, Yao Z, Hajjar DP, et al. Peroxisome proliferator-activated receptor gamma activation by ligands and dephosphorylation induces proprotein convertase subtilisin kexin type 9 and low density lipoprotein receptor expression. J Biol Chem 2012 Jul 6;287(28):23667-77.

198. Tao H, Aakula S, Abumrad NN, Hajri T. Peroxisome proliferator-activated receptor-gamma regulates the expression and function of very-low-density lipoprotein receptor. Am J Physiol Endocrinol Metab 2010 Jan;298(1):E68-79.

199. Schneider WJ. CHAPTER 20 – Lipoprotein receptors. In: D. E. Vance, J. E. Vance, editors. Biochemistry of lipids, lipoproteins and membranes (fifth edition). ; 2008. .

200. Ding Y, Svingen GF, Pedersen ER, Gregory JF, Ueland PM, Tell GS, Nygard OK. Plasma glycine and risk of acute myocardial infarction in patients with suspected stable angina pectoris. J Am Heart Assoc 2015 Dec 31;5(1):10.1161/JAHA.115.002621.

201. Zhu X, Song J, Mar MH, Edwards LJ, Zeisel SH. Phosphatidylethanolamine N-methyltransferase (PEMT) knockout mice have hepatic steatosis and abnormal hepatic choline metabolite concentrations despite ingesting a recommended dietary intake of choline. Biochem J 2003 Mar 15;370(Pt 3):987-93.

202. Erion DM, Shulman GI. Diacylglycerol-mediated insulin resistance. Nat Med 2010 Apr;16(4):400-2.

203. Liu SP, Li YS, Chen YJ, Chiang EP, Li AF, Lee YH, Tsai TF, Hsiao M, Huang SF, Chen YM. Glycine N-methyltransferase-/- mice develop chronic hepatitis and glycogen storage disease in the liver. Hepatology 2007 Nov;46(5):1413-25.

204. Funai K, Lodhi IJ, Spears LD, Yin L, Song H, Klein S, Semenkovich CF. Skeletal muscle phospholipid metabolism regulates insulin sensitivity and contractile function. Diabetes 2016 Feb;65(2):358-70.

205. Jacobs RL, Zhao Y, Koonen DP, Sletten T, Su B, Lingrell S, Cao G, Peake DA, Kuo MS, Proctor SD, et al. Impaired de novo choline synthesis explains why phosphatidylethanolamine N-methyltransferase-deficient mice are protected from diet-induced obesity. J Biol Chem 2010 Jul 16;285(29):22403-13.

206. Ling J, Chaba T, Zhu LF, Jacobs RL, Vance DE. Hepatic ratio of phosphatidylcholine to phosphatidylethanolamine predicts survival after partial hepatectomy in mice. Hepatology 2012 Apr;55(4):1094-102.

207. Li Z, Agellon LB, Allen TM, Umeda M, Jewell L, Mason A, Vance DE. The ratio of phosphatidylcholine to phosphatidylethanolamine influences membrane integrity and steatohepatitis. Cell Metab 2006 May;3(5):321-31.